DISSERTATION

INTEGRATED OPTIMIZATION OF COMPOSITE STRUCTURES

Submitted by

Daniel Lang

Department of Systems Engineering

In partial fulfillment of the requirements

For the Degree of Doctor of Philosophy

Colorado State University

Fort Collins, Colorado

Spring 2022

Doctoral Committee:

Advisor: Donald Radford

Daniel Herber
Edwin Chong
Paul Heyliger

ABSTRACT

INTEGRATED OPTIMIZATION OF COMPOSITE STRUCTURES

Many industries are exploring the application of composite materials to structural designs to reduce weight. A common issue that is encountered by these industries, however, is difficulty in developing structural geometries best suited for the materials. Research efforts have begun to develop optimization methodology to help develop structural shapes but have thus far only partially addressed optimization of the geometry.

This dissertation provides a literature review of past efforts to develop optimization methodologies. Through that review it is identified that the subprocesses required to fully optimize a composite structure are mold shape optimization, ply draping analysis, kinematic partitioning, connection and joint definition, ply topology optimization and manufacturing simulations. To date, however, these subprocesses have primarily been applied individually and have not been integrated to develop fully optimized designs.

In this research, a methodology is proposed to integrate established composite design and subprocesses to develop optimized composite structures. The proposed methodology sequentially and iteratively improves the design through mold shape optimization, ply draping analysis, kinematic partitioning, connection and joint definition, ply topology optimization and manufacturing simulations. Throughout the proposed methodology, checks are also integrated to ensure that the developed design meets design objectives and constraints.

To test the methodology a case study is conducted to develop composite rail vehicle structures. As part of this case study, it is hypothesized that a composite structure designed

through a fully integrated methodology will demonstrate reduced costs, mass and improved manufacturability compared to a structure where functions have only been partially integrated.

When the proposed fully integrated methodology is applied to create a case study design, the hypothesis is validated. The design generated by the fully integrated optimization methodology has a 37% lower mass and a 56% lower cost to manufacture than a design that is developed through a partially integrated methodology. The case study also demonstrates that structures developed through the proposed methodology have improved manufacturability.

ACKNOWLEDGMENTS

I would like to thank Dr. Donald Radford for patiently guiding and supporting me through my PhD degree. I would also like to thank the rest of my research committee: Dr. Daniel Herber, Dr. Edwin Chong, and Dr. Paul Heyliger your thorough review and feedback on my research have greatly improved the quality of my research. Finally, I would like to thank my wife Casey for being patient and supporting me in my lifelong quest to educate myself.

DEDICATION

I dedicate this work to my parents Cynthia and Carl, for instilling a lifelong love of learning and for your support throughout my education. I will never be able to thank you enough for your dedication and sacrifices that have allowed me to reach this lifelong goal.

TABLE OF CONTENTS

LIST OF TABLES

LIST OF FIGURES

CHAPTER 1: INTRODUCTION

Many industries are seeking to reduce energy consumption and greenhouse gas emissions. One strategy that is being explored by researchers in these industries is the application of composite materials in structural design. Composites offer a higher specific stiffness and can be readily molded into complex shapes to reduce the number of components, reducing the mass of a structure. Adoption has been slow in many industries, however, due in part to a lack of understanding of how to develop, accurately model and validate an optimal composite structural shape [1]. Many industries create suboptimal designs referred to in the composites industry as "black metal", where structural shapes that were designed for metals are re-used and composite materials are applied to them[2]. These designs are suboptimal because the structural geometries have been created with respect to the material properties and manufacturing processes common to metals, rather than composites, and as a result fall short of producing comparable or improved function to metallic designs.

Another reason for minimal composite application by other industries is due to the expense associated with creating physical prototypes of composite structures and testing them to validate designs [3]. Instead, computer simulation is viewed as a more efficient methodology to refine and validate designs. Many industries, however, lack maturity in composite modeling and simulation and therefore have not developed methodologies to accurately predict structural performance or to optimize designs [4]. Industries that are mature in composite application, such as aerospace have developed proprietary modeling and validation tools that are specific to their application but are not available or relevant for other inexperienced industries looking to apply composites [5]. Without more accurate modeling and validation methodology, many research studies that have focused on black metal designs may present inaccurate weight savings projections for composite structures that are not actually achievable through manufacturing.

Due to the potential for inaccurate results when composites are applied to black metal geometries, it is logical that a methodology be established to develop structural shapes specifically for the materials. In recent years, many research efforts have focused on optimizing composite structural geometries to improve application in structural design [6]–[8]. The intent of geometric optimization is to produce structural shapes that are better suited for composite material application and manufacture. Thus far, however, these efforts have focused primarily on optimizing material layout within the existing black metal geometry and have neglected optimization of the overall structural shape. Ignoring the overall structural geometry has perpetuated the practice of developing black metal designs that are not fully optimized and may not be feasible for manufacturing or service.

Advancements outside the area of composite shape optimization have developed other design methodologies that may help to develop and validate structural geometries specific for composite materials. These design methodologies include overall structural shape development, improved modeling of joints and connections, structural partitioning, and manufacturing simulations [9]–[13]. To date, however, these outside processes have not been organized and integrated to create a comprehensive composite structural shape optimization methodology.

1.1 Research Purpose

The purpose of this research is to organize, integrate and advance existing design processes to develop a methodology which creates optimal shapes for composite structures. This methodology will be developed in an attempt to help industries that lack experience with composites replace black metal structures, with shapes that are better suited for composite application. This methodology will leverage commercially available software tools and advance practices beyond what has been published in previous research with the intent of encouraging more rapid adoption by industry. The final purpose of this research is to identify key requirements and processes to be included in a future software application that integrates the overall methodology proposed to provide a more streamlined approach to designers.

1.2 Contribution to Literature

This research advances current practices within the design field by providing a consistent methodology to optimize the geometry of composite structures to improve performance, manufacturability, and costs. As demonstrated in the literature reviewed, past research has only optimized material layout within black metal geometries, which is not suitable to develop optimal overall structural geometries. Additionally, this research identifies key constraints on the geometric optimization that must be considered to develop a shape that meets material and manufacturing requirements. These contributions have been demonstrated as novel, through publication in two peer reviewed journal articles and the proceedings from one conference [14]–[16].

1.3 Terminology

Anisotropic: a material that has different mechanical properties depending on the direction in which load is applied.

Autoclave: is a composite manufacturing process which cures composites under heat and pressure.

Black Metal: is the practice of applying composites to a structural geometry that was originally designed for metallic materials.

Composites: As it will be used through the rest of this document, refer to fiber reinforced plastics (FRPs). Specifically, in this context FRPs are assumed to consist of a polymer matrix and a continuous fiber reinforcement.

Fibers: Although there are numerous types of reinforcements that can be used in FRPs, this study focuses on carbon fibers (CFRP). Fibers are typically produced as layers of oriented fibers that are each referred to as a "ply".

Isotropic: Is a material type that possess identical properties regardless of direction

Laminate: When multiple ply layers are combined to form a thicker overall assembly, it forms a laminate.

Layup: Is a composite manufacturing process where plies are layered in a mold or on a tool surface to develop a laminate.

Matrix: A matrix is a material which binds fibers together, protecting them from the environment and transferring stresses from one fiber to another. This study focuses on a common type of polymer matrix: epoxies.

Partitioning: The common composite design process of subdividing an overall structural geometry into smaller laminate or ply regions.

Ply: Within the composite material each layer of fibers, constitute the ply. Composite plies have anisotropic material properties, meaning that they have different mechanical properties depending on the direction in which load is applied to the fibers.

Quasi-Isotropic: Designers often implement a laminate design where plies are stacked in alternating order to create an overall structure that has in-plane properties which are functionally isotropic. An example of a stacking sequence that would constitute a quasi-isotropic laminate would be 8 plies oriented in the following directions: 0°, 45°, -45°, 90°, 90°, -45°, 45°, and 0°. Through-thickness properties remain matrix dominated.

2 CHAPTER 2: BLACK METAL DESIGN AND OPTIMIZATION

Many industries have become interested in the application of composite materials, due to their high specific material properties. The transportation sector, in particular, has invested significant research efforts into developing composite structures, as the high specific material properties offered by the materials can lead to reduced energy consumption and greenhouse gas emissions by vehicles [17]. With weight savings of up to 50% achievable over traditional metallic structures, composites are viewed as a possible strategy in reducing transportation's contribution to climate change [18].

Despite the promise of weight savings improvements over traditional structural material types; however, composites remain limited in their application in most transportation sectors. Composites experts have partially attributed this issue to the inexperience of many structural designers in developing optimal shapes for composite application [19]. It has been observed that designers who lack experience with composites frequently apply the materials to structural geometries that were developed for metallic materials and manufacturing out of convenience and due to a lack of understanding for how to best apply the materials. This practice has been termed "black metal" design by those within the composites industry.

Figure 1 provides an example from rail vehicle design of a common cast steel bogie structural shape, and a composite black metal replica made from composites that was the focus of research [20]. It can be seen from the figure that the composite black metal truck frame has identical shape to the original cast steel structure. Replicating steel structural geometries with composite materials is common practice, not just in rail vehicle design, but in most industries that lack experience with the materials [21].

Figure 1 *(a) Cast steel rail vehicle bogie structural geometry, and (b) black metal composite replica* [20]

The reason that black metal structures have impeded the application of composites in many industries, is because these designs can often fail to meet the weight savings expectations of the designers. One study, for example, designed and manufactured two separate automotive trunk structures from composite materials: one black metal design, and one that was specifically designed for composite application [22]. In that study, it was found that the structure specifically designed for composites was 22% lighter than the black metal design. The composite specific design also provided 77% greater stiffness than the black metal design, which was an important performance criterion for the structure.

Black metal shapes produce suboptimal weight savings and performance, in part, because they neglect the compositional differences between metals and composites that result in dissimilar material properties [21]. Metals, and many other materials familiar to structural designers, have uniform “isotropic” composition through the thickness of the material, meaning they possess identical properties regardless of direction. Composites on the other hand possess different micro and macro material properties through the thickness. As structural shape is partially determined based on mechanical properties, the increased micro and macro complexity of composites offers geometric freedom, which is a design advantage over many other materials, but applying these properties to black metal geometries constrains the design to not fully realize these freedoms.

Within the composite material each layer of fibers, referred to as a ply, constitute the micromechanical properties of the structure [23]. The individual ply of the composite has anisotropic material properties, meaning that there are different mechanical properties depending on the direction in which load is applied to ply. The fibers of a composite offer the greatest strength when load direction is aligned with the fibers. If the load is applied transverse, or out-of-plane (through the ply thickness), the strength is substantially reduced. Figure 2 illustrates load alignment with the fibers (shown as direction 1), transverse (shown as direction 2), and out-of-plane (shown as direction 3). Altering fiber coordinate system orientation can change the shape of a structure by creating more efficient load paths. Additionally, composites are available in various feedstocks, some of which have fibers aligned at multiple angles which can also affect shape.

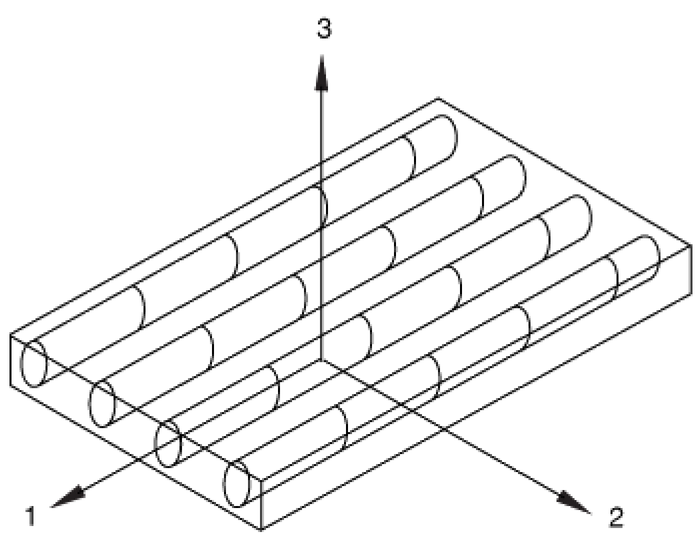

Figure 2 Load applied longitudinally (1), transversely (2) and out-of-plane (3) to a composite

When multiple ply layers (plies) are combined to form a thicker overall assembly, referred to as a laminate, macromechanical properties are developed [24]. When plies are layered at alternating angles, the composite laminate can provide overall in-plane mechanical properties that are different from the individual ply layers. Therefore, the sequencing of ply angles can affect the shape of the structure due to the resulting alterations in macromechanical material properties. These alterations would not be accounted for in a black metal design. Figure 3 illustrates how multiple plies can form a laminate. In the example shown in Figure 3, plies are oriented at angles of 45, -45 and 90 degrees from the original ply coordinate system (shown as 0 degrees). This type of arrangement can be beneficial in situations where multi axis loads are applied to the structure, or when distributing the loads out in multiple directions is beneficial.

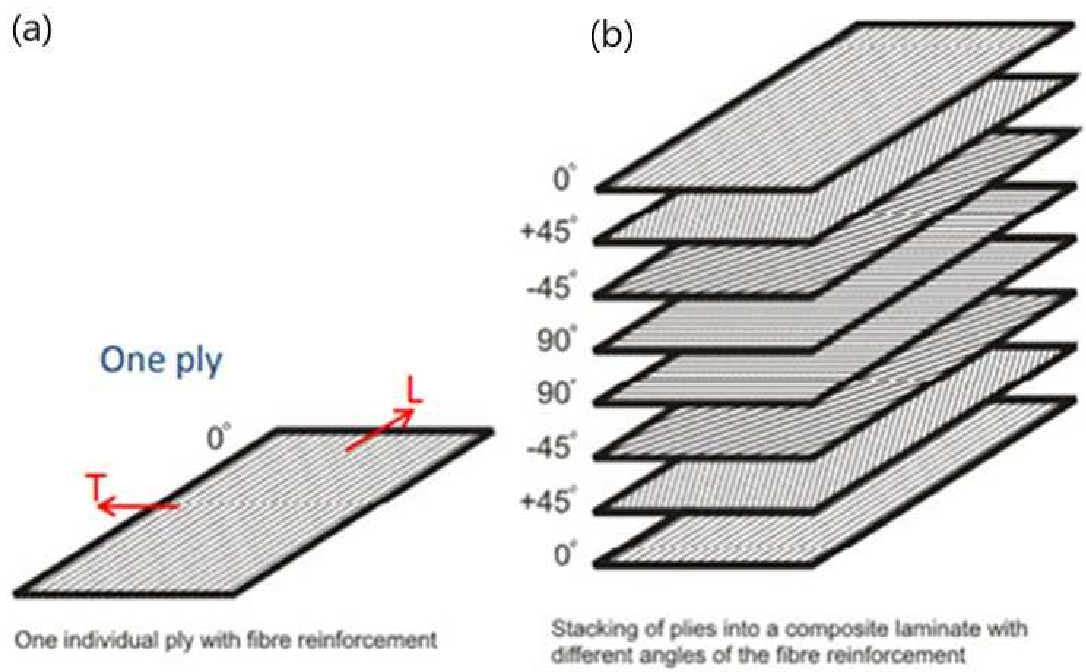

Figure 3 A composite ply (a) vs. a laminate (b) [15]

2.1 Black Metal Design Literature Review

To better understand the design processes that are leading researchers to design black metal structures, a literature review was conducted. Through this review it is evident that the manner in which structures are modeled and optimized through Finite Element Analysis (FEA) software is contributing to the prevalence of black metal designs. The following subsections provide details on common FEA practices observed in the literature reviewed and noted limitations of the current approach.

2.1.1 Black Metal FEA Modeling

In addition to compositional and material property differences mentioned previously in this section, black metal geometries can produce suboptimal performance because they do not account for the differences between metallic and composite manufacturing. Composite manufacturing imposes different constraints on a structural shape than metallic processes, and therefore should be considered during design [25]. Composites are typically manufactured through a process where composite plies are layered in a mold, which defines the shape, to produce the laminate, this process is referred to as *layup*. Molding of the composite provides improved geometric freedom when designing the laminate compared to many metallic manufacturing processes. Where multiple structural components, joints, welds and fasteners may be required in a metallic design, composite laminates can be shaped to reduce or eliminate these inefficiencies [26].

Rather than beginning with the development of molded structural shape to best utilize composite materials, however, typical black metal design processes begin by modeling metallic structural geometries to represent the mold surfaces for composite parts [27]. Modeling often begins with importing a black metal structural shape into the FEA software from another design suite such as a Computer Aided Design (CAD) or 3D modeling program [28]. Once imported into an FEA program the surfaces of the black metal shapes represent mold surfaces to simulate composite ply layup.

Before ply geometries can be defined and layup can be simulated, however, the surfaces of the model geometry are next divided into much smaller subregions to create FEA “elements”

[29]. FEA simulation requires element assignment to the geometry to provide more accurate simulation of mechanical performance at subregions of the structure. The geometry of each element subregion is selected by the user from a set of predefined types in the FEA program [30]. Most FEA programs provide two major types of elements to mesh a structural model: 2D and 3D. 2D elements are usually used to model simple thin structures, while 3D elements are better suited for thicker more complex structures. Within these major element types, there are a number of element shapes that can be selected by the FEA program. The reason there are multiple element shapes available, is so that the model surface is accurately represented through the mesh. Figure 4 shows common FEA shapes for 2D and 3D element types.

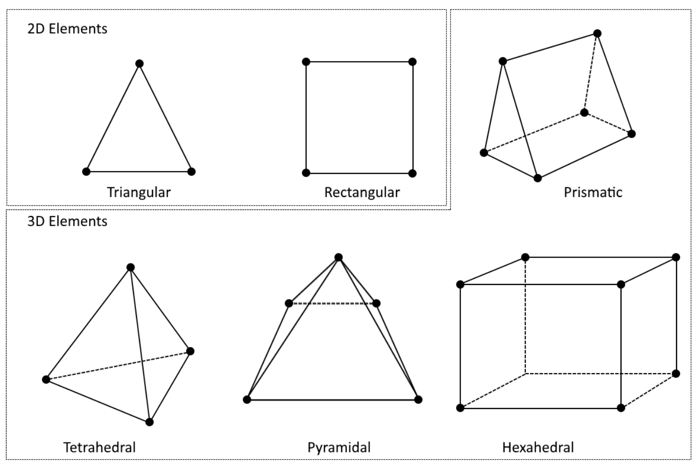

Figure 4 2D and 3D FEA element types [31]

Composite plies are usually manufactured to be very thin (<0.25 mm), so to realistically capture the mechanical performance of individual plies commercially available FEA software packages only allow for the material to be modeled as two-dimensional elements [32]. As the name implies, two-dimensional elements only represent shape in two dimensions (x and y). While ply thickness, the third dimension (z), can be mechanically and mathematically simulated as a parameter it is not geometrically represented by the elements. Similarly, modeling of multiple plies laminated as a stack at a single FEA element location is done through mathematical parameters and is not represented geometrically.

With the black metal geometry meshed, fiber angles must be assigned to the elements so that ply and laminate details can be developed [33] In the literature reviewed it was noted that most research related to black metal design defines fiber angle referenced off of model coordinate axes (x, y, or z). This is, however, an inaccurate way of defining fiber angle, as fiber path can deviate based on structural geometry [34]. Figure 5 provides an example from literature of four fiber angles being assigned to elements within an aircraft wing design. In this figure, the ply thicknesses are visualized for the reader, but are not actually geometrically represented in the model.

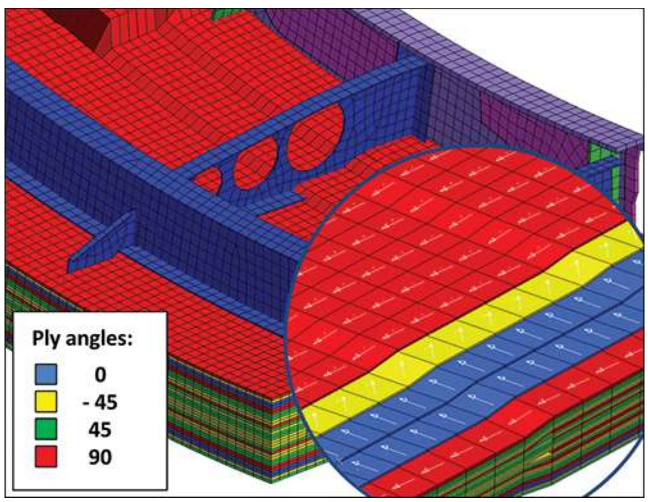

Figure 5 Example of fiber angle definition applied to elements in an aircraft wing design [33]

Figure 6 provides a summary example of the general process noted in literature for modeling black metal structures [35]. Here a CAD drawing is imported (Figure 6 (a)) and meshed with 2D elements (Figure 6 (b)). Following meshing, the surfaces of the black metal floor panel serves as the mold surfaces, from which ply layup can be simulated (Figure 6 (c)). Here a 6-ply laminate is modeled off of the black metal floor panel geometry. Again, ply thickness is visualized for the reader (Figure 6 (c)), but not actually represented geometrically in the FEA model.

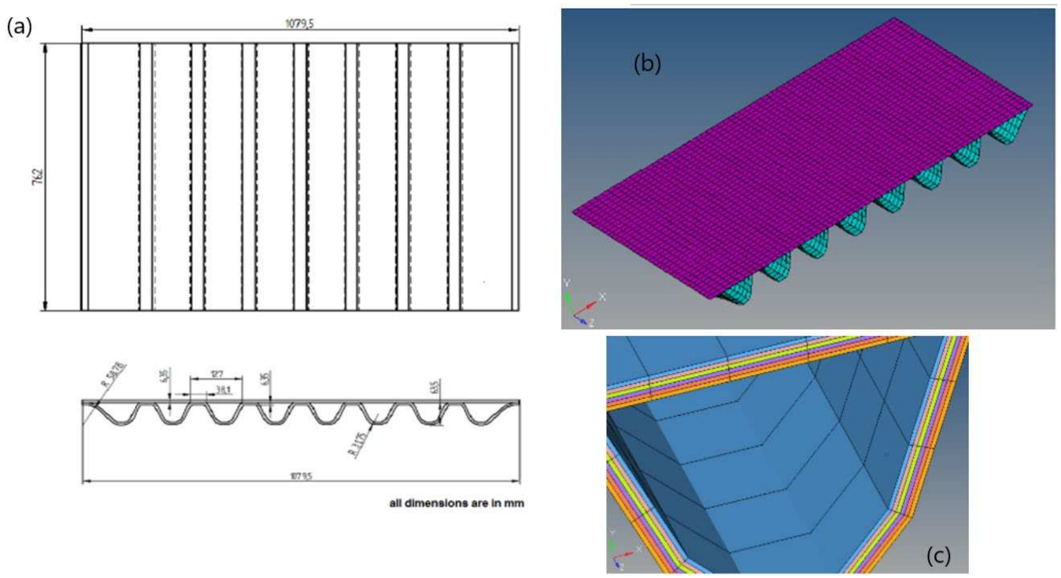

Figure 6 Example of black metal FEA modeling process of a bus floor structure from literature [35]

Recently, research has focused on modeling composite materials with 3D elements [36]. Modeling composites with 3D elements is advantageous as it adds an additional dimension of geometric definition. Referring again to Figure 4, there are twice as many 3D element types when compared to 2D. Therefore, modeling composites from 3D elements also offers the ability to more accurately capture the geometry of composite materials. To date, however, modeling composites with 3D elements is not possible with commercially available FEA software and requires time consuming modeling and custom software to accurately capture the materials anisotropic properties [37]. Therefore, little research has been done in modeling composites with 3D elements, and the work that has been completed has been on small simple structures to prove out the concept [38]. Figure 7 provides an example from literature of a simple woven composite mat that was modeled from 3D elements. Due to the complexity and the lack of established methodology surrounding using 3D elements to model anisotropic properties, this approach was not considered further as part of this research.

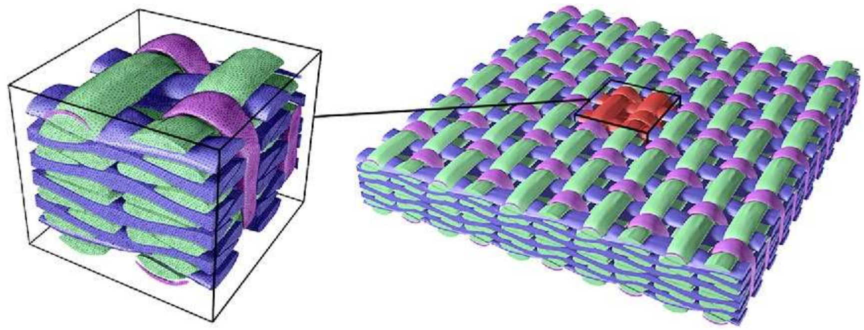

Figure 7 FEA modeling of woven composites using 3D elements [37]

2.1.2 Black Metal Optimization

In addition to the shape flexibility offered by composites previously mentioned in this section, composite manufacturing also offers increased geometric flexibility for ply design. Ply shape flexibility is advantageous in design because plies can be stacked up in certain areas of the structure to provide increased strength, but less layers can be used in other low stress regions. So, material can be distributed throughout the structure as needed to resist the stresses through both variations in the amount of material, fiber orientation, and local stacking sequence of the laminate. This type of thickness variation within a metallic part could only be achieved through expensive casting or machining processes. The flexibility of ply shapes means that a ply geometry does not necessarily have to match to dimensions of the overall laminate, adding complexity to the shape development process.

Following the modeling of a black metal structure a common next step is to conduct structural optimization to exploit the shape and section flexibility of composite plies, referred to as topology [39]. Ply topology optimization research has become prevalent amongst industries that lack experience with composites, as it is viewed as a methodology to assist designers in improving black metal designs [40]. Ply topology research has been aimed at providing designers with optimal ply shapes to improve structural performance [41]. Ply topology optimization essentially identifies optimal composite material allocation to be laid up over a given mold geometry. When applied to a black metal structure, however, there may be limits to the extent that ply topology optimization can improve structural performance.

Many optimization algorithms have been presented in literature to address the demand for ply topology optimization, but the most commonly applied is a gradient descent-based approach which is included in many commercially available FEA programs [6]. The general form of gradient descent optimization is given by Equation 1. The gradient algorithm is governed by an objective function, ψ_o, which seeks to minimize a particular parameter of the design. Optimized solutions are constrained by functions, ψ_i, to develop designs which meet other requirements. The optimization algorithm works to meet the objective function by modifying the design space, which are the plies within the model. The optimal ply design space that is identified through optimization, p_j, is bounded by the lower p^l, and upper, p^u limits. The upper limit is the initial ply geometry prior to optimization, while the lower limit can be defined by the user to restrict the degree to which plies are modified from their starting point.

Objective Function:	$\psi_o(p) \rightarrow \min\ (target)$	(1)
Subject to constrain function(s)	$\psi_i(p) \leq X$	
Design Space	$p^l \leq p_j \leq p^u$	

Ply topology optimization has been applied in research with the intent of satisfying a wide range of functional goals such as maximizing structural damping, improving aerodynamics, minimizing buckling, or reducing stress in composite structures [42]. As previously noted, however, one of the benefits of composite materials in structural design is the potential to reduce weight when compared to traditional structural materials. Therefore, most published research has modified equation 1 to create an objective function that minimizes mass by eliminating ply area [43]. While optimizing ply topology to meet other design objectives and constraints have been studied [44], this research, and the examples from literature provided in this section relate to deriving structural designs with minimal mass.

For optimization problems that have the objective of minimizing mass, constraint equations, $\psi_i(p)$, are required to keep the algorithm from eliminating the entire structure. Similar to objective functions, many constraints have been researched, but the most commonly applied have been compliance and failure requirements [45]. Compliance is the inverse of stiffness, and therefore when applied as a constraint ensures a minimum level of load transfer efficiency by a structure. Similarly, most designers seek to develop designs which will not fail while in use, so requirements to ensure that the structure will not fail are also commonly applied as constraints. While other constraints have been researched, failure and compliance constraints are the most commonly applied, so this research, and the examples from literature provided in this section relate to these constraints.

In composite ply topology optimization, the optimal design space, p_j, is ply geometry. During optimization initial ply shapes are essentially eroded to support the objective of minimizing mass. Ply erosion is constrained by the governing equations, $\psi_i(p)$, so that the structure maintains the required compliance and does not fail. Constraints are verified by FEA software during optimization by evaluating mechanical performance and confirming no violations are created during the process.

With the structure modeled and the algorithm formulated, optimization can next begin. Ply topology optimization is an iterative process, with the three major subprocesses: Free-Sizing,

Sizing, and Shuffling. Figure 8 illustrates the iterative optimization process. Details on the iterative subprocesses are provided below.

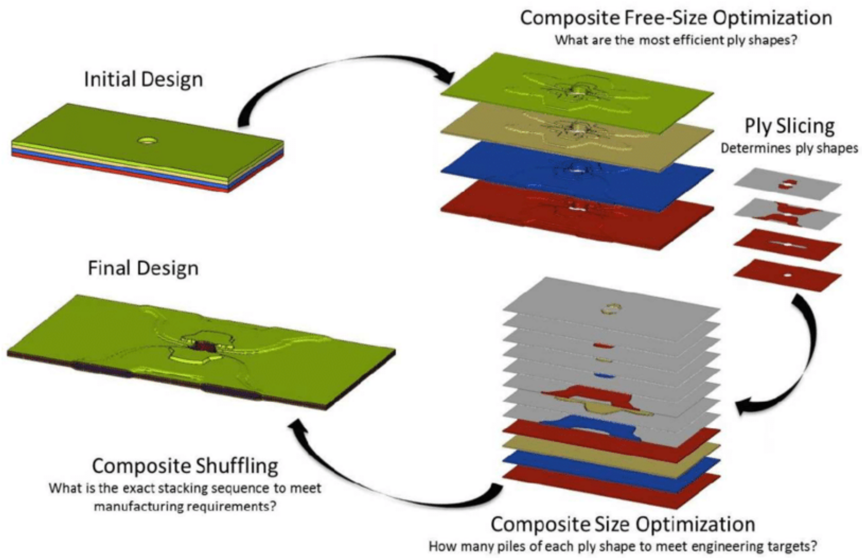

Figure 8 Iterative ply topology optimization process [46]

The first process in ply topology optimization is termed "Free-Size" optimization [47]. This is the process where the aforementioned ply shape erosions occurs. During Free-Size mechanical performance at each individual FEA element is evaluated, and initial ply shapes are eroded to meet established objectives and constraints [48]. Free-Size erosion modifies both 2D ply shape and overall ply thickness. With respect to shape, erosion eliminates ply area at elements that are not needed to meet the constraints to reduce mass. With respect to thickness, Free-Size erosion reduces the overall ply thickness to support the objective of minimizing mass, while still meeting the established constraints.

Because the gradient based Free-Size erosion is subtractive and not additive, prior to starting the optimization designers must first develop a laminate construction that includes all material types and fiber angle orientations to be considered during erosion. The candidate plies within the laminate must also be set to a thickness to satisfy the constraints (failure and compliance). It should be noted that these initial ply thicknesses may be modeled at an unrealistic thickness (>0.25 mm) to meet the established constraints. This issue is corrected during the next step termed “Sizing” optimization. During Sizing, the original ply thicknesses that was increased to meet design constraints are sliced, to develop plies of a manufacturable thickness (<0.25 mm). The exact thickness is defined by the designer based on manufacturing reports.

Figure 9 provides a visual representation of ply erosion following ply shape optimization. Here ply shape varies in dimension from the overall laminate shape within the design of a composite chair armrest [49]. In this example, the laminate makes up the overall shape of the armrest, but the individual plies have varying dimensions and shape to give added support to the armrest around holes and other geometric stress risers to avoid failure and provide the required stiffness.

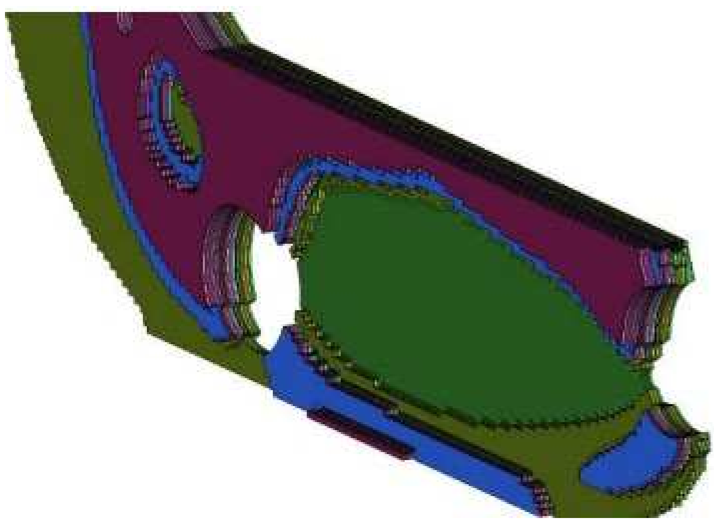

Figure 9 Example of variation in shape between ply and laminate within the design of a composite chair armrest [49]

The final subprocess of ply topology optimization is termed “Shuffling”, which find the optimal organization of plies within a laminate [50]. When thicker plies are sliced during Sizing optimization it can leave numerous plies of the same fiber angle stacked consecutively within a laminate. This organization, however, is suboptimal, as stacking plies of the same orientation consecutively is understood to develop interlaminar forces, such as torsion that can lead to failure. The Shuffling process reorganizes ply order within laminates to reduce or eliminate interlaminar issues. Figure 10 provides an example from literature of how plies of the same fiber orientation are iteratively dispersed within a laminate to improve performance [35].

Iteration 0	Iteration 1	Iteration 2	Iteration 3	Iteration 4
11101	12101	12101	12101	12101
12101	15101	15101	15101	15101
13101	12201	12201	12201	12201
14101	15201	15201	15201	15201
15101	11101	13201	13201	13201
11201	11201	13101	13101	13101
11202	13101	11101	11101	11101
12201	12202	11201	11201	11201
12202	15202	14201	14201	14201
13201	14101	14101	14101	14101
13202	11202	11202	11202	11202
14201	16201	16201	12401	12401
14202	12301	12301	15401	15401
15201	15301	15301	12202	12202
15202	13201	12202	15202	15202
16201	14201	15202	12301	12301
16202	16202	12401	15301	15301
12301	12401	15401	16201	16201
15301	15401	14202	13202	13202
16301	16301	13202	16301	16301
12401	13202	16301	16202	16202
15401	14202	16202	14202	14202

Legend
90.0 degrees
45.0 degrees
0.0 degrees
-45.0 degrees
-90.0 degrees

Figure 10 Example results of shuffling optimization, showing reductions in the number of plies stacked consecutively of any one fiber orientation [35]

Ply topology optimization algorithms develop structural solutions based on the loading condition, boundary conditions, objectives, constraints, initial design space established by the designer [51]. Modifying some, or all, of the governing algorithm will develop a solution that is optimized specific to the unique structural details provided. This allows designers the ability to optimize structures to a service environment, rather than duplicating existing designs that are not custom tailored for a specific application.

As applied in the literature reviewed ply topology optimization has been successful in developing designs which predict weight savings over steel structures. These promising results have attracted industries with less experience in composites, such as rail vehicle manufacturers, to begin researching the application of the materials in structural design. For example, ply optimization was used in one study to develop a composite locomotive front-end structure design that provided a 51% reduction in the mass compared to a steel design [52].

2.1.3 Uncertainty and Limitations of Black Metal Methodology

Despite the promising results, there have been limitations and simplifications identified with the application of ply topology optimization in the literature reviewed. The primary limitations are the lack of geometric flexibility dictated by 2D elements and the propensity of gradient descent algorithms to arrive at local, rather than global minima. Furthermore, there have been simplified assumptions in the way ply topology optimization experiments have been conducted in the literature reviewed including defining the design space based on black metal geometries, not modeling connections between laminated regions, and a lack of integration with validating processes.

The first limitation of ply topology optimization is due to deficiencies in the available simulation tools [53]. As explained in Section 2.1.1 , FEA software requires that composite plies be modeled with two-dimensional elements. As a result, commercially available Finite FEA software has not been designed to optimize plies with three-dimensional elements [54]. As demonstrated in Figure 4, there are twice as many FEA 3D element shapes as 2D shapes. This limits the algorithms geometric flexibility in modifying ply topology during optimization.

When combined with the manner in which gradient descent algorithms erode initial ply area, modeling composites with 2D elements can limit the ability of the algorithm to reorient fiber planes to take advantage of fiber material properties and best support load transfer [55]. As explained in the introduction to this chapter, composite fibers offer the greatest mechanical properties when loading is applied in-plane with fiber direction. 2D elements are only capable of simulating fibers in the two-dimensions in which the plies are modeled. Therefore, if the design space (ply area), is initially defined in a manner where fibers are out of plane with load application, the algorithm will be incapable of orienting plies in an optimal orientation.

For structures that have been specifically designed for composites, the limitation of ply topology optimization to alter the plane in which fibers are oriented may not be an issue. Black metal structures, however, are not designed with the intent of orienting fibers in-plane with load application. As a result, when ply optimization is applied to a black metal design, the process may be incapable of fully optimizing the structure [22].

The limitations of ply topology optimization, and the issues that can occur when applied to a black metal design are evident in a study published by Chen et al. [40]. In that study, a black metal hat section designed to support batteries on an electric vehicle was modeled with composites and optimized using the common ply topology optimization methodology explained in Section 2.1.2. Figure 11 shows the hat structural shape, meshed with 2D elements and the loading direction. From this figure it can be seen that the battery load is being applied vertically in the “Z” direction. Figure 12, however, shows the ply orientations and shapes following optimization. In reviewing these two figures, it can be noted that at the location in which load is applied the fibers are oriented out of plane, running in the X and Y axes. While the vertical walls of the structure are oriented in the Z direction, this was not through design or optimization, but rather a circumstance of the original black metal geometry. The optimization was successful in reducing the mass of the hat section by over 34%. The final design, however required an isotropic metal ply (shown in Figure 12) to be inserted in the laminate to support the out of plane load in the trough section of the hat shape. Despite the improvements over a metallic structure, the results of the optimization indicate that further improvements may be possible if shape modifications outside of material allocation to the 2D ply axes were considered.

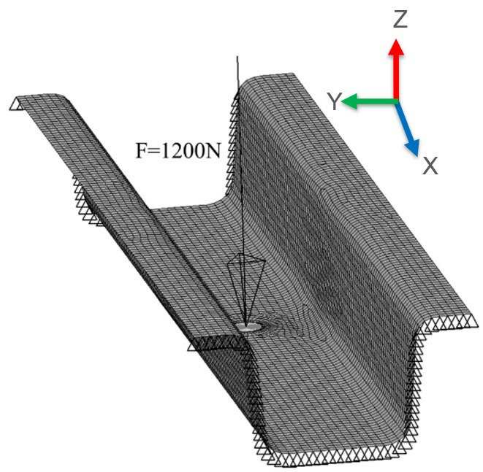

Figure 11 Black metal hat section, loading direction and coordinate system [40]

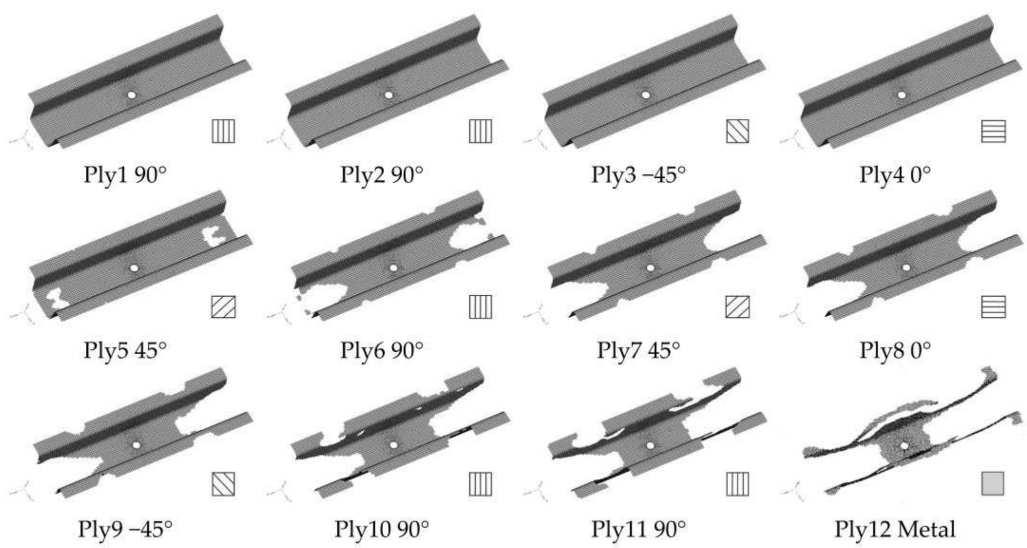

Figure 12 Fiber orientations and ply topology following optimization [40]

The other major limitation of ply topology optimization is due to the type of optimization algorithm typically used to complete the optimization. There are two primary optimization algorithms used to conduct topology optimization: *gradient based* and *gradient free*. Gradient based algorithms are the most commonly applied in research and are included in most FEA software packages because they arrive at solutions faster than the gradient free algorithms [56]. The reason gradient-based algorithms have faster processing times than gradient free algorithms is because the algorithm only considers a single solution, rather than comparing multiple options. While this reduces processing time, it does introduce the possibility that there are alternative solutions that could result in improved results.

Gradient based algorithms work through iterative derivation of the objective function [57]. The derivation process is governed by three processes: direction, step sizes and convergence checks. The direction is set by the user through the developed objective function. As previously stated, objective functions are typically formulated to minimize mass, meaning that the direction is in the negative gradient direction. During each iteration, the derivative of the objective function results in a step that provides steepest gradient, or slope moving the design towards a reduced mass by eroding the ply geometries. The degree to which plies are eroded during each iteration, and the number of iterations it takes to reach a solution is governed by a step size. FEA solvers typically adjust step size throughout the iterations, starting with greater reductions in geometry initially, and moving to smaller refinements as the process progresses. This is done so that the algorithm does not reduce ply geometries too far and violate the established constraints such as stiffness or failure criterion. The final process in the gradient-based approach is a convergence check, which assess results after each iteration to determine if a minimal mass solution has been identified that meets all constraints.

The concept of gradient based algorithms is visualized in Figure 13 [58]. In the Figure, the red dots represent possible initial starting ply geometries. The blue arrows represent the iterative process, and demonstrate the concepts of direction, step size and convergence checks. The direction of geometry change is negative as the derivative of the objective function is taken to identify a downward slope. This negative progression results in ply erosion to reduce mass. The step sizes start with large changes in ply geometry and become smaller as the convergence check identifies that the algorithm is approaching a minimal solution. The light blue dots represent optimization solutions.

Figure 13 also demonstrates the inherent issues with gradient based optimization. As can be seen in the figure there are multiple solutions possible for a given design. There are typically multiple *local minima*, shown in light blue in the figure. These local minima do achieve mass savings through ply erosion but are not the optimal design configuration for the structure. Instead, a *global minima* exists that achieves a greater degree of mass savings. The primary issue with gradient descent algorithms is that they have a tendency to arrive at local, rather than global minima. This is because the process only considers one final configuration and erosion progression.

Figure 13 also shows that there are multiple starting points for an optimization problem, shown as red dots in the figure. These dots represent alternative starting ply geometries to be optimized. As shown in the figure, a different starting ply geometry may result in different local minima, or even the global minima. If the user does not use a manual trial and error approach to test multiple alternatives, it is possible that a local, rather than a global minimum, will be reached. The user also has no way of knowing if a global minimum has been reached, as there can be a nearly unlimited number of design solutions for any structure.

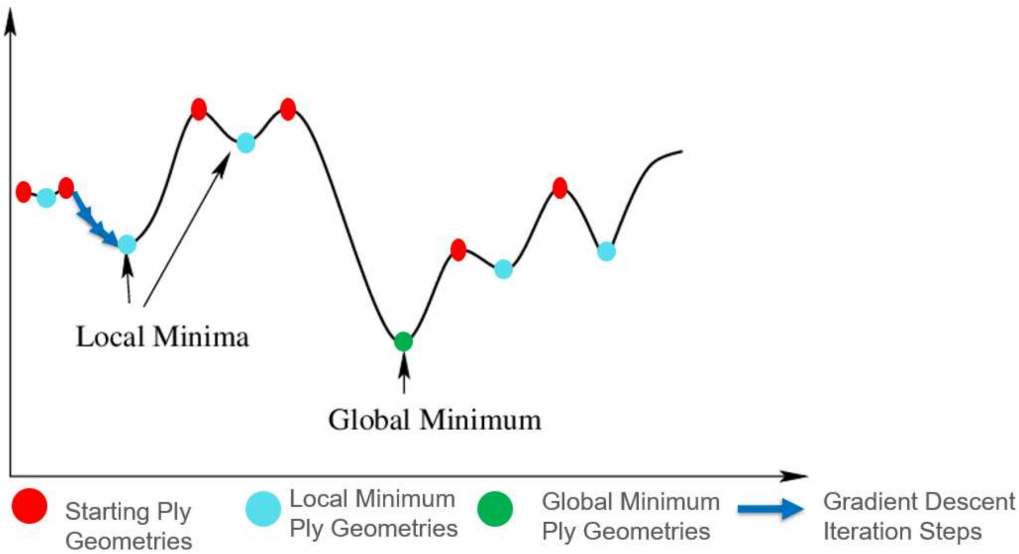

Figure 13 Local and global maximum and minimums [58]

Other gradient-free algorithm types do not optimize through derivation, but instead use search functions to identify optimal solutions. Gradient-free algorithm types include evolutionary, genetic, geometry projection, level-set, and phase field [7]. Unlike gradient based algorithms, gradient-free algorithms consider multiple design solutions to identify the global minima. Processing times for these algorithms is far longer than gradient based, however, as numerous solutions must be considered. As a result, commercially available FEA software does not include these algorithm types and they have been applied with less frequency in research. Custom gradient-free software has recently been developed in research but has only been developed to the point of assessing very simple composite structures at this point [59]. Furthermore, the code is not commercially available, limiting the progression of research in this area.

Instead of investing effort in developing custom gradient-free programs, research has more commonly explored modifying starting ply geometries to obtain improved results with the commercially available gradient-based software [12]. This research has shown partitioning the overall structure into smaller initial ply regions can guide gradient based algorithms towards greater mass reductions. The research has also shown that the geometry of the partitions should be developed based on composite specific design principles to achieve optimal results.

When conducting research on black metal structures, however, researchers have not used composite specific design principles to partition structures. Instead, black metal structures are typically partitioned to mimic the geometry of individual pieces of metal in the original steel design. Take, for example, a study conducted by Wu et al. to perform Ply optimization on an automotive door. [60]. In the study, an existing steel car door geometry was imported into an FEA program, meshed in two-dimensional elements, and an optimization process was conducted with the objective of minimizing mass while providing comparable stiffness to the existing steel design. Prior to optimization, the overall structural geometry was partitioned into 32 regions to create the initial ply geometries, as is illustrated in Figure 14. These partitions were based on the way in which the original mertal door had to be partitioned for manufacturing with steel. No consideration was provided in the research for whether the partitioned areas were ideal for composite manufacturing.

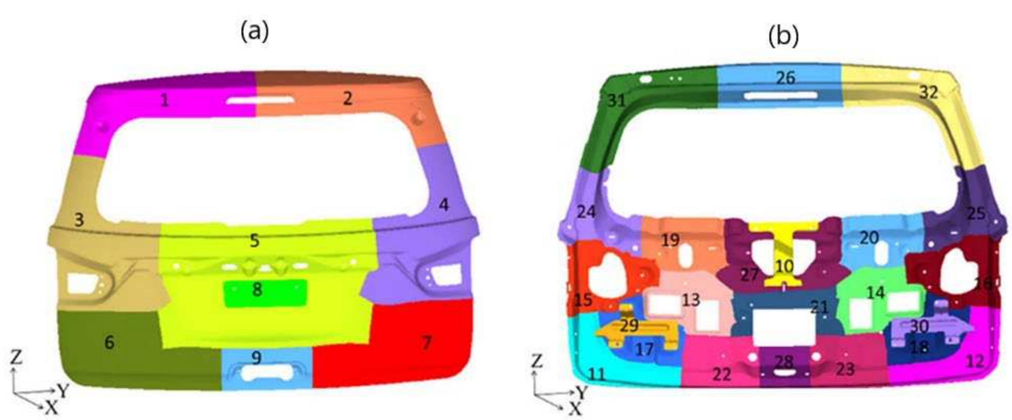

Figure 14 Example of laminate partitioning during the ply optimization of a black metal car door (door exterior panel (a), interior panel (b)) [60]

Like much of the literature reviewed, the researchers were able to achieve a 59% reduction in mass compared to a steel design and meet the stiffness requirement following ply topology optimization. The study did not, however, consider alternative initial ply geometries to determine if even greater mass savings were possible. Furthermore, while some level of partitioning was likely necessary, the high degree of segmentation used in this study likely may have actually limited the mass savings achievable. The level of partitioning used does not take full advantage of composites' ability to reduce the number of structural components. Furthermore, due to the segmentation, the final laminates were composed of hundreds of complex ply shapes, likely making the design too expensive to manufacture.

The ply area partitioning of the overall door structure also introduced another common researcher error noted in the literature reviewed: simplification of ply overlap and joint modeling [61]. To actually manufacture the comoposite door, ply regions would either need to overlap to create connections, or adhesive joints would be needed. The study did not include these details, but instead assumed that the paritioned areas were connected with material that had matching material properties to the plies. The actual geometry and mass of the connecting ply areas, however, was not modeled. This means that the final design developed in this study would not be manufactuable, and that the weight savings achieved are likely unrealistic.

The final simplification noted in the literature reviewed has to do with validation of the results. Despite major mass reductions reported, there has been no method to determine if the projected improvements are actually achievable. Furthermore, no consideration has been made for whether the mass savings achieved would be considered cost effective to execute due to the complex final designs developed during these studies [62]–[67]. Most research has not included physical prototyping, simulation or testing of the developed designs [38], [68]–[71]. Consequently, the results published may be overly optimistic.

CHAPTER 3: PRELIMINARY EXPERIMENT

As discussed in the previous chapter, many industries replace existing geometries designed for metallic manufacturing with composite laminates leading to suboptimal designs. Researchers have attempted to improve these designs by conducting ply optimization to tailor ply topology to suit the required function of the structure. While these studies have demonstrated promise in the application of composites, the methodology used may not be capable of developing finalized designs due to a lack of geometric flexibility of ply optimization simulations, and simplified assumptions. Furthermore, most research has used simple structural geometries that are lightly loaded such as wall and floor panels, and therefore the results may not be transferrable to more complex, heavily loaded structures. As a result, many of these studies predict major benefits that may not be achievable. To assess the current methodology being applied in the literature, a preliminary experiment was conducted [15].

3.1 Preliminary Methodology

The methodology for this experiment was based on the general practices noted in the literature reviewed. The major difference between the preliminary experiment and the examples reviewed in literature is the structure which the methodology is applied to. As previously noted, black metal design and optimization methodology has primarily been applied to simple structural geometries that are lightly loaded. In this preliminary experiment, however, the established methodology is applied to heavily loaded structure with a complex geometry. This was done to assess black metal design and optimization methodologies with respect to other structural types and to gather information and requirements to develop improved methodology. Figure 15 (a) summarizes the current types of structures optimized in published research and compares it to the complex structure used in this experiment Figure 15 (b).

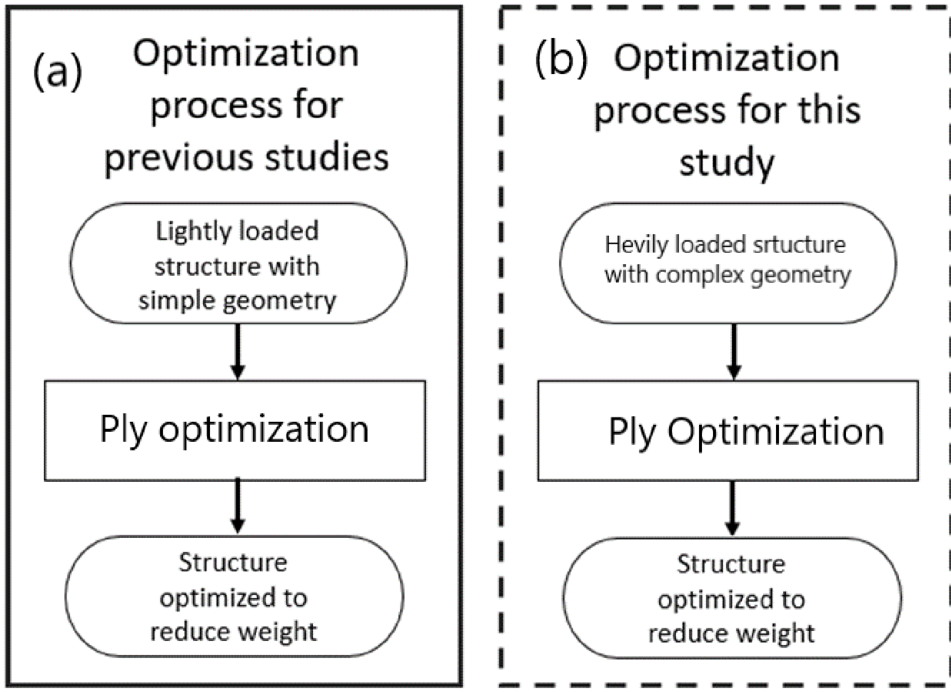

Figure 15 (a) Common subject matter and optimization methodology used in the literature reviewed [50], *and (b)the subject matter and methodology applied in the preliminary experiment* [15].

3.2 Steel Model Geometry and Requirements

A common rail vehicle structure was selected to test the applicability established black metal design and optimization methodology on a complex geometry that is heavily loaded. During rail vehicle operation, significant forces are applied to the bogie structure during propulsion and braking. To distribute these forces, common rail vehicle designs transmit them out of the bogie frame via a traction rod, through an anchor bracket and into car body side sill. From experience, anchor brackets are only designed to support longitudinal forces, and are not designed around lateral or vertical loads. The European rail vehicle design standard, EN13749, provides equation 2 for determining the specific longitudinal loading values for structures such as anchor brackets [72]:

$$F_{XC} = m_1 \cdot a_{xc} \tag{2}$$

Where F_{xc} is the longitudinal force, m_1 is the mass of the vehicle, excluding the bogies, and a_{xc} is the longitudinal acceleration of the vehicle. A typical rail vehicle, excluding the bogies, has a mass (m_1) of 44,000 kg [73]. The European standard states that longitudinal acceleration, a_{xc}, is equal to the deceleration rate during emergency braking, which is typically 1.40 m/s^2 [74]. Inserting these mass and acceleration values into equation 2 results in a F_{xc} value of 61 kN. There are four anchor brackets that must support this load, so the 61 kN is divided over those structures for an individual bracket load of approximately 15 kN. A safety factor of 2.0 was applied to the calculated load in this study to ensure an appropriately conservative design was developed, resulting in a design load for each bracket of 30 kN.

While other loading conditions could be considered, the load developed for this study is consistent with the industry standard and represents the most conservative condition the structure would experience during service. EN13749 identifies emergency braking deceleration as the event that will result in the highest loading condition and states that it is more extreme than vehicle acceleration or other typical service loads. Designing a structure against other loads associated with other service conditions would result in a structure that is not suitable for the most extreme service condition that is being used in this study.

In the literature reviewed, black metal design and optimization was mostly applied to simple structural geometries such as flat panels that experience relatively light loading of roughly 1 kN or less [35]. Figure 16 illustrates that the anchor bracket is a complex, heavily loaded structural component, very different from the structures which have formed the basis for past research.

Figure 16 Example anchor bracket arrangement on a rail vehicle

The anchor bracket structure, of Figure 16, from a rail vehicle, was modeled in Altair HyperWorks finite element analysis (FEA) software. First the existing steel anchor bracket was modeled to develop a baseline mechanical performance metric for the study. In the existing design the main body of the bracket structure is a hollow welded fabrication, manufactured from 6.35 mm thick ASTM A36 steel, with a mass of 25.46 kg. The main body of the bracket has weld shelves to accommodate fillet weld connections between the pieces of steel. The main structure was modeled using 2D shell elements. A solid 80 mm thick ASTM A36 steel machined block at the base of the anchor bracket accepts forces from the traction rod through two bolts. This machined block was modeled using 3D hexahedral elements. The connection between the 2D elements and the 3D elements in the steel anchor bracket were modeled using multi-point constraint equations to simulate a weld and were constrained against three degrees of freedom, but rotational degrees of freedom were unconstrained. The modeling of the 2D and 3D element connection is common practice used in the simulation of welded joints [75]. The total anchor bracket structure is 506 mm tall and 335 mm wide. With the cast block and other attached components, the total structure and has a mass of 48.36 kg. The anchor bracket is affixed to the side sill structure with six mounting bolts. Figure 17 depicts how the model was constrained at the top bolting plate of the structure to represent the fixity associated with the mounting arrangement on the vehicle's side sill.

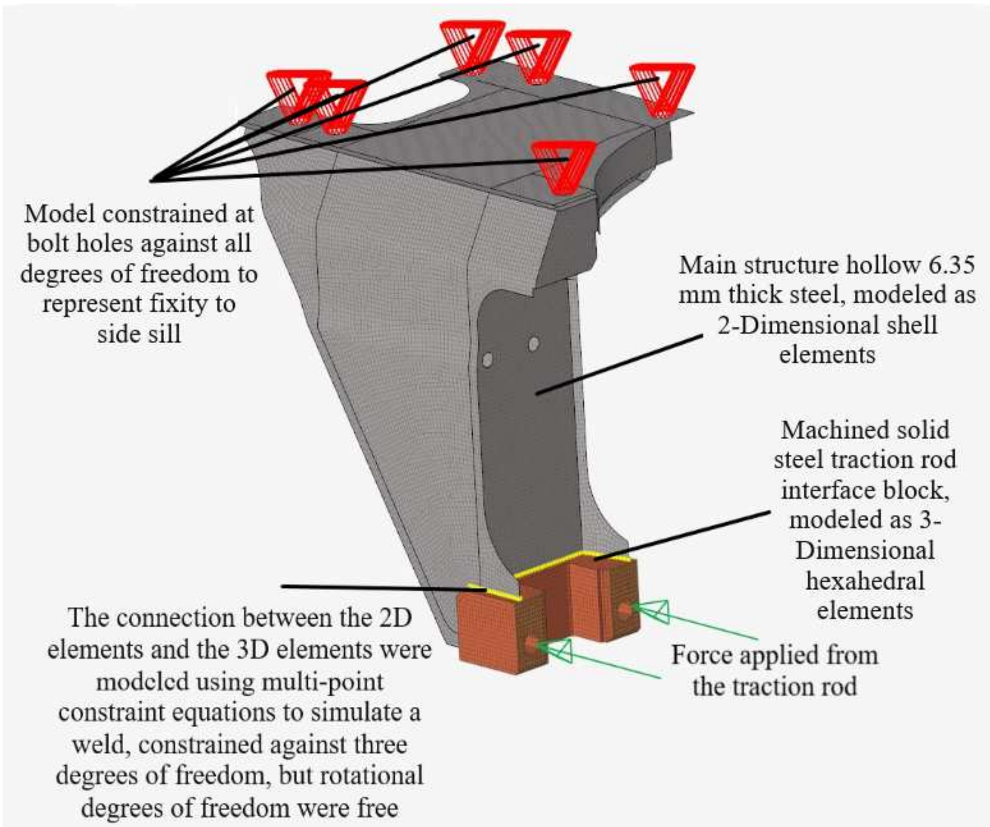

Figure 17 Steel anchor bracket model geometry, boundary condition, and force application

Table 1 provides details for the steel structure that was modeled:

Table 1 Steel anchor bracket model details

FEA Mesh Details	
Model Detail	Value
Elements	104,857
Anchor bracket main structure element type	2-Dimensional shell
Anchor bracket machined traction rod interface block element type	3-Dimensional hexahedral
Steel Structure Dimensions and Mass Details	
Model Detail	Value
Anchor bracket main structure thickness	6.35 mm

Anchor bracket machined traction rod interface block thickness	80 mm
Model height	506 mm
Maximum model width	335 mm
Main Structural Mass (hollow section)	25.46 kg
Total Structural Mass (including cast block and other attached components)	48.36 kg
ASTM A36 Steel Material Properties	
Model Detail	Value
Youngs Modulus, E [76]	204.08 GPa
Shear Modulus, G [76]	8000 MPa
Poisson's Ratio, ν [76]	0.30
Mass Density, ρ [76]	0.0078 g/mm3
Applied Force	30.00 kN

The functional requirement of the anchor bracket is to transmit forces between the traction rod and the side sill, suggesting that a reduction in structural flexibility improves the efficiency of this force transfer. Therefore, the flexibility of the existing steel structure was modeled for use as a benchmark parameter for the proposed composite design. This is a common benchmark that has been used in other black metal design and optimization studies [45]. Compliance, C, is the flexibility of a structure and is the inverse of stiffness (k) and is given by Equation 3 [53]:

$$C = \frac{1}{k} \tag{3}$$

Stiffness (k) is the amount in which a structure resists elastic deflection when force is applied, and is given by Equation 4:

$$k = \frac{F}{\delta} \tag{4}$$

Where F is the force applied and δ is the resulting displacement in the structure. The FEA model was used to calculate an overall structural compliance of 3.82E-09 mm/N for the steel design. This compliance value will be used as a constraint during the composite optimization process.

3.3 Black Metal Materials

The same steel geometry was next modeled replacing the steel material with composites. Consistent with the materials used in the literature reviewed, the composite type modeled in this preliminary experiment were carbon fiber plies reinforced with epoxy polymer matrix, referred to as Fiber Reinforced Polymers (FRP). This research modeled all FRPs as preimpregnated plies, referred to as prepregs, which were the most commonly applied in the literature reviewed [77]. As the name implies, prepreg plies are sold with the epoxy resin already impregnated into the fiber material. This is advantageous as it eliminates a manufacturing step, but also typically ensures higher and more consistent mechanical performance from each ply.

As explained in Chapter 2, FRPs are different from the metallic materials currently used to construct anchor brackets due to their anisotropic behavior. Anisotropic materials have varying properties depending on the direction that load is applied. FRP's can, however, be manufactured or constructed to provide more consistent performance in various direction by the use of fabrics which weave fibers at various angles or by assembling "laminates" which stack multiple unidirectional plies in varying directions, thus enabling tailoring of material properties within the plane. Laminates with unidirectional plies are structurally more efficient, were more commonly used in the literature reviewed, and were therefore selected as the FRP construction to simulate in this study.

To accurately model and optimize the anisotropic properties of composite materials FEA software was again used. Hexcel 8852 AS4 carbon fiber was selected as a representative unidirectional epoxy FRP prepreg material. Common practice observed in the literature reviewed was to use material properties from lab-based test reports. Therefore, properties relevant to this study, for the composite material, was obtained from National Center for Advanced Material Performance (NCAMP) testing reports and the relevant data are provided in Table 2. The anisotropic properties of the composites are evident in Table 2 through the varying moduli and strength values in different directions.

Table 2 Composite material properties

Material Property	Hexcel 8852 AS4 Carbon [78]
Modulus of Elasticity in Longitudinal Direction, E1	131,620.92 MPa
Modulus of Elasticity in Lateral Direction, E2	9,2388.98 MPa
Poisson's Ratio, ν	0.36
In-plane shear modulus, G12	4,826.33 MPa
Mass Density, ρ	0.0016 g/mm3
Longitudinal tensile strength parallel to the fiber angle, Xt	2558.51 MPa
Compressive strength parallel to the fiber angle, Xc	1731.48 MPa
Transverse tensile strength normal to the fiber angle, Yt	64.05 MPa
Compressive strength normal to the fiber angle, Yc	285.72 MPa
Shear strength, S	91.56 MPa
Manufacturable ply thickness (*T*)	0.19 mm

3.4 Black Metal Geometry, Partitioning and Connections

A practice noted in the literature reviewed, was that for larger more complex structures designers often leave portions of black metal structures modeled from metallic materials [79]. This is done to reduce complexity, and because it is understood that certain metallic structures are not suitable for composite manufacture. This practice was included in the preliminary experiment. Figure 18 shows that for the preliminary study the solid machined block which interfaces with the traction rods remained modeled as steel, as this geometry would be difficult to manufacture from composites without a comprehensive redesign of the complete anchor bracket. The connection between the steel machined block and the composite structure was modeled as a multi-point constraint equation that allows for six degrees of freedom to simulate an adhesive joint. The modeling of the connection is consistent with the approach used in the literature reviewed [79].

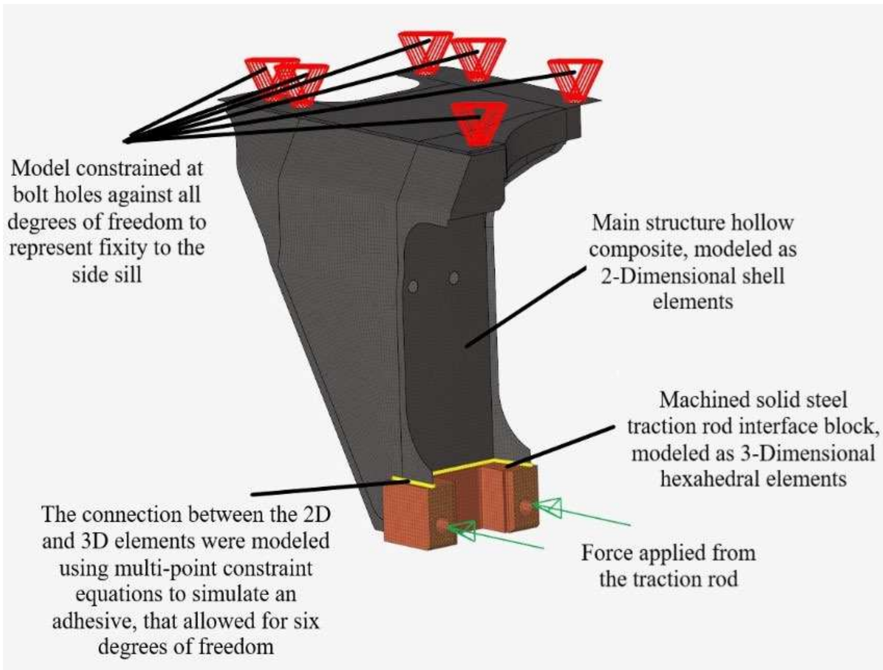

Figure 18 Black metal composite anchor bracket model geometry, boundary condition, and force application

As explained in the previous chapter (subsection 2.1.3), the composite sections of black metal geometries are typically partitioned based on steel manufacturing and material constraints [60]. Typically, when replicating a metallic design with composites, sections of the structure that were manufactured from a single piece of metal becomes the geometry of a composite laminate in a black metal design. This is one of the many deficiencies of black metal structures, as they do not exploit the benefits of composites to reduce structural components or to mold the material into complex structural shape. To mimic the method of structural partitioning noted in literature, the anchor bracket was next divided into laminate regions based on the metallic design. Figure 19 depicts this partitioning, and how the geometries of the 8 steel plates making up the hollow main body of the anchor bracket were used as shapes to model 8 composite laminates.

As also explained in the previous chapter, common practice in black metal design and optimization studies is to simplify the modelling of connections between these partitioned ply and laminate regions [61]. Common practice is to assume that the partitioned sections are connected with material that has matching properties to the surrounding plies or laminates. The actual ply and laminate geometries of the connecting material, and accurate structural performance are not, however, typically modeled. To mimic this practice noted in literature, individual laminates in the anchor bracket model were assumed to be joined with material that had matching properties to the composites for this preliminary experiment, but accurate modeling of connecting material was excluded. Figure 19 shows that there were no connecting plies between the 8 laminate regions of the anchor bracket. This is another deficiency of black metal designs, as they may overpredict mass reductions and structural performance due to simplified modeling of the composite structure.

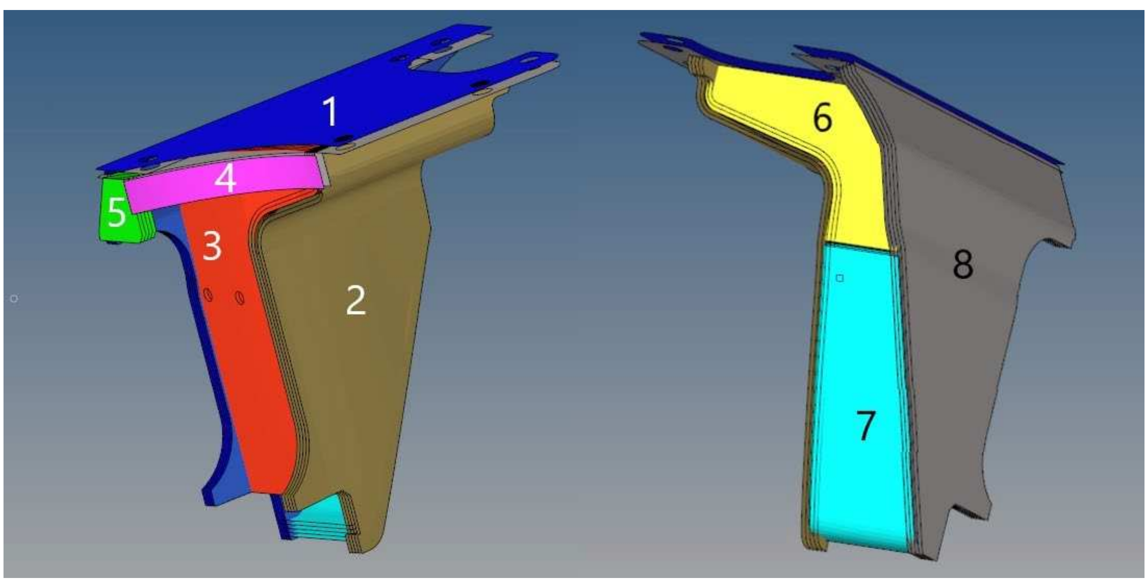

Figure 19 Anchor bracket geometry divided into eight manufacturable composite laminates

3.5 Black Metal Ply Optimization

With the preliminary black metal model developed and requirements established, the next step in the preliminary experiment was to optimize the design. Optimization of composites is complicated due to the materials' anisotropic nature. With advances in analysis tools and added experience related to fiber reinforced composites, structural designers have developed optimization techniques to alter design geometries to better utilize these anisotropic materials [9], [42], [43], [60], [80]–[84]. As discussed in Chapter 2 (subsection 2.1.2), these optimization techniques, both globally and locally, are used to alter the number of plies, ply thickness, and ply shape to reduce the weight of the design.

The optimization process is consistent with composite material forms and manufacturing techniques common to the aerospace industry, where the standard material utilized is in the form of prepregs (like the ones modeled in this experiment) which can be easily cut into unique geometries and be layered in a mold as part of the manufacturing process. This approach enables the development of structures that provide increased thickness and strength in areas of high stress while reducing thickness in low stress areas to reduce mass. Cutting the plies into smaller geometries can reduce the efficiency of load transfer due to fiber discontinuity, but the optimization process can balance those negative effects against the benefit of reduced mass and still meet the structural requirements.

The optimization process is governed by optimization algorithms which are included in many commercially available FEA programs such as Altair HyperWorks. As previously explained in Chapter 2 (subsection 2.1.2), optimization algorithms typically have an objective function and constraints which govern the structural modifications. These objectives and constraints can be custom coded by designers to achieve a range of unique optimization results for a structure. Based on relevant literature, it was identified that the most common objective of optimization research was to minimize the mass of a structure [66].

As previously discussed, findings from the same review of the literature, suggested that optimization is typically constrained by criteria such as compliance, failure criterion, ply thickness and stacking sequence [45]. In the previous subsection (3.2), the compliance constraint for the structure was defined. The simulated compliance of the steel structure (3.82 E-09 N/mm) was used as a constraint for the black metal optimization.

Failure is the next common constraint applied in optimization studies. Because of the anisotropic nature of the material, analyzing failure in composite structures is different from the process used to assess the metallic structures that are common in the rail vehicle industry [85]. There are several failure theories that are used within the composites industry, including: Maximum Strain, Maximum Stress, Tsai-Hill, and Tsai-Wu [86]. Each theory has been developed, and validated, to predict different types of composite failures. The Maximum Stress failure criteria is one of the most applied in the literature reviewed, and thus was selected as the failure theory to be applied as a requirement to the black metal model [87]. Maximum Stress theory simultaneously predicts failures in both the fiber and matrix of a composite laminate structure. The Maximum Stress failure criterion is given by Equation 5:

$$F = -X_c < \sigma_1 < X_t ; \; -Y_c < \sigma_2 < Y_t ; \; |\tau_{12}| < S \tag{5}$$

Where *Xc, Xt, Yc, Yt*, and S are the longitudinal tensile strength parallel to the fiber angle, compressive strength parallel to the fiber angle, transverse tensile strength normal to the fiber angle, and compressive strength normal to the fiber angle, and the in-plane shear strength of each material respectively. These values were obtained from the NCAMP testing report and are listed in Table 2 [78]. The other values (σ_1, σ_2 and τ_{12}) are the stress state expressed in the three principal axes of the material and are calculated by the FEA solver. The FEA software calculates Maximum Stress failure criterion for each element in the model. Any element with a failure criterion value exceeding one is predicted to be a location on the structure where a failure will occur.

Ply thickness is also commonly considered in black metal optimization studies [78]. This is because prepreg materials are only commercially available in certain thicknesses. Therefore, the final design must include plies with thickness that matches that which is available. For this preliminary experiment, the manufacturable ply thickness constraint was (T) was set to match that listed in the NCAMP report (0.19 mm) and is shown in Table 2.

Ply stacking sequence is the final constraint commonly applied to composite structures. Stacking consecutive plies of matching fiber orientation can create interlaminar forces such as sheer that over the service life of a structure can lead to failure [88]. Common composite design standards require that no more than two plies of any fiber orientation be stacked consecutively in a laminate to avoid these issues [89]. Therefore, this common design constraint was used for this preliminary experiment.

With the optimization objective and constraints formulated an optimization algorithm could be developed. The general optimization algorithm (equation 1) provided in Chapter 2, was custom programmed based on the objective and constraints established for this preliminary experiment, and are summarized by Equation 6:

$$\text{minimize } f(x) \tag{6}$$

subject to

$C \leq 3.820\text{E-09 mm/N}$,
$F \leq 1$,

$T = 0.19$ mm

$P \leq 2$,

Where *f(x)* is the objective function, set to minimize mass. The constraints on the optimization process are compliance (*C*), failure criterion (*F),* minimum laminate thickness *(Lx),* manufacturable ply thickness used during the sizing optimization *(T),* and the maximum number of successive plies of any angle used during shuffling optimization (*P).*

It is important to note that optimization is non-linear, and each solution is unique to the boundary conditions, loading, and constraints applied to the process. Applying different loads or constraining the optimization process in a different way would result in unique ply geometries and thicknesses. Furthermore, altering the boundary condition, or changing the direction that forces are applied would result in the quantity and thickness of plies of each angle to change to efficiently transfer the loads.

With the optimization algorithm formulated, ply details next had to be defined to begin the optimization process. Typical unidirectional plies are stacked in orientations of 0°, -45°, 45° and 90° in composite laminate design. FEA simulates fiber angle within each element in the model to accurately predict structural performance. Common practice in black metal design is to define fiber angle based on FEA model coordinate axes (x, y, z) [27]. Figure 20 provides an example of this common practice applied to the anchor bracket plies in laminate 8. Here the 0° ply direction was aligned with the y axis, as shown in Figure 20 (a). the other ply angles: 45°, -45°, and 90° are then offset angles from the 0-degree direction, as shown in Figure 20 (b), (c), and (d) respectively.

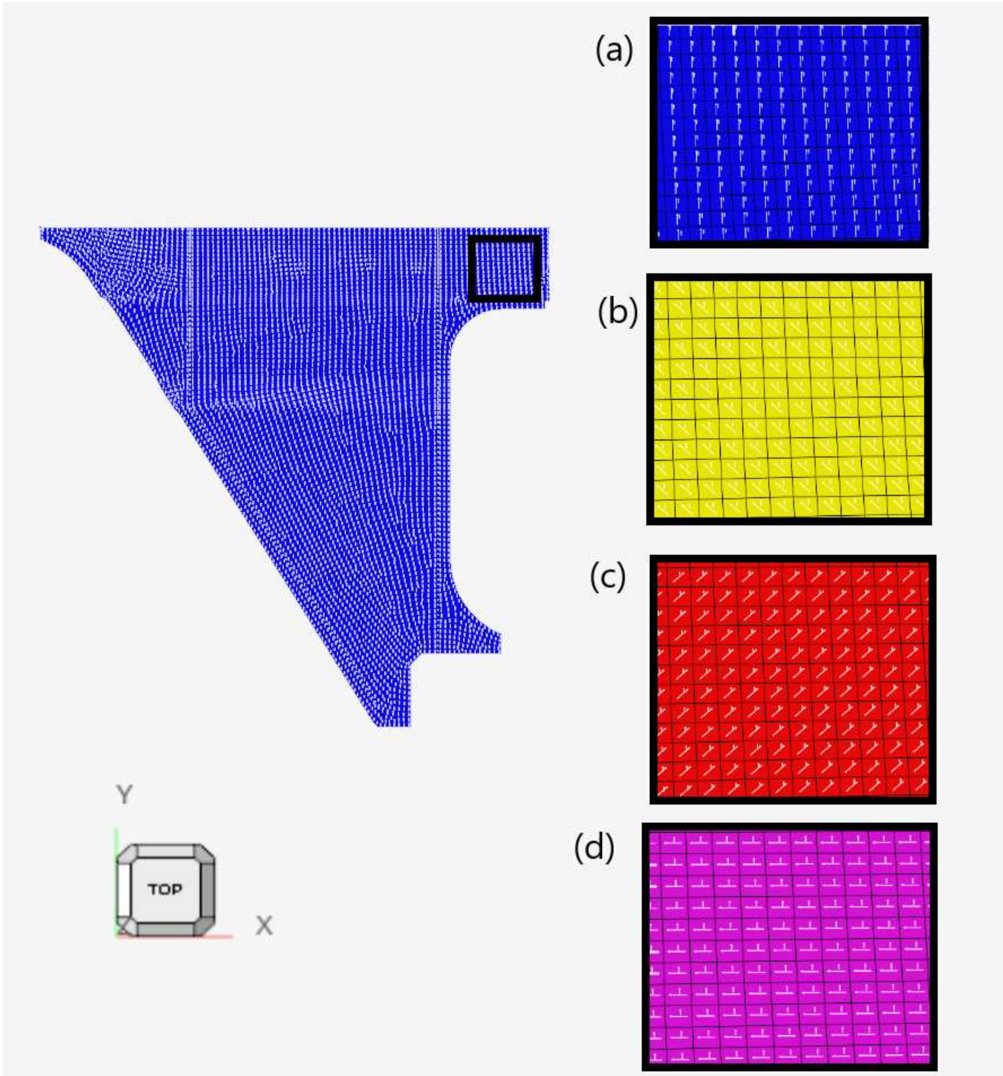

Figure 20 Example of fiber angle definition for laminate 8, showing detailed eliminate orientations for the various ply angles: (a) 0°, (b) 45°, (c) -45°, (d) 90°

Consistent with the practices noted in the literature reviewed, initially anchor bracket design was simulated as a Uniform Thickness Model (UTM) where all plies were modeled with identical thickness and shape within each laminate, as shown in Figure 21 and Figure 22. As a starting point for the simulation and optimization, each laminate was modeled as 8 plies oriented in the following directions: 0°, 45°, -45°, 90°, 90°, -45°, 45°, and 0°, as shown in Figure 21. This type of laminate is referred to as "quasi-isotropic" and was selected as a baseline construction because it provides similar in-plane characteristics to the isotropic materials typically used in rail vehicle structures [90].

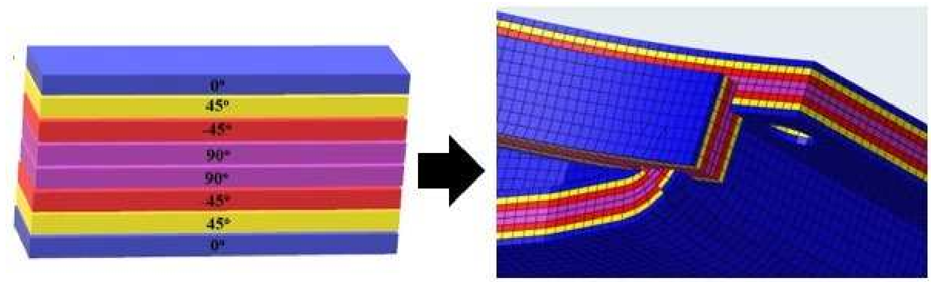

Figure 21 UTM laminate design with 2D element thicknesses visualized to show dimensions in 3D

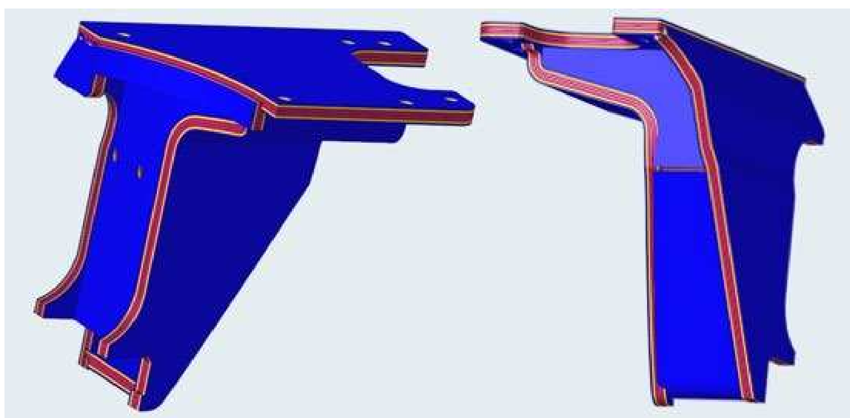

Figure 22 UTM structure with 2D element thicknesses visualized to show dimensions in 3D

As explained in Chapter 2 (subsection 2.1.2), composite optimization processes erode initial ply geometries to reduce mass. Therefore, prior to initiating optimization, structures must at least meet the established compliance and failure requirements referenced previously in this section. If the structure does not at least meet the minimum design requirements, it is not possible to erode ply dimensions, and therefore optimization cannot begin. To meet the minimum design requirements, plies are typically thickened to determine a starting point for the optimization.

For the anchor bracket, the thickness of each laminate was initially set to 6.35 mm, equal to the thickness of the original steel structure, by setting the thickness of each of the 8 plies within each laminate to 0.79 mm. During a preliminary check of the simulation the model failed to meet the compliance and failure requirements when the UTM laminates were 6.35 mm thick. Thus, the thickness of all ply stacks within each laminate in the UTM models were iteratively increased until the model achieved the requirements for compliance and failure. The model met the requirements when the initial laminate thickness was set to 40 mm (~6.30 times thicker than the 25.46 kg steel structure) with a corresponding mass of 39.72 kg.

As previously explained, AS4 carbon fiber prepreg plies are typically manufactured to be 0.19 mm thick, so clearly the resulting 8 plies making up the 40 mm laminate section are unrealistically thick. However, prior to, and during the initial stage of optimization plies represent candidate fiber angle “*stacks*” and are not meant to represent ply thickness realistically. As explained in Chapter 2 (subsection 2.1.2), the composite optimization is an iterative process consisting of three primary processes: free-sizing, sizing and shuffling. The iterative process is illustrated and summarized in Figure 23.

Figure 23 (a) shows the previously explained UTM laminate cross section with 8 ply stacks that are each 5 mm thick. Figure 23 (b) shows the first optimization step, free-sizing, during which the fiber angles of the UTM stacks are treated as candidate ply types for the optimizer to choose from. The optimization process identifies optimal shapes and section thicknesses for each ply type from stacks in the UTM model. Following free-sizing, the model has more ply stacks than the UTM model, the overall laminate thickness has changed, the ply stacks do not have uniform shape or thickness, and the plies are still unrealistically thick. During the second optimization step of sizing, shown in Figure 23 (c), the stacks of each orientation developed during free-sizing are subdivided into actual manufacturable thicknesses. Following sizing, there may be numerous plies of the same fiber orientation stacked consecutively, so the third and final optimization process of shuffling reorganizes the plies within each laminate to ensure that plies of each fiber orientation are disbursed, as shown in Figure 23 (d). This is done to reduce interlaminar forces that can develop when numerous plies of a particular orientation are stacked consecutively.

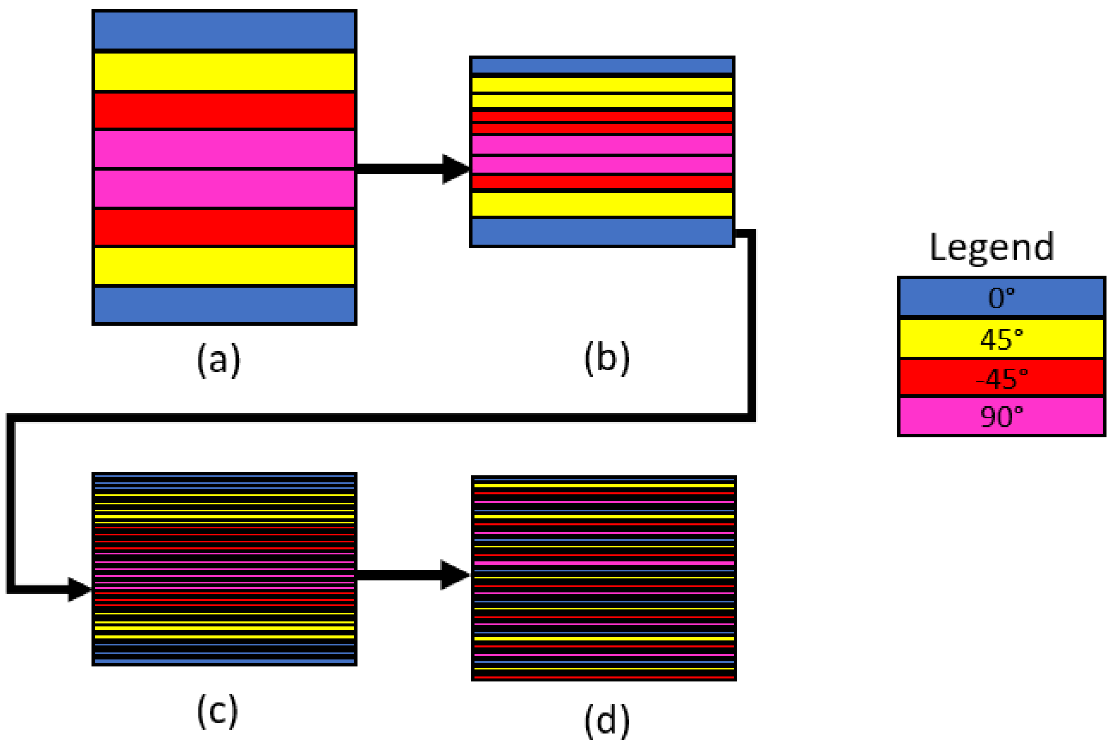

Figure 23 Example laminate and ply thickness throughout modeling and iterative optimization processes: (a) UTM, ***,*** *initial model ply stacks are thickened to meet constraints prior to optimization, (b) free size, ply thickness and geometry are modified to optimal, but unrealistic configurations (c) sizing, unrealistically thick plies are subdivided into multiple plies to meet realistic manufacturable thickness, (d) shuffling, plies are reorganized to so that plies of the same fiber orientation are not stacked consecutively.*

3.5.1 Free-Sizing Optimization Results

As explained in the previous subsection, the objective of the optimization was to reduce mass, while meeting all established constraints. As explained in Chapter 2 (subsection 2.1.3), free sizing optimization is governed by a gradient based approach which reduces the mass of the initial UTM model to identify optimal ply details for the structure. Gradient based algorithms work through iterative derivation of the objective function (equation 6) [57]. The derivation process is governed by three processes: direction, step sizes and convergence checks, and can be visualized in Figure 24. The negative slope in the figure represents the direction for the anchor bracket optimization, as mass was minimized iteratively. The X axis in the figure shows that it took 59 iterations to converge at a solution. During each iteration, the derivative of the objective function results in a step that provides steepest gradient, or slope reducing mass by eroding the ply geometries. The figure also shows the extent to which plies were eroded during each iteration, and the number of iterations it took to reach a solution were governed by a step size. The FEA solver adjusted step size throughout the iterations, starting with large reductions in ply geometry and mass initially. After each iteration a convergence check is completed to ensure that the algorithm did not reduce ply geometries too far and violate the established constraints. The convergence check also informs subsequent step sizes, moving to smaller refinements as the process progresses and the design gets closer to violating the constraints.

Figure 24 also shows that the results of the free-size optimization was a reduction in the mass of the carbon fiber model. The composite structure in UTM model had a mass 39.72 and was the starting point for the optimization. Over the course of the 59 iterations, the mass was reduced to 15.20 kg through ply erosion. At the conclusion of the free size iterations, the developed structure still met all established constraints.

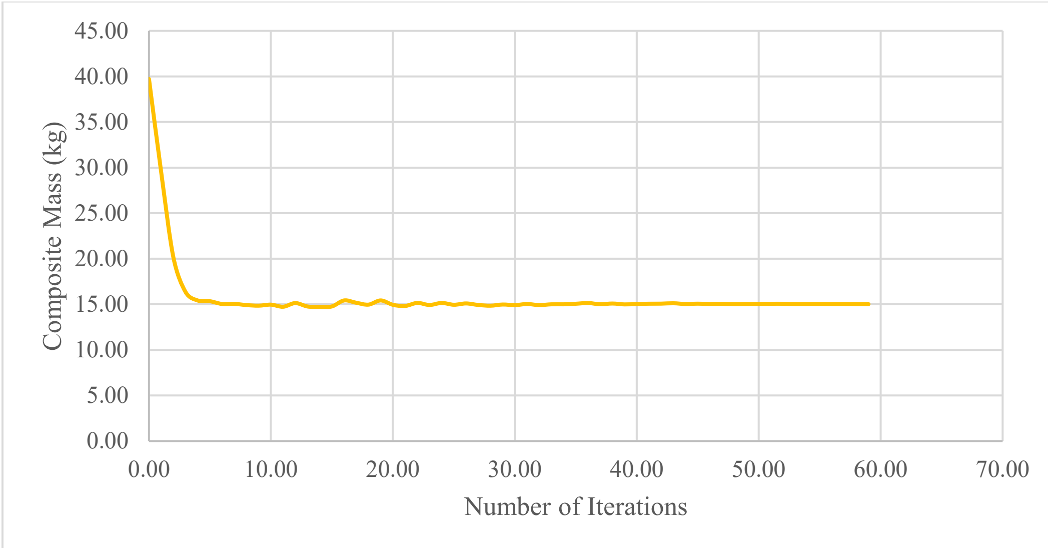

Figure 24 Iterative gradient descent free size results

As explained previously, prior to optimization the plies in the UTM model did not represent actual manufacturable plies, but rather candidate fiber angle and ply geometry stacks. During the free size operation, the initial 5 mm thickness of the ply stacks was modified to the optimal section thickness for each candidate fiber angle. While the section thickness of each stack is uniform following free size, there was variability between stacks in the structure. The geometries were also eroded to the optimal ply topology for each fiber angle stack. This resulted in more plies than were in the original UTM model, as the ply regions were subdivided during erosion.

Figure 25 shows the overall geometry of the black metal structure following the free size optimization operation. During the process the number of stacks was increased from 64 uniform thickness stacks (8 plies in each of the 8 laminates) in the UTM model, to 240 stacks of varying thickness and geometry for the free sized model.

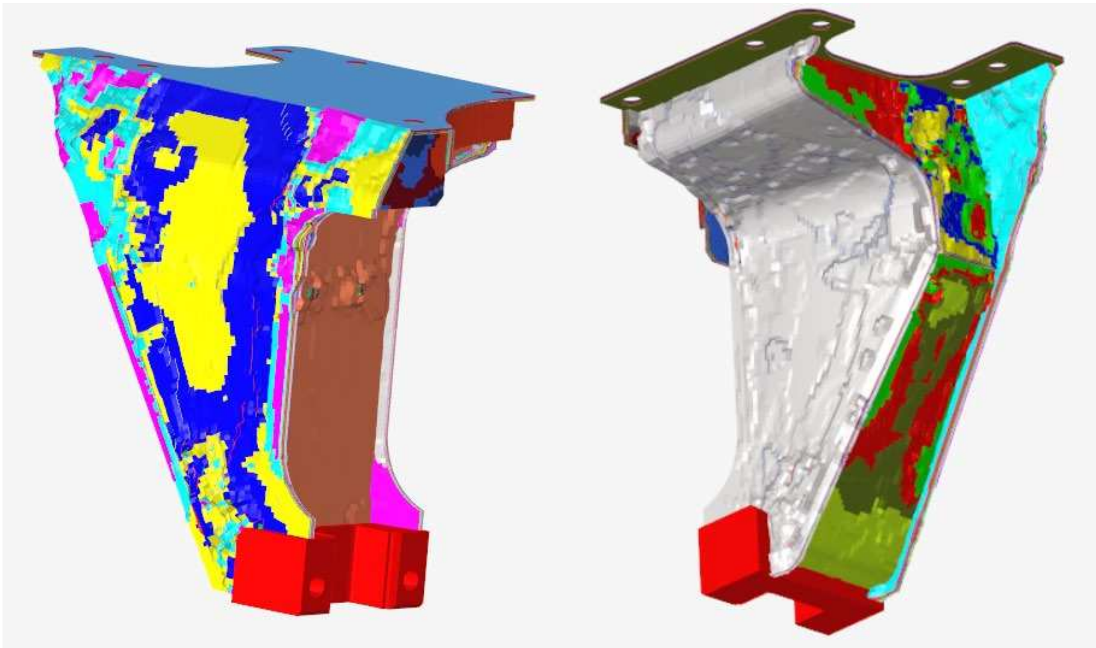

Figure 25 Black metal composite free sizing optimized topology

Prior to optimization, all 8 laminates in the UTM model had uniform thicknesses of 40 mm. Following optimization, however, the resulting laminates had thickness values of roughly 38 mm in the connecting areas where laminates intersect, while most other areas were thinned to values ranging from 6-20 mm. This is logical, as the geometry that the composites were applied to has sharp angles in the connection areas between the laminates that were designed to allow for welding of metallic plates. In the composite model these sharp angles cause stress concentrations and resulting high failure criteria values that the optimization operation satisfies by maintaining thickness in these areas. In a composite-specific geometry, the transitions from surface-to-surface would be much less severe and the overall geometry would take on more biologically inspired contours. Figure 26 shows the thickness of the laminates following the optimization operation.

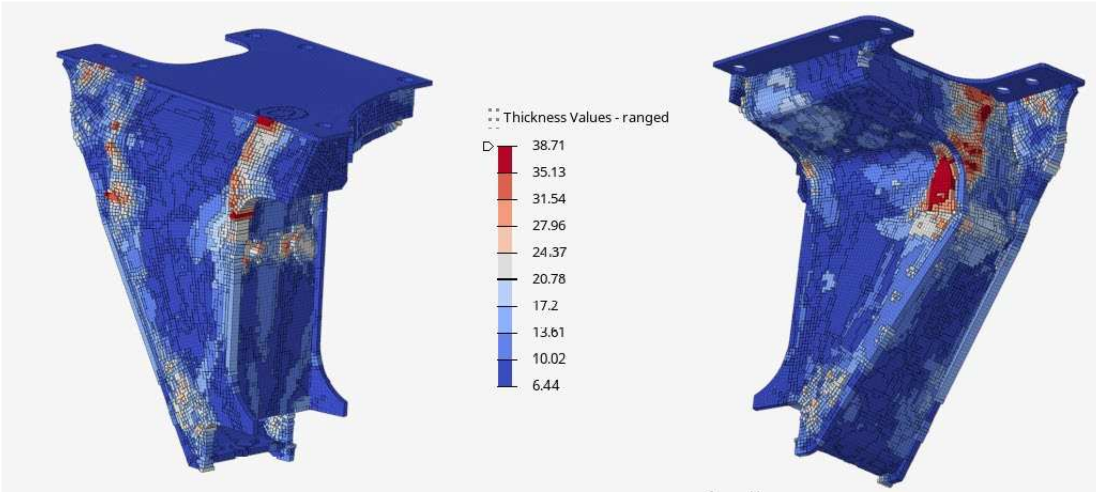

Figure 26 Thickness (mm) contour plot of black metal composite free size optimized topology

As an example of how free sizing optimization altered each ply geometry, Figure 27 shows the modification of a 0° ply within laminate 8 of the carbon fiber structure. The ply topology was altered to remove area without allowing the overall compliance of the structure to fall below the constraint value. The number of plies within the laminate increased from 8 to 30 following free sizing, but overall thickness of the laminate decreased in many areas as each individual ply was thinned.

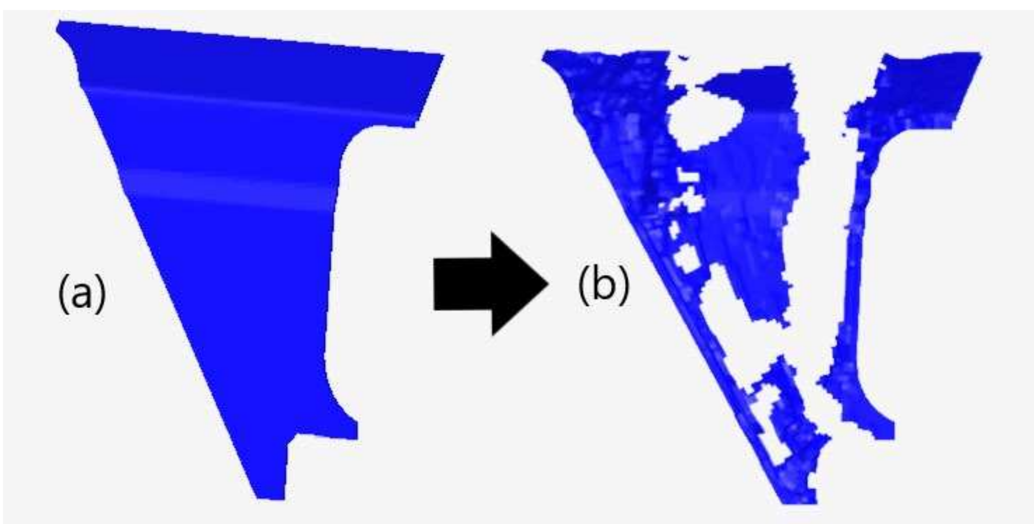

Figure 27 (a) Original carbon UTM fiber ply geometry, and (b) TO results for laminate 8, [0°/90°] plies

3.5.2 Sizing Optimization Results

As discussed previously, the free sizing process allows for composite plies to be modified to any thickness. In this study the free sizing solver allowed for many plies to have thicknesses below 0.05 mm, and plies that were as thick as 3.57 mm. This deficiency led to plies which are either too thick or too thin to be manufactured [17], [35], [91], [92]. Therefore, the next step in the optimization process is conducted to define manufacturing optimization constraints to be applied in the model. This process is referred to as sizing optimization. Here the previously defined ply thickness constraint, *T*, was used so that each ply was required to be divisible by 0.19 mm, the manufactured thickness of a cured ply, as provided in the NCAMP material test.

Application of the sizing process to the free sized model increased the total number of plies in the component from 240 plies of variable thickness to 1063 plies with uniform manufacturable thickness. Following sizing, the number of plies within each laminate varied between 34 plies and 209 plies to make up the 1063 ply total. Figure 28 shows the change in laminate topology following the SO operation. The thicker plies of up to 2 mm were divided into multiple plies that were 0.19 mm, while thinner plies were thickened to meet the manufacturing requirement. Due to the thickening of some thinner plies, and the fact that the laminate thicknesses were not always exactly divisible by the manufacturable ply thickness, the SO model increased in mass by 1.72 kg compared to the free sized model. This brought the total mass of the composite part of the structure to 16.92 kg, which is still a 33% reduction in mass compared to the hollow section of the steel design. This structure continued to meet the compliance and failure criterion constraints that had been previously applied.

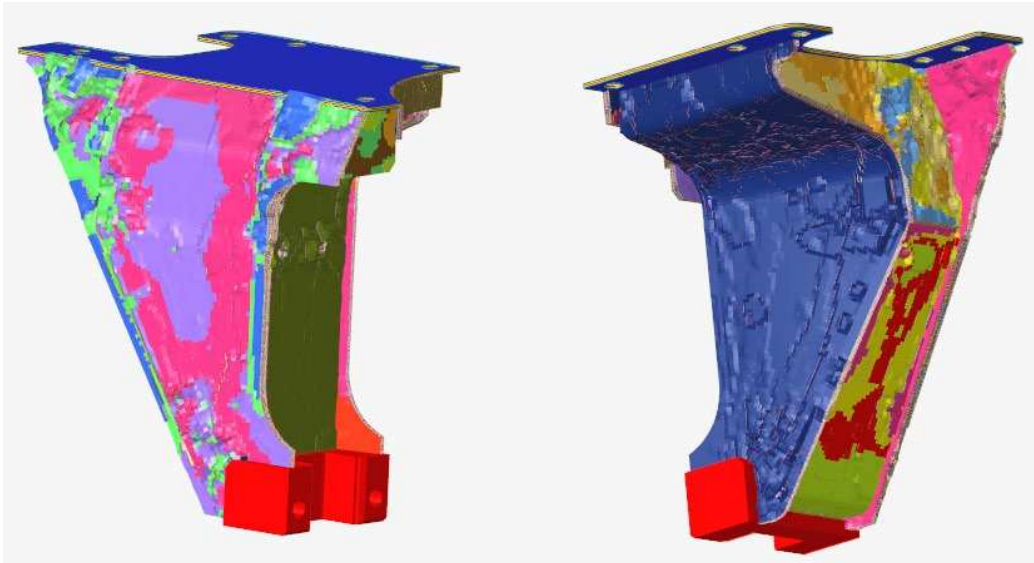

Figure 28 Black metal composite sizing optimized topology

3.5.3 Shuffling Optimization Results

The final process of ply optimization is shuffling optimization. Shuffling optimization is a subroutine within many composite FEA solvers which reorders plies within a laminate to find an optimal solution [93], [94]. The primary purpose of shuffling optimization is to disperse plies of matching fiber orientation to improve laminate performance [95], [96]. Stacking consecutive plies of the same fiber orientation can create interlaminar forces such as sheer that over the service life of a structure can lead to failure [88]. While these interlaminar forces are accounted for in the FEA model, the force considered in this study was a single static load. Repeated cyclic fatigue loading that the structure would likely experience in service could result in failure. As previously stated, common composite design standards require that no more than two plies of any fiber orientation be stacked consecutively in a laminate to avoid these issues, and thus was used as a constraint in the shuffling optimization [89]

The shuffling optimization was successful in reorganizing all 8 laminates while still meeting all constraints. During this process ply geometry and thickness remain the same from the previous process of sizing optimization. Therefore, the overall structural mass of 16.92 kg and the 1063 plies remained the same from the previous step of sizing optimization. Figure 29 shows the overall geometry of the structure following the shuffling optimization process.

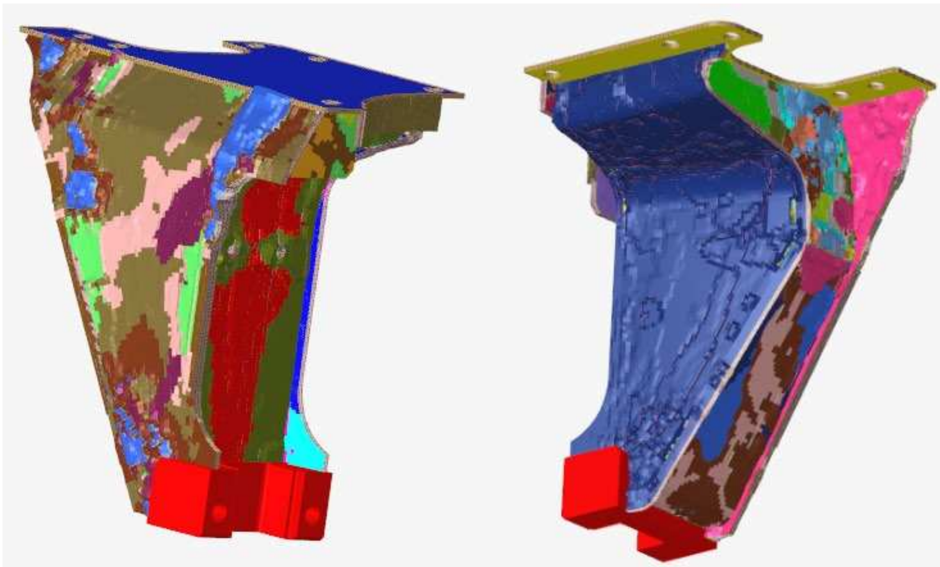

Figure 29 Black metal composite shuffling optimized topology

Table 3 provides an example of shuffling optimization results for Laminate #1 in the anchor bracket structure. Like the previous two optimization processes, the shuffling process is iterative. In the case of Laminate #1 the solver took four iterations to find the optimal laminate configuration and meet the constraint of not stacking two plies of the same orientation. While the solver met the constraint of not stacking more than two plies of the same orientation consecutively after the first iteration, the solver ran further iterations to determine the optimal laminate configuration to support the compliance and failure constraints.

Table 3 Shuffling optimization results for Laminate #1

Iteration 0	Iteration 1	Iteration 2	Iteration 3	Iteration 4
1030	1034	1034	1033	1033
1031	1039	1033	1030	1030
1032	1030	1030	1039	1039
1033	1043	1039	1040	1040
1034	1035	1040	1031	1031
1035	1040	1031	1034	1034
1036	1031	1035	1035	1035
1037	1044	1043	1043	1043
1038	1036	1044	1044	1044
1039	1041	1042	1042	1042
1040	1032	1041	1041	1041
1041	1045	1032	1032	1032
1042	1037	1036	1036	1036
1043	1042	1037	1037	1037
1044	1033	1045	1045	1045
1045	1046	1046	1046	1046
1046	1038	1038	1038	1038
1047	1051	1060	1060	1060
1048	1060	1053	1053	1053
1049	1047	1051	1051	1051
1050	1055	1061	1061	1061
1051	1052	1055	1055	1055
1052	1061	1047	1047	1047
1053	1048	1048	1048	1048
1054	1056	1056	1056	1056
1055	1053	1062	1062	1062
1056	1062	1052	1052	1052
1057	1049	1054	1054	1054
1058	1057	1063	1063	1063
1059	1054	1057	1057	1057
1060	1063	1049	1049	1049
1061	1050	1050	1050	1050
1062	1058	1058	1058	1058
1063	1059	1059	1059	1059

Legend
90.0 degrees
45.0 degrees
0.0 degrees
-45.0 degrees

As previously explained, composite failure is assessed on an element-by-element basis using the Max Strain failure criterion during the optimization processes. The failure criterion values for the structure following the last process of shuffling show maximum composite failure values of less than one predicting that no failure would occur. Figure 30 shows the locations of the maximum failure criterion values for all plies within the black metal structure following shuffling. It can be seen in the figure that the sharp angles between the laminate sections created elevated failure criterion values.

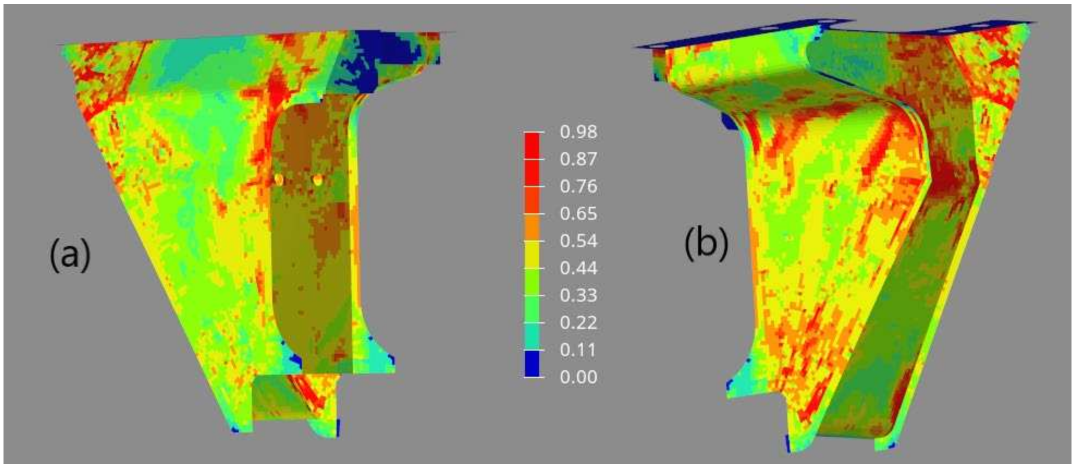

Figure 30 Black metal composite failure criterion results

3.5.4 Optimization Results Summary

Figure 31 provides a visual summary of the FEA models created during the preliminary experiment. Table 4 provides key structural details for the same models. Figure 31 (a) shows the initial steel model that was used to generate the compliance constraint for the optimization, and that was used as a point of comparison for the mass of the black metal composite structure. The main hollow section of the steel bracket was replaced with composite materials to generate the UTM model shown in Figure 31 (b). The composite portion of the UTM model had a mass of 35.31 kg and had 8 laminates each composed of 8 plies (64 plies total). The UTM model was then optimized through free sizing optimization which reduced the mass to 15.20 kg, but increased the total number of plies to 240, as shown in Figure 31 (c). Next the sizing optimization was conducted on the model which increased the mass of the composite section to 16.92 kg and increased the total number of plies to 1063, as shown in Figure 31 (d). Finally, shuffling optimization was conducted which did not increase the mass of the structure or the total number of plies, but reorganized the plies within each laminate to identify the optimal stacking sequence, as shown in Figure 31 (e). The composite section in the final FEA model developed, the shuffling model, provided 33% reduction in mass compared to the hollow main section of the steel structure.

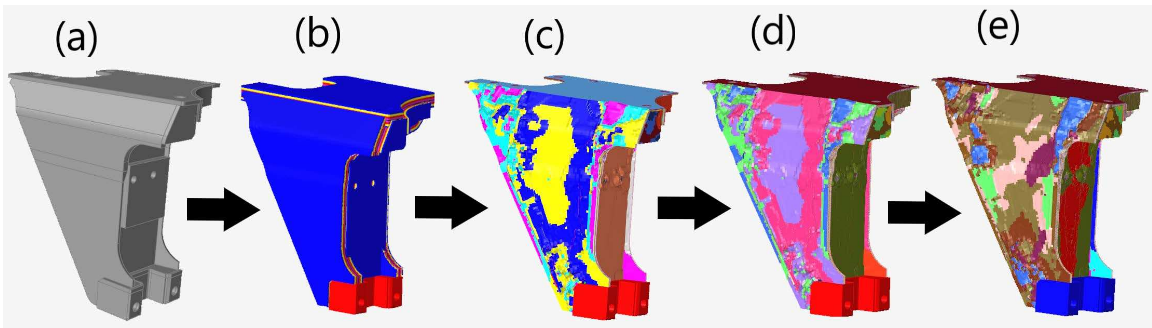

Figure 31 Topologies of the models developed in the preliminary experiment (a) steel structure, (b) uniform thickness model, (c) Free-size model, (d) sizing model, (e) shuffling model

Table 4 Model properties.

Model Property	(a) Steel Structure	(b) Uniform Thickness Model	(c) Free-Size Model	(d) Sizing Model	(e) Shuffling Model
Plies in laminate 1	0	8	16	34	34
Plies in laminate 2	0	8	32	166	166
Plies in laminate 3	0	8	32	190	190
Plies in laminate 4	0	8	32	80	80
Plies in laminate 5	0	8	32	72	72
Plies in laminate 6	0	8	32	209	209
Plies in laminate 7	0	8	32	136	136
Plies in laminate 8	0	8	32	176	176
Total number of plies in structure	0	64	240	1063	1063
Average ply thickness -mm	0	5	0.87	0.19	0.19
Variation in ply thickness - mm	0	0	3.58	0	0
Mass of main structure -kg	25.46	35.31	15.20	16.92	16.92
Total structural mass (including metal structure) - kg	48.36	58.21	36.10	37.82	37.82

Figure 32 provides a summary of the entire black metal ply optimization process for an example Laminate #1 to illustrate the changes that occurred during optimization. Figure 32 (a) shows the UTM model where all plies were modeled with uniform thickness and geometry. During that step the plies represent candidate fiber angle and geometry stacks and were unrealistically thick to meet the initial constraints. Next Figure 32 (b) shows the results of the free sizing process, where the optimal geometry and section of each of the candidate stacks was identified. Figure 32 (c) shows the subsequent step of sizing optimization where the candidate ply stacks were sliced to plies of uniform manufacturable thickness. Finally, in in Figure 32 (d) the plies within Laminate #1 were reorganized so that no more than two plies of any orientation were stacked consecutively, and to fine the optimal laminate configuration.

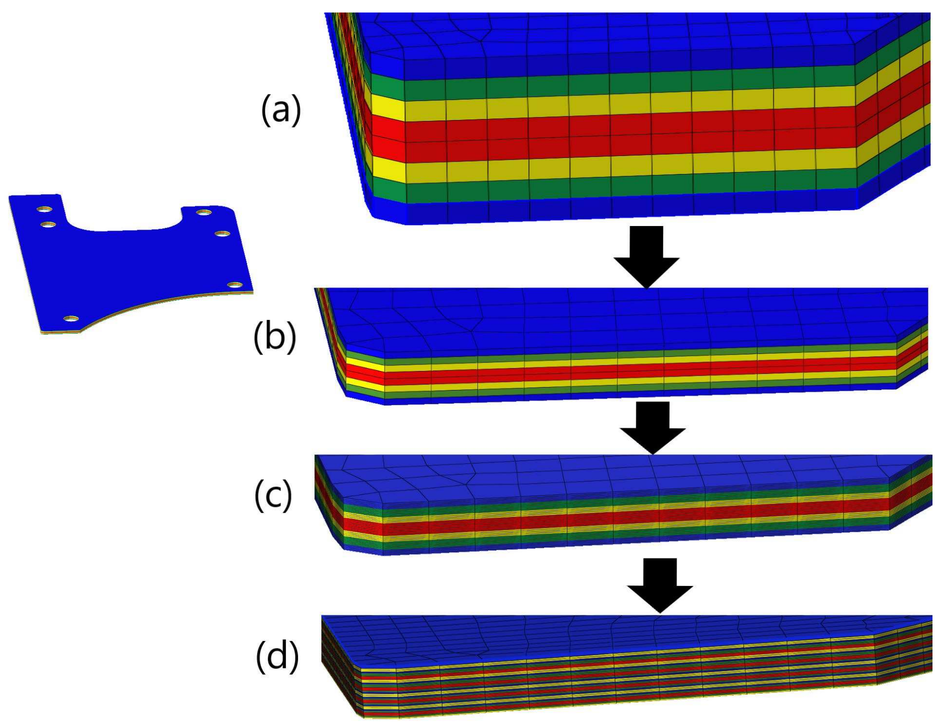

Figure 32 Example of ply and laminate configurations throughout the ply optimization processes: (a) UTM, where plies are treated as candidate angle and geometry stacks, (b) free-sizing, where plies are resized to find optimal geometry and section thickness for each fiber angle, (c) sizing, where plies are sliced to create plies of uniform manufacturable thickness, (d)

shuffling, where plies of any fiber orientation are dispersed within the laminate to improve structural performance.

3.6 Discussion of Preliminary Methodology

In previously published research, black metal design and optimization methodologies have been developed to design structures for industries that lack experience with the composite materials [97]. While these studies have predicted promising mass savings potential over steel structures through simulation, to date the methodology has only been applied to structures that have simple geometries and that are lightly loaded. In this study, common black metal design and optimization methodologies that have been published were applied to a complex heavily loaded structure to identify if they would be applicable. The 33% mass reduction over the steel design predicted in this study were comparable to weight savings accomplished in previous black metal research on simpler structures that experience lower loading [35].

It is possible, however, that even greater mass savings could be achieved if the black metal methodology was improved. This study replicated a practice noted in the literature reviewed where portions of a black metal structure remain modeled with metallic materials. In this preliminary experiment, the cast block at the base of the structure was modeled from steel, as the structural shape was deemed to be infeasible to manufacture with composites. In a composite specific design, the connection between the anchor bracket and the surrounding rail vehicle structure would likely be integrated into the overall structural geometry and manufactured from composites to increase the mass saving potential of the structure.

While the mass savings predicted were in line with those previously published, and there is potential to create even greater reductions, the results are likely inaccurate due to the modeling assumptions included in the established methodology [92]. Furthermore, the developed structure is likely not feasible for manufacture. The process and results do, however, provide insights into what improvements to the methodology must be made to develop complex heavily loaded composite structures.

The mass savings results of the preliminary experiment are likely inaccurate because the model replicated the common assumption noted in literature where connections between ply and laminate area are modeled in a simplified manner. The modeling assumed that the 8 laminates were connected with material that had matching mechanical properties to the surrounding plies and laminates, but no connecting material was actually modeled. In a manufactured solution plies would have to be added between the laminates to provide structural connection, likely significantly increasing the mass of the structure.

The other assumption made during this preliminary experiment that may result in inaccurate results is the manner in which fiber paths were modeled. In this study the common practice where fiber paths are aligned with a model coordinate axes (x, y, z) and fiber alignment was contiguous was used [27]. In reality, however, fiber paths are often noncontiguous in complex structures, especially ones that contain curvature. Deviations in fiber path can cause alterations to structural performance that were not considered in this experiment [98]. These deviations may have reduced the mass savings achieved during optimization, and therefore may reduce the accuracy of the results.

The final design developed during this preliminary experiment is also likely not feasible for manufacturing. The way the structure was partitioned into laminates based on the black metal geometry did not take advantage of composite materials ability to be molded into complex shapes and eliminate components. Instead, the 8 laminate regions had 90° angles between them which reduced the efficiency of the design with respect to compliance and failure criterion. This caused the optimization process to maintain thicker sections at the connection area between laminates, as shown in Figure 33. These inefficient connections also increased the number of plies to over a thousand for the final design, likely making the construction of the final composite structure a time-consuming and expensive process. Figure 33 also demonstrates that the limitation of ply optimization to only modify structural shape two dimensions. Due to this limitation the ply dimensions cannot be altered to connect between the different three-dimensional planes of the overall structure to improve the efficiency of the design.

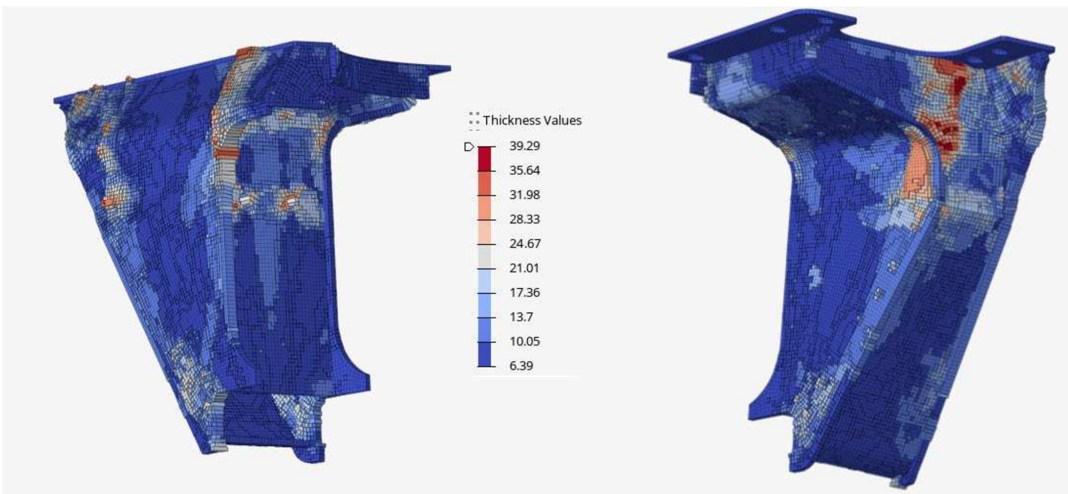

Figure 33 Laminate thickness (in mm) of the final design, showing increased thickness in connection regions due to the black metal geometry

Despite the issues noted with the black metal methodology in this preliminary experiment, composites do offer the promise of light-weighting complex heavily loaded structures, as has been demonstrated in other industries such as aerospace [99]. It is possible that methodologies developed by those industries could be incorporated into the ply optimization methodology to more fully redesign structures for composite application. For example, in a composite specific design, the overall laminate geometries would likely be redesigned to take on a more biologically inspired contour. This would leverage the advantage that composites offer to be molded into complex shapes and reduce the number of components. It is evident from this preliminary experiment, however, that this requires optimization beyond the two-dimensional capability of existing ply optimization software. Also, incorporating composite manufacturing simulation into the established methodology would provide feedback on manufacturing feasibility and help to refine design details such as the connections in the anchor bracket structure to improve the design.

CHAPTER 4: COMPOSITE SPECIFIC DESIGN AND OPTIMIZATION

Chapter 2 provided a literature review demonstrating that black metal design and optimization is a common focus of research in industries that lack experience with composites. The preliminary experiment, discussed in Chapter 3, highlighted the deficiencies of the optimization methodology prevalent in the literature reviewed when it is applied to a complex black metal structural geometry that is heavily loaded. This demonstrates that the current methodology being applied in industries that lack experience with composites is inadequate to develop final composite designs for many applications. The inadequacy of the methodology is evident in the lack of composite material application in many industries. Other industries have, however, been successful in developing structural shapes specifically for composites. As an example, the aircraft industry has spent decades researching, developing, and testing composite structures, as shown in Figure 34 (a). The knowledge developed has assisted the industry in developing complex aircraft structures constructed from roughly 50% composite materials which supports heavy loads during flight, as shown in Figure 34 (b) [100].

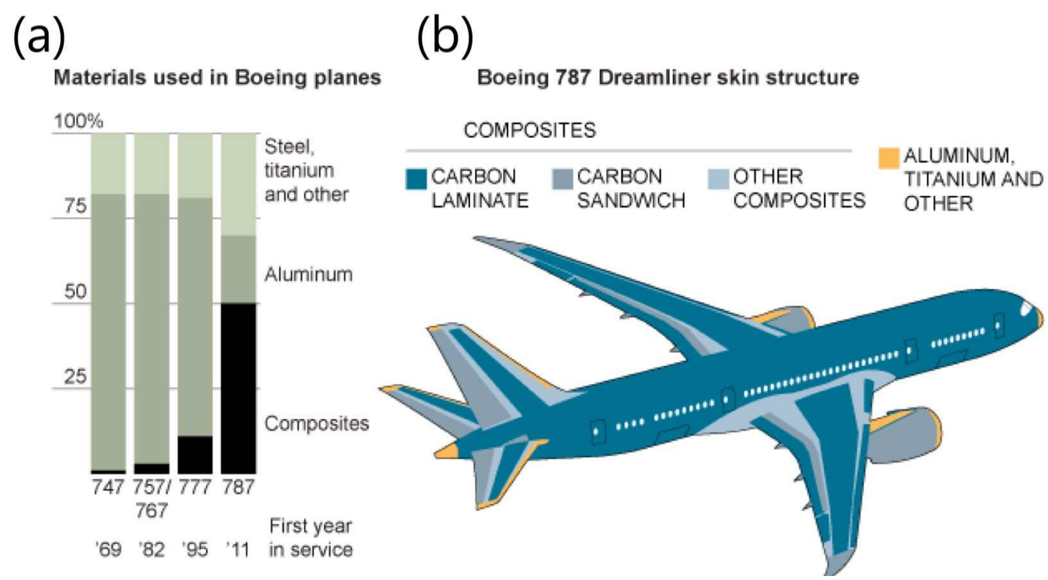

Figure 34 (a) Increase in composite application through the years in Boeing aircraft, and (b) demonstration of aircraft structures produced with composites [101], Industries such as aerospace have developed maturity in composite design and optimization by designing structural shapes specifically for composite materials, rather than using black metal design. This research has led to a recognition that the composite material must be designed in parallel with the structure, and that the form of manufacture affects optimal structural shapes and the structure's ability to perform a desired function [102]. Thus, unlike structural development utilizing more traditional materials, efficient structures developed with composite materials must simultaneously optimize the structural geometry, the material and the manufacturing approach to meet the desired design functionality. A common composite specific design and optimization philosophy, used by industries with composites experience, is summarized in Figure 35, where function, material, shape and manufacturing are simultaneously considered throughout the design processes [102].

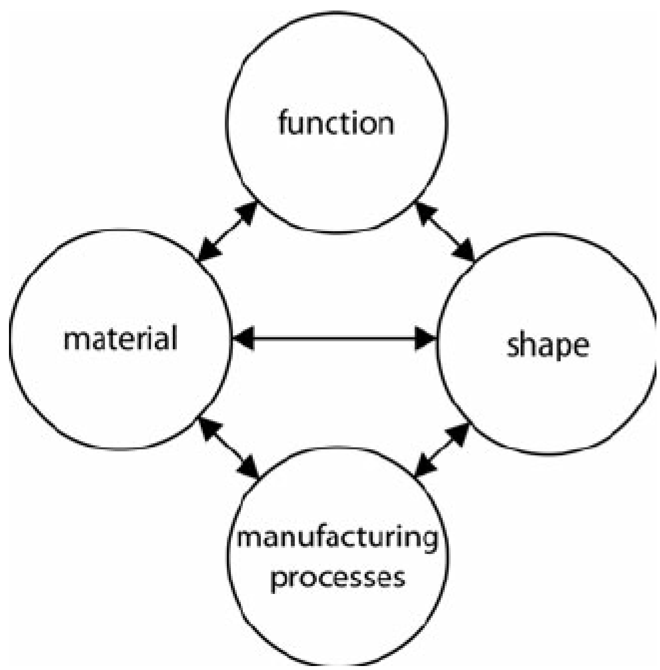

Figure 35 Composite specific structural design methodology [102]

4.1 Composite Specific Simulation

The knowledge generated through decades of research by industries that have maturity in composite application has been used to develop custom simulation tools to assist in developing composite structural shapes. For example, a research group developed a custom simulation tool for Boeing to assist with composite design [103]. This simulation tool allows Boeing to evaluate major aspects of composite structural design that were absent in the black metal methodology reviewed in Chapter 2, such as manufacturing, costs, weight, materials, partitioning, connections, and joints. The simulation tool can also be used to conduct analyses and optimization to develop finalized designs. Similar tools have been developed by Northrop Grumman and other aerospace designers [5]. These tools have assisted aircraft manufacturers in achieving a greater level of composite application in structural design than many other industries through designs that carefully balance the many competing design requirements of composite structures.

While the function of these simulation tools, and the successes achieved by the aerospace industry using them, have been published, they are proprietary to the companies who have developed them [5]. Furthermore, the tools have primarily been developed to assess structures specific to the aircraft industry such as fuselages and wings. Therefore, these established tools are not available or applicable for other industries. The existence of these tools, though, demonstrates a clear demand for their functionality by designers. Furthermore, most of these proprietary tools were introduced between the mid 90's and the present, coinciding with increased application of composites, as shown in Figure 34 (a). Therefore, utilizing simulation and modeling tools may be the fastest way to increase the application of composites in other industries.

To increase application of the material type, other industries could develop custom simulation tools similar to aerospace to assist in developing composite specific structural shapes. While this may be the best long-term solution, a strategy that will likely result in faster adoption of composites would be to leverage commercially available software tools. This is a common Systems Engineering concept of leveraging legacy systems when appropriate [104], [105]. In specific, the concept of software reuse is commonly cited in Systems Engineering research as a preferred solution in many instances [106]. Reusing software offers the key benefit of more rapid adoption of a methodology by many researchers, which can lead to further improvements to the methodology. Faster adoption can also help to identify additional requirements and functionality for a future software solution by the research community.

Fortunately, there are many other commercially available composite software tools that could be combined with ply topology optimization to fulfill similar functionality to custom tools which have demonstrated success in industries such as aerospace. These tools include three-dimensional shape optimization, optimizing structural shape to suit manufacturing, partitioning, connection modeling, and simulations to validate designs. In reviewing additional literature, however, the methodology associated with these simulation tools must be improved, and a strategy for integrating the various tool functions together must be developed.

4.2 Three-Dimensional Mold Shape Optimization

The first simulation tool that would logically improve composite design methodology for many industries is three-dimensional shape optimization. Logically, three-dimensional optimization would offer an additional dimension of geometric flexibility for developing composite structures and allow for more efficient connection between structural planes compared to the existing two-dimensional ply topology approach. As discussed in Chapter 2 (subsection

2.1.1), however, FEA programs do not allow for three-dimensional elements to be assigned anisotropic properties. Also discussed in that chapter, some research has begun to develop custom simulation tools to model composites with three-dimensional elements, but these applications have been very basic to-date and are not suitable currently for widespread application by industry [37].

Most FEA programs do allow for the modeling and optimization of three-dimensional elements with isotropic properties. Similar to ply optimization, three-dimensional isotropic optimization erodes the originally defined geometry of a structure to support function. With the flexibility of a third dimension however, the erosion is conducted over a volume, rather than a two-dimensional area. As an example of the benefits that an additional dimension can offer, consider the three-dimensional and two-dimensional optimization of an aircraft wing geometry shown in Figure 36. During a three-dimensional optimization of a wing made from isotropic materials, a volume is created which has rounded edges to support aerodynamics, as shown in Figure 36 (a) [107]. Although this optimization was completed with isotropic materials, the geometric features developed would offer benefits to a composite wing structure, as plies could span from the top, around the curvature to the bottom of the wing providing continuous fiber load paths. For comparison, Figure 36 (b) shows a two-dimensional optimization of a composite aircraft wing modeled with 2D elements. The composite optimization is limited geometrically to modifying the structure within the original two-dimensional plane that the plies were modeled in. Due to the dimensional limitation, the rounded contours that were developed in the isotropic optimization were not created, meaning that plies for the top and bottom surfaces of the wings did not have continuous fiber load paths, limiting the efficiency of the design [108].

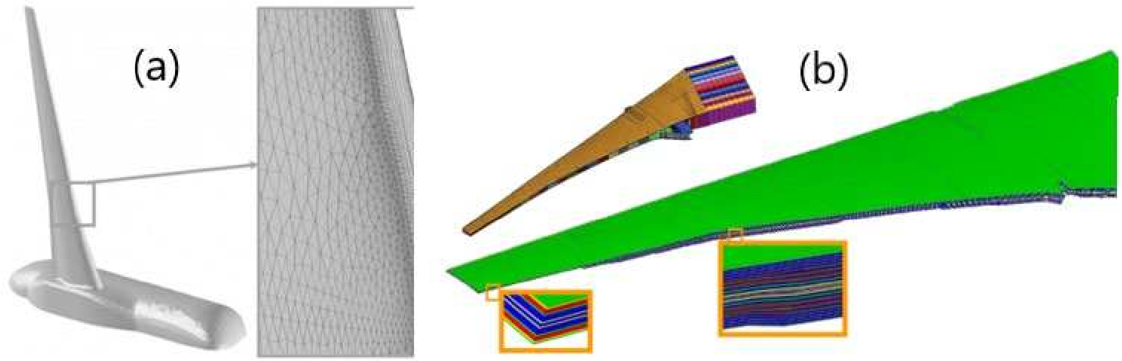

Figure 36 Comparison of three-dimensional (a) and two-dimensional (b) geometric optimization of aircraft wings[107], [108]

As discussed in Chapter 2 (subsection 2.1.1), composites can be modeled on three-dimensional geometries, such as the aircraft wing shown in Figure 36 (a), once the isotropic optimization is completed. This can be done by remeshing the surfaces of the developed structure with two-dimensional shell elements. Once completed, anisotropic properties can be applied to the developed structure. This would essentially result in the optimization of the overall molded shape, rather than just optimizing ply material allocation within a predefined black metal structural geometries.

The primary drawback of using three-dimensional optimization with composites, is that the mechanical differences between isotropic and anisotropic materials means that although the structural shape is optimal for isotropic mateirals, it may be suboptimal for anistropic material application. In some circumstances, however, the shapes developed through three-dimensional isotropic optimization may be applicable for composites. For example, structures developed for vehicles typically required multi-axis structural performance to provide support in dynamic loading environemnts, as explained in Chapter 3. Therefore, vehicle designers often implement a laminate design where plies are stacked in alternating order to create an overall structure that has properties which closely mimic in-plane isotropy [90]. For these types of composite applications, isotropic three-dimensional optimization may be an appropriate way to develop overall structural shapes.

Despite the potential for isotropic three-dimensional optimization to be used to develop quasi-isotropic laminate mold shapes, this practice has been far less explored within composite research. Recently however, researchers have begun approximating composite mechanical performance by modeling three-dimensional elements with approximated isotropic laminate properties to conduct mold shape optimization [38]. This practice may allow for the development of optimal mold shapes rather than using black metal geometry to define the overall structural shape.

As an example of mold shape optimization, a series of studies by Kuczek et al. developed an optimal composite rail car frame through the use of three-dimensional isotropic elements [83], [109]. Figure 37 summarizes the process used in that representative study. First the researchers developed a FRP design which layered fibers in various directions to provide multi-axis support for the typical dynamic loads that a rail car experiences, as shown in Figure 37 (a). The multi-axis laminate was modeled as three-dimensional elements with isotropic properties, approximating the in-plane properties, as shown in Figure 37 (b). The researchers compared the anisotropic two-dimensional elements of Figure 37 (a) and the approximated three-dimensional isotropic elements of Figure 37 (b) and determined that there was only a 2% difference in mechanical performance for their application, which was deemed to be acceptable. Next, as shown in Figure 37 (c), a total vehicle volume was established as a sum of three-dimensional elements created in the previous step. Dynamic loading and boundary conditions were applied to the volume. Finally, the three-dimensional volume was created by eroding the volume through optimization to create the optimal rail car frame shape.

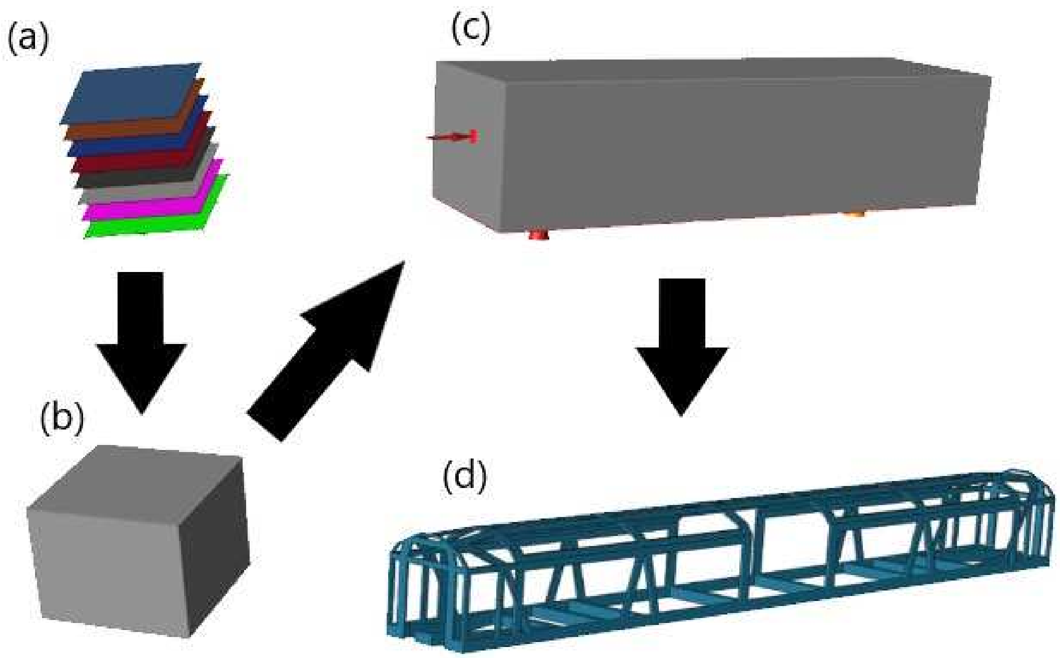

Figure 37 Example of anisotropic approximation with three-dimensional isotropic elements [83]*: Mechanical anisotropic fiber properties for a laminate (a), are converted to a single three-dimensional element with comparable isotropic properties (b), an initial three-dimensional volume is established with boundary constraints and loads applied (c), the volume is eroded to develop a composite rail car frame (d)*

As shown in Figure 37, the developed composite frame is one that could be realistically molded with composites. Furthermore, this type of shape would not have been developed through the erosion of two-dimensional elements applied to a black metal design. Studies like this have demonstrated that in cases where quasi-isotropic laminates are used, simplifying plies into a single element with the mechanical properties of the resulting laminate can accurately simulate structural performance such as stiffness.

Simplifying the modeling of laminates as isotropic three-dimensional elements does neglect some ply micromechanics. For example, individual ply simulation would be required to determine interlaminar strength of a composite structure. Due to the interface between plies, there are stresses that can develop within the laminate. Therefore, simplifying the properties of multiple plies limits the accuracy of stress and failure modeling. Logically, following mold optimization, the developed shapes should be re-meshed in two-dimensions and ply details modeled to fully simulate structural performance. Kuczek et al. identified this as a logical next step for their research, but to date have not published results for this type of conversion. If completed, this would also allow for the previously demonstrated benefits of ply optimization to be applied to the developed molded shapes. This step, however, has thus far not been included in the published research [110]–[115].

4.3 Manufacturing Optimization

Another area where the methodology proposed by Kuczek et al. could be improved is through the consideration of alternative manufacturing processes. In their studies the developed railcar structure was constrained to only be produced through composite tube structural shapes [83]. These would likely be manufactured through a process such as filament winding or pultrusion [116]. While this is logical for a railcar frame, tube shapes have limited applications in structural design. Pultrusion and filament winding manufacturing is not suitable for producing more complex structural shapes that are required in many applications. Expanding the methodology proposed by Kuczek et al. to consider manufacturing methods such as hand layup which are suitable for complex molded shapes, would greatly increase the geometric flexibility of the methodology. Developing shapes suited for hand layup with three-dimensional optimization has not, however, been explored in research to date.

While geometric flexibility is advantageous in composite design, shape development should be constrained to an extent. Research has shown that using constraints during shape optimization is important to ensure that the developed geometry can be feasibly manufactured through the production methodology being considered [117]. This has not, however, been explored in three-dimensional composite shape optimization research for common manufacturing methods such as hand layup.

Because optimization algorithms included in FEA software are designed for the three-dimensional optimization of isotropic materials, constraints specific to those materials and their associated manufacturing processes are included in the software and have been examined in research. These geometric constraints include milling, turning, extrusion, casting, forging, and rolling of isotropic materials [94]. Figure 38 demonstrates the effects of manufacturing constraints on a three-dimensional isotropic process. In this example, the wire frame represents the original three-dimensional design space volume. Figure 38 (a) shows the developed geometry without manufacturing constraints. Constraining the optimization under the assumption that the structure would be produced through rolling the material, however, radically changes the developed geometry, as shown in Figure 38 (b).

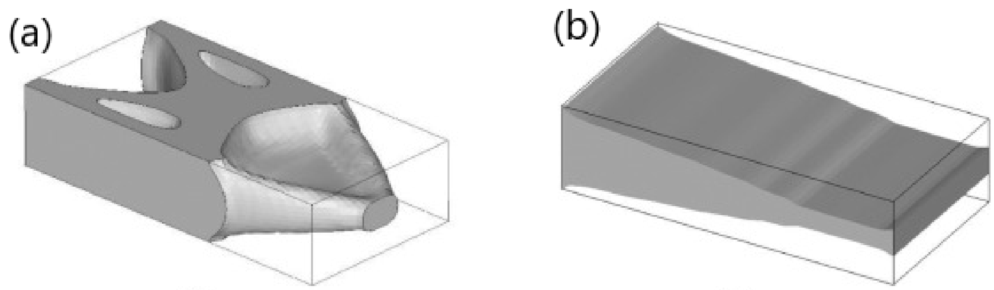

Figure 38 Example of an isotropic optimization without manufacturing constraints (a) and with a rolling constraint applied (b) [117]

These manufacturing constraints designed to simulate metallic manufacturing are not, however, applicable to composites. This is because FRP composites are primarily produced by laying up plies over a mold shape to develop the structure. Through this manufacturing methodology, hollow interior sections are possible, advantageous to weight savings, and in some cases required to provide access to layer plies inside the mold. The metallic manufacturing process that is most similar to molding FRPs would be casting, where molten metal is poured into a mold cavity. With castings, however, hollow sections require complex molds and can introduce defects into the metal part. Therefore, manufacturing constraints specific to FRP molding need to be developed to improve adoption of the material type.

4.3.1 Ply Draping, Partitioning and Connections

As modeling plies with two-dimensional elements is common practice, there are composite manufacturing simulations available in many FEA programs for those element types that could be used to constrain designs and optimize them with respect to manufacturing. The most researched types of simulators are those that simulate the process of draping plies as they are being laid up to form a laminate [118]. Industries that have experience with composites use ply draping simulators as part of their design process because they can be used to more accurately predict structural performance and material defects that can occur during manufacturing but have thus far not been incorporated into black metal design and optimization studies.

Ply draping simulators are designed to accurately predict two primary effects that the process of ply draping has on composite structures: fiber angle deviation and ply thickness. When flat ply shapes are draped over complex curved mold geometries during hand layup, fiber angles can be locally skewed due to wrinkling of the ply [119]. These fiber angle deviations are known as fabric shear [120]. During draping, fiber tows and unidirectional tape can be locally altered. Figure 39 illustrates how unidirectional materials can be sheared and fiber angles can be altered by a value of θ [121]. These local fabric distortions can create stress concentrations that can reduce structural performance, leading to increases in required weight to prevent failure [122].

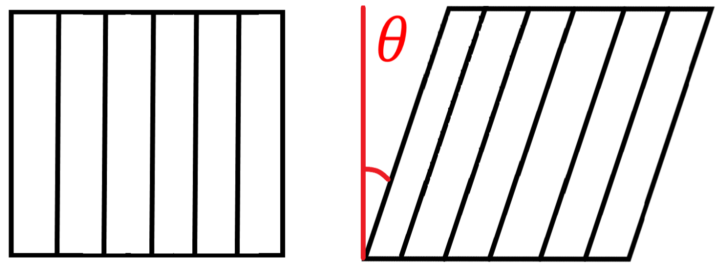

Figure 39 Local fiber orientations neglecting the effects of draping (left) and accounting for them (right) for unidirectional material

The other primary effect that ply draping has on a composite structure is deviations in ply thickness. During draping simulation, the ply thickness at each element location is also calculated based on the degree of fabric shear, θ. The thickness of each element within a FEA model is given by Equation 7 [118]. Where t is the local ply thickness of an element following ply draping and t_o is the thickness of the ply when laid flat. For large and complex structures, the effects of draping and fabric shear on structural performance can be significant[123].

$$t = t_0/\cos(\theta) \tag{7}$$

Ply draping simulators have been validated in research as accurate when compared to physical test specimens [122]. Ply draping simulators can accurately predict where local fabric shear and wrinkling will occur based on structural geometry and re-assign material orientation within FEA model elements to represent the issue [124]. An example of a ply draping simulation that was validated through physical prototyping is shown in Figure 40.

Figure 40 Manufactured composite part (a) compared to a ply draping simulation (b) [122]

For the reasons mentioned above, ply draping can affect structural topology due to reductions in structural performance associated with fiber misalignment. As a result, it should be considered as a constraint during optimization. Logically constraining ply shapes to minimize fabric shear would result in improved performance and alter the shape of a structure. To date, however, optimization studies have not considered the effects of ply draping or been constrained to minimize fabric shear. Instead, common practice when modeling composite structures has been to define fiber orientation to be aligned with respect to a model coordinate axis (x, y, or z), rather than accounting for localized fabric shear resulting from the structures mold geometry, as discussed in Chapters 2 and 3 [27]. Models which neglect the effects of ply draping simulate fiber path in a contiguous manner, regardless of structural geometry. While this approach is accurate for simple flat geometries, it may not accurately account for fiber angle deviations that can occur as plies are draped over complex mold shapes [34].

Ply draping can also be used to assist designers with the partitioning of plies to improve structural performance. A methodology termed kinematic draping is a method of optimizing ply draping to minimize fabric shear [124]. During kinematic draping ply area is assessed, and if fabric shear is predicted the ply area is partitioned into subregions. Published research has demonstrated that in the case of more complex structures, partitioning may be necessary to achieve optimal mass reductions of part [125]. To date, however, studies have not incorporated ply optimization with kinematic draping. Using kinematic draping to partition a part and constrain the optimization, rather than metallic constraints as has been used in black metal studies is, however, a more logical way to constrain the process and optimize the structure with respect to composite specific manufacturing.

Ply draping could also potentially alleviate a primary deficiency of the common algorithm used to perform ply optimization. As discussed in Chapter 2 (subsection 2.1.3), a limitation of the gradient-based algorithms used to optimize ply topology is that they can arrive at local, rather than global minima [58]. This means that there is a potential that alternative designs could achieve further mass reductions than those arrived at by the algorithm. A common strategy employed in literature outside of composite research is to guide gradient based algorithms towards greater reductions by altering the initial design space for the optimization [51]. With respect to composites, this would mean constraining the initial ply and laminate geometries in an effort to obtain increased mass reductions. A logical approach to constraining the ply optimization process would be to use ply draping to alter ply and laminate geometries prior to optimization. Figure 41 was previously presented in Chapter 2 (subsection 2.1.3) as Figure 13 to demonstrate the deficiency of gradient based algorithms. It is represented here to demonstrate how alternative starting points, or ply geometries, could theoretically result in greater mass reductions. To date, however, this has not been considered in published research.

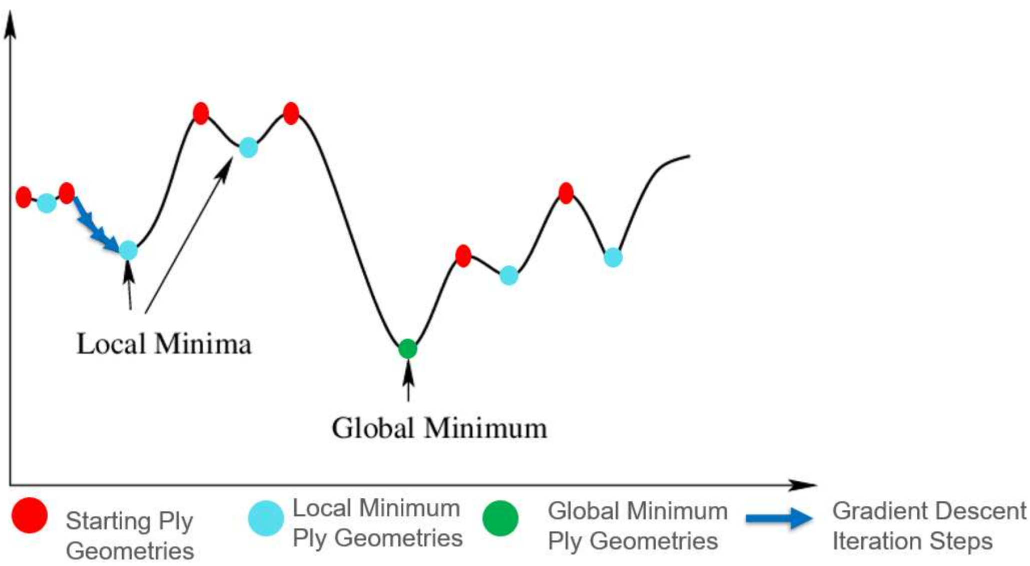

Figure 41 Gradient descent solutions showing that the alternate starting ply developed by kinematic draping geometries could lead to improved mass reductions [58]

4.3.2 Validation Simulations

As previously discussed, the current black metal ply optimization methodology can result in the development of designs which are not feasible for production due to a high degree of manufacturing complexity and associated costs. Therefore, the final area that optimization methodology could be improved in is the inclusion of manufacturing validation. As previously cited, however, an impediment to composite application is the complexity of developing manufacturing procedures and the expense of developing manufacturing procedures and prototyping parts [126]. Instead, research indicates that computer-based simulations can be an effective way to evaluate composite structural manufacturing and performance [135]. Applying these validation tools to optimization research may lead to faster development of manufacturable designs and feedback on the manufacturing feasibility of designs [128]. Production simulation has been the most researched method of validation and has demonstrated promise in the literature reviewed [77], [129]–[132]. Primary outputs of these simulations are feedback on the costs, effort and time predicted to produce a particular composite structure.

Logically, these production simulations are designed to replicate common composite manufacturing processes in a virtual environment. These simulators are typically able to model production through a number of procedures, but the two most common processes associated with FRP structures are ply layup and curing [133]. Ply layup is the previously described process where plies are layered in or around a mold to for a laminated structure. Plies can be layered through a number of processes included automated ones, but manual labor to layup plies by hand is the most common. As described in Chapter 3, common ply types used in FRP design are preimpregnated plies that are sold with resin pre-infused into the fibers. During layup the resin is tacky, meaning that following the layering process the structure must be cured to solidify the plies and stiffen the structure. Different curing methods are available, but autoclaves which cure FRP structures under heat and pressure are the most commonly used.

While the major manufacturing processes used to produce FRP structures are fairly consistent, the methodology in which effort and costs associated with them are simulated varies. The primary methodologies are grouped into three categories: analogous, parametric and bottom-up simulators [5]. Analogous simulation leverages historical data related to the manufacturing of various types of composite parts. This typically requires structures to be grouped into categories of common structural shapes. The design being reviewed is then compared against the historical data for similar shaped parts produced through similar production processes, and adjustments are made to compensate for any differences between the design being reviewed and the historical data. This methodology is ideal for aerospace, where many of the structural shapes are repeated regularly such as fuselages and wings. For other industries that are seeking to develop new structural shapes, however, this methodology may be inaccurate.

Parametric based simulators utilize metrics associated with a design to predict the costs, effort and time associated with manufacturing the structure through a specific set of processes [134]. Examples of parameters that could be used to assess a design include part size and wall thickness. The simulator than scale historical data based on variances in those selected parameters to estimate effort and costs. The primary issue with parametric simulators is that if metrics vary too significantly between structural alternatives and the historical data considered the results could be inaccurate.

Bottom-up simulators are considered to be the most accurate for new structural designs, as they simulate each step in the manufacturing process individually and combine them to generate results. These simulations are used in research and industry to determine how structural geometry will affect each step in manufacturing when a final design enters production [99], [129], [135]. For example, the simulator will examine how the laminate design will affect the costs associated with designing the mold and tooling, the effort to lay up the plies within the mold, and the time to cure the composite structures [130]. While bottom-up estimation can be a more time consuming process and does require data specific to a manufacturing operation to be accurate, it is considered to be the most applicable simulation methodology when creating new composite designs.

Figure 42 provides a graphical depiction of the bottom-up methodology for the common manufacturing processes of layup and curing. It can be seen in the figure that the subprocesses of manufacturing are broken down to accurately estimate each of them. It can also be seen that each subprocess is evaluated with respect to laminate and ply geometry. The simulation also considers how structural geometry effects tooling effort and costs such as mold design. Finally, the Figure shows how the results of the subprocesses are combined to generate the total tooling, effort and costs associate with the design.

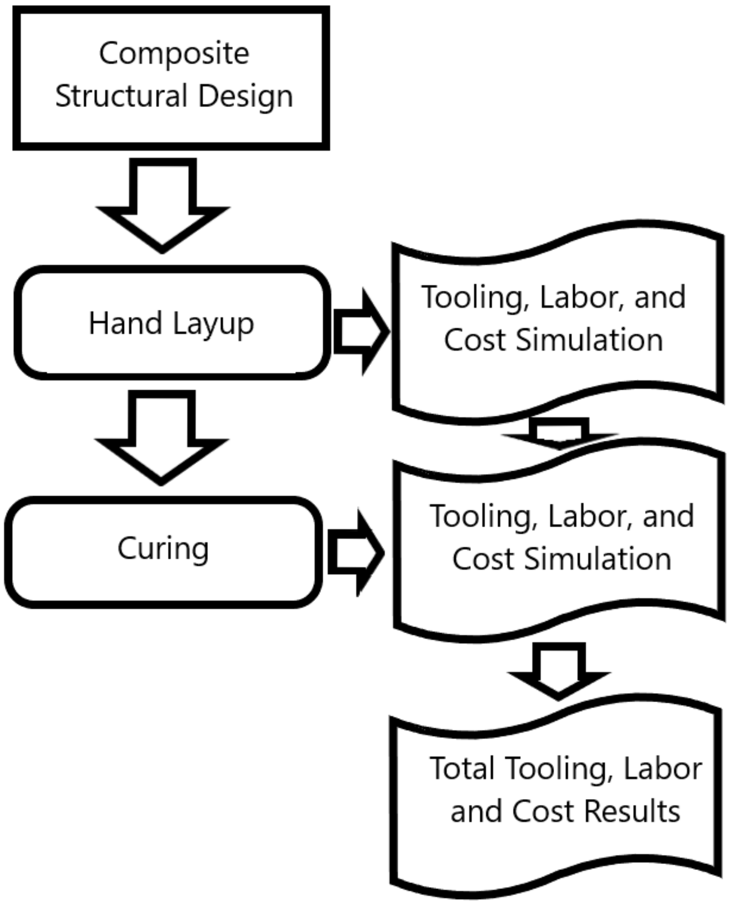

Figure 42 Depiction of bottom-up manufacturing simulation

It should be noted that manufacturing simulation is incorporated into proprietary simulation tools developed by industries that have maturity in composite application, such as aerospace, demonstrating its value as part of the design process. As previously mentioned, however, these tools are not available or applicable to other industries. Due to demand by industries that are interested in beginning to apply composites, all three of the major manufacturing simulation methodologies have recently been developed into commercially available software [136]. To date, however, these types of simulators have not been integrated into composite optimization methodology.

4.4 Integrated Methodology

The design and optimization processes and methodologies discussed previously in this chapter would be logical improvements to the established ply topology optimization methodology discussed in Chapter 2. To realize these improvements, however, the processes would need to be integrated into ply topology optimization to develop a more comprehensive composite design methodology. The need for this integration has been recently noted in literature in a few studies [1], [9], [21]. While these studies have noted the need for an integrated methodology, and began to formulate conceptual frameworks, none of them have advanced as far as applying said frameworks to case studies to validate the proposed approaches.

One example of an integrated approach is shown graphically in Figure 43 [1]. In this study the authors hypothesized that Geometry, Architecture, and Process (GAP) are the key design parameters which must be simultaneously optimized to develop a composite design. The authors reiterated what has been explained previously in subsection 4.1, that mold and ply geometry must be optimized with respect to the manufacturing processes that will be used to produce the part. The authors leveraged the concept of analogous manufacturing simulation discussed in the previous subsection (4.3.2) to categorize structures by their "Architecture" as shown in Figure 44.

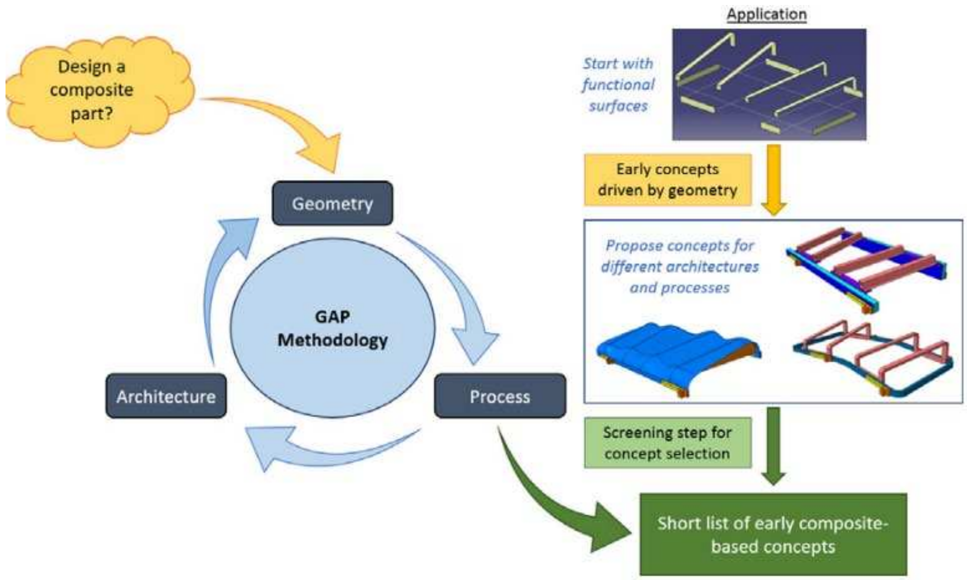

Figure 43 Geometry, Architecture, Process (GAP) composite design methodology [1]

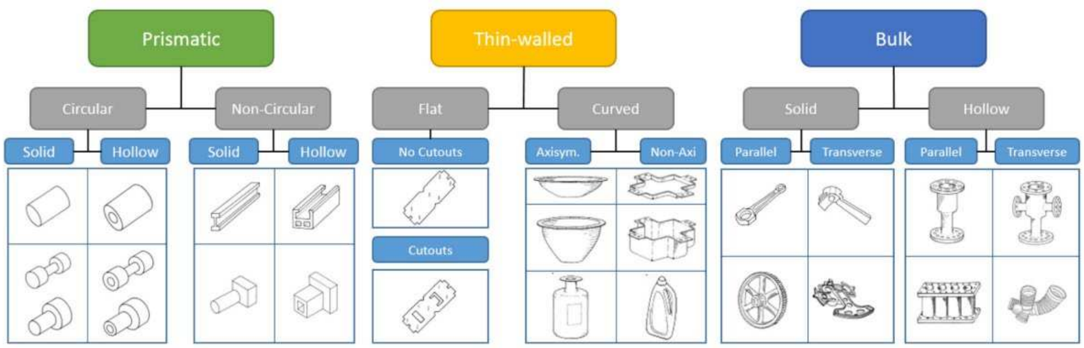

Figure 44 Example from literature of "Architecture" types used to optimize composite structures [1]

This study demonstrates interest by industry to develop an integrated design and optimization methodology [1]. The study did not, however, identify ways to integrate other key composite design and optimization processes such as ply topology optimization and draping analyses. Additionally, while the study did provide some basic high level case studies of how the proposed methodology could be applied, it did not provide sufficient details for a reader to use the methodology to develop fully optimized final designs.

A more advanced example from literature of a conceptual methodology for integrating composite design and optimization processes is provided in Figure 45 [21]. In this study the authors proposed a complex multistage process which iteratively develops a composite structural design. It can be noted in the figure that the proposed integrated methodology references many of the subprocesses previously discussed in this dissertation. For example, during the "System and Subsystem level" definition proposed by the authors the initial topology of the mold is developed. During the same level, composite joints that are typically neglected during black metal design are defined in terms of position, functionality, and shape. In the "Component level" the authors propose to fulfill ply optimization (termed "topology optimization" in the figure) and manufacturing simulation to validate the design.

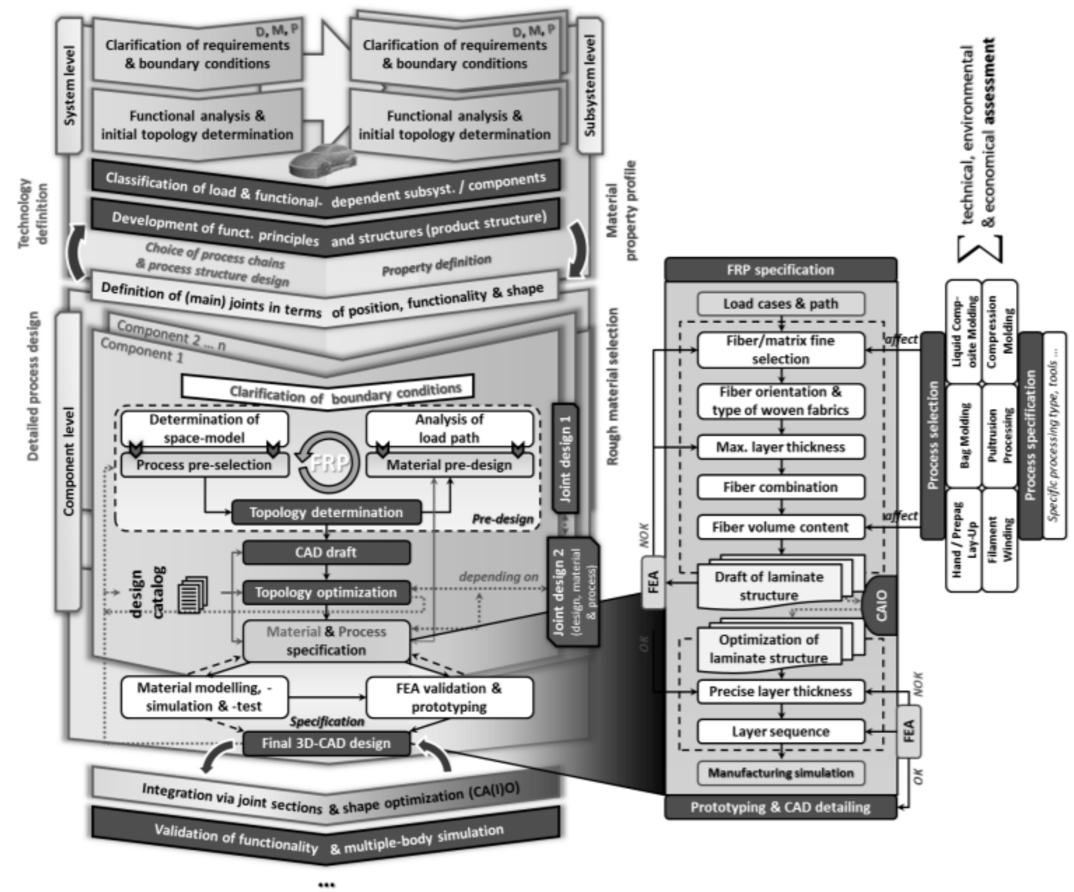

Figure 45 Composite design and optimization process [21]

Like the first study [1], this one demonstrates the interest of industry in developing an integrated methodology [21], but the authors do not provide specific details or a case study explaining how to execute the subprocesses within the proposed approach. Furthermore, the methodology does not include other subprocesses such as ply draping that are likely necessary to achieve accurate results.

The final example from literature is a series of studies conducted by automotive researchers at Volvo to develop optimal automotive floor pan structures and demonstrate the advantages of functional integration in composite design [9]–[11], [13]. One study combined ply topology optimization with joint design and partitioning functions [9], and a separate study combined ply draping with partitioning and joint design functions [11]. While neither of the studies fully integrated all identified two-dimensional composite ply design functions, that advancement would be a logical next step for the research. Also, neither study provided details on how the overall molded floor pan shape was designed, meaning that the methodology would not be suitable for replacing black metal designs. Integrating three-dimensional mold shape optimization, as proposed by Kuczek et al. [83], [109], would advance Volvo's methodology by also developing an optimal overall molded shape. Finally, neither study integrated a manufacturing simulation to provide feedback and validation on the developed designs.

Despite not fully integrating all functions, the results of the Volvo studies were structures that offered cost savings of over 40% and reductions in mass of 7% when compared to designs that were not developed through an integrated approach [9]. It is logical to assume that full integration may result in even greater mass and cost reductions. Therefore, there is a demand for a new methodology which will yield more comprehensive optimization through the integration of multiple commercially available composites design tools.

CHAPTER 5: PROPOSED METHODOLOGY

In the previous chapter, composite specific design methodologies and processes were introduced that may offer benefits if integrated with the black metal design and optimization methodologies introduced in Chapters 2 and 3. The previous chapter also demonstrated an interest throughout industry to develop such an integrated methodology to develop finalized designs that can exploit the benefits of composite while being constrained to the specific material type. As discussed, however, while conceptual methodologies for integration have been proposed, specific processes have not been developed to validate the effectiveness of an integrated approach. Therefore, there is a demand to develop an integrated methodology that provides specific details to designers on how to fully design and optimize a composite structure.

It is evident from the literature reviewed that development of an optimal structural shape is directly related to better implementation of composite material and improved manufacturability and must be fundamental to any integrated methodology. Therefore, this research formalizes a new methodology which integrates, ply and mold shape optimization, constraints, and validation to develop improved designs. In response to the literature reviewed and industry trends, the intent of this research is to develop this methodology within a simulation-based framework to improve the efficiency of the design process.

5.1 Two Step Optimization

As discussed in Chapter 4 (subsection 4.1), the methodology proposed in this research is designed to leverage existing commercially available software tools and established methodologies to aid in more rapid application of composites throughout industry. Due to the lack of integration between these software tools and the functional deficiencies highlighted in the previous chapters, the developed methodology must be an iterative one that sequentially develops optimal structural shapes for composite application. Through review of the literature the requisite methodologies required to develop a fully optimized designs can be logically organized into two major steps: mold shape optimization and ply shape optimization.

5.1.1 Step One: Mold Shape Optimization

The first step in the proposed methodology is based primarily on the mold optimization process proposed by Kuczek et al., which was discussed in Chapter 4 (subsection 4.2) [83], [109]. According to those studies, the optimization must be conducted in three dimensions, to provide maximum flexibility to the design, and exploit composite material benefits. Also according to those studies, the overall structural shape, or mold geometry, should be optimized to meet design goals and be constrained with respect to shape, function, materials, and manufacturing requirements. Other literature reviewed confirms the conclusion by Kuczek et al. that three-dimensional optimization is conducted by first identifying the maximum space in which a structure can occupy and creating a solid volume of that size from which the structure will be developed [137], [138].

As discussed in Chapter 4 (subsection 4.2), limitations with existing software tools prevent the modeling three-dimensional elements with isotropic properties. As a result, researchers have developed an approximation method of modeling elements with quasi-isotropic laminate properties [83]. To do this the elements are meshed to match a typical laminate thickness, and in-plane quasi-isotropic properties are applied. It is anticipated that future software development will eliminate the need for this approximation, by allowing for isotropic properties to be applied to three-dimensional elements.

Next, a check process must be conducted to confirm the accuracy of the quasi-isotropic laminate property approximation [83]. To do this, a separate model should be created using two-dimensional elements with accurate anisotropic properties to simulate the performance of the plies and resulting laminate more accurately. The three-dimensional elements created with isotropic properties should be compared against the two-dimensional elements to confirm it accurately represents the in-plane properties of the desired laminate construction.

Next, constraints are applied to the volume so that the developed structural shape meets design requirements [139]. The intent of the optimization is to develop an optimal mold geometry, so the constraints applied during this subprocess relate primarily to manufacturability [133]. For example, if a female mold is desired, the boundary constraints must be established such that a mold cavity is formed. With the constraints applied, the volume is subsequently optimized through erosion to identify the optimal mold shape.

Finally, the mold geometry must be converted from 3D elements to a 2D shell which represents the optimized laminate shape. This is done by remeshing the surfaces of the mold with 2D elements and eliminating the developed optimized 3D volume. This conversion must be conducted so that accurate anisotropic materials properties can be applied and so that the subsequent step of ply optimization can be conducted.

5.1.2 Step Two: Ply Optimization

Once a mold geometry has been formed, the next major step in the optimization process is to conduct ply optimization. The second step in the optimization methodology is primarily based on a series of studies by the Volvo group that was discussed in Chapter 4 (subsection 4.4) [9]–[11], [13]. In those studies, it was identified the integrating the ply design functions of draping, joining, connections, and topology. One study combined ply optimization with joint design and partitioning functions [9], and a separate study combined ply draping with partitioning and joint design functions [11]. The proposed methodology in the current research fully integrates all of those functions investigated by the Volvo group and advances the methodology by also incorporating production simulations that have been demonstrated as beneficial in other literature [77], [129]–[132]. Furthermore, the studies by the Volvo group did not include a methodology to develop the overall structural mold shape, so integrating the first step described in the previous subsection with ply optimization also advances the currently published methodologies.

Of importance during ply shape step is the organization of the subprocesses. The order of the subprocesses should be draping, partitioning, joint design, topology optimization and production simulation. Like mold optimization, ply optimization should begin with the development of shape constraints to ensure that all subsequent subprocesses are conducted in a way that meet design requirements. From literature these constraints typically include manufacturability, stiffness, failure criterion, and cost considerations [117].

Ply draping analysis should be conducted next, and before ply topology is modified, to ensure that accurate material properties are referenced during the optimization. With draping conducted first, the later subprocess of topology optimization will be conducted with respect to any structural defects that may be identified, such as wrinkling and fabric shear, and alter the design accordingly to still meet the objectives and requirements established. Without draping conducted first, the topology optimization process may develop solutions that overestimate performance of the developed structure.

Ply draping must also be conducted prior to topology optimization to inform structural partitioning and joint design. For complex structures kinematic draping processes can be applied to partition the mold shape into subregions [124]. This partitioning has typically been conducted to minimize fabric shear and wrinkling defects. If the simulation determines that partitioning is necessary, connections between the subregions must be defined and modeled to accurately represent structural performance. While the subsequent step of topology optimization can partition ply geometries in a similar manner to kinematic draping, the gradient-based algorithms are known to arrive at local minima that may not represent the most optimal ply topology [58]. Therefore, by conducting kinematic draping ahead of ply optimization the partitioned plies may guide the gradient-based algorithm towards more accurate results.

After the laminate, ply and connection details have been established, material allocation can next be optimized through ply topology optimization. The process for this optimization has been well documented in literature, and follows the approach applied in the preliminary experiment discussed in Chapter 3 [60]. First, ply topologies are optimized to identify the optimal thickness and shape. Next plies are sliced to develop plies of a manufacturable thickness. Lastly the plies are shuffled within the laminate to determine the optimal stacking sequence, and to minimize interlaminar shear.

The last part of the optimization process is to conduct a manufacturing simulation to demonstrate that the design produced can be feasibly manufactured. Both laminate and ply details generated from the optimization processes are inputs to the manufacturing simulation [24]. Mold geometry is assessed to determine how the shape may affect costs and production. Ply geometries are also analyzed to determine their effect on the overall cost of the part.

As the structure is sequentially optimized, the results must be reviewed to ensure that developed design continues to meet the design requirements initially established. Should the design fail to meet the requirements, subroutines of the optimization should be repeated with parameters modified to develop a fully optimized solution. Figure 46 summarizes the proposed fully integrated methodology.

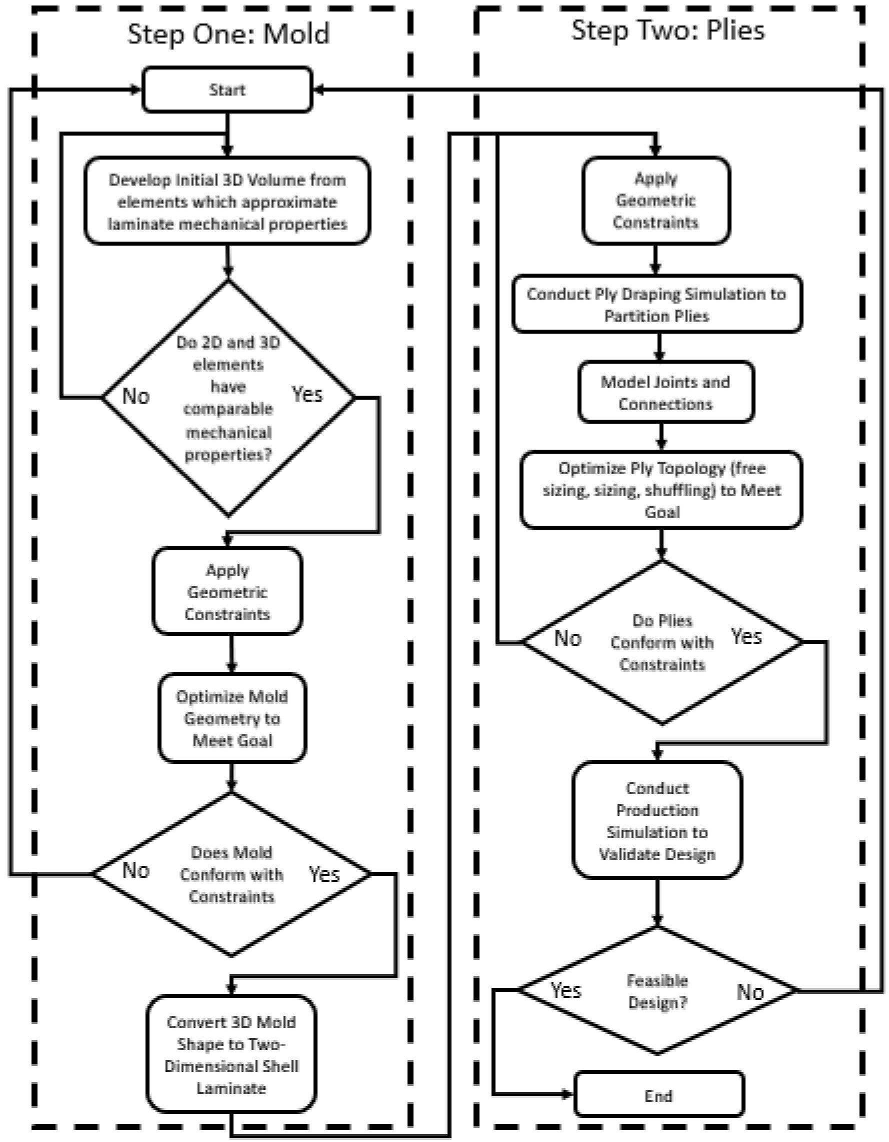

Figure 46 Proposed fully integrated optimization process

CHAPTER 6: FINAL EXPERIMENT

A final experiment was next designed to test the effectiveness of the developed methodology. Like the preliminary experiment, discussed in Chapter 3, the final experiment focuses on a rail vehicle anchor bracket. Where the preliminary experiment was designed to test the ply topology optimization methodology implemented in the literature reviewed, the final experiment is designed to show how increasing levels of integration between the required design processes for composite structures will lead to increased structural performance with respect to mass, manufacturability, and production costs. In the final experiment, an experimental design will be produced through the application of the complete fully optimized optimization and will be compared against a black metal control design that is only produced through the second step of ply optimization.

Figure 47 shows the fully integrated methodology proposed in Chapter 5, as it will be applied to develop an anchor bracket design in the final experiment. This experiment will develop a model through fully integrating all required composite optimization processes to redesign the anchor bracket structure for composite materials. This structure will hereafter be referred to as the *fully optimized design*. As discussed, the process for fully optimizing the design will be completed through two major steps of mold and ply optimization. Each major step has a number of subprocesses which will be conducted to sequentially develop a design that is optimized for the material type and associated manufacturing processes and will meet all defined constraints.

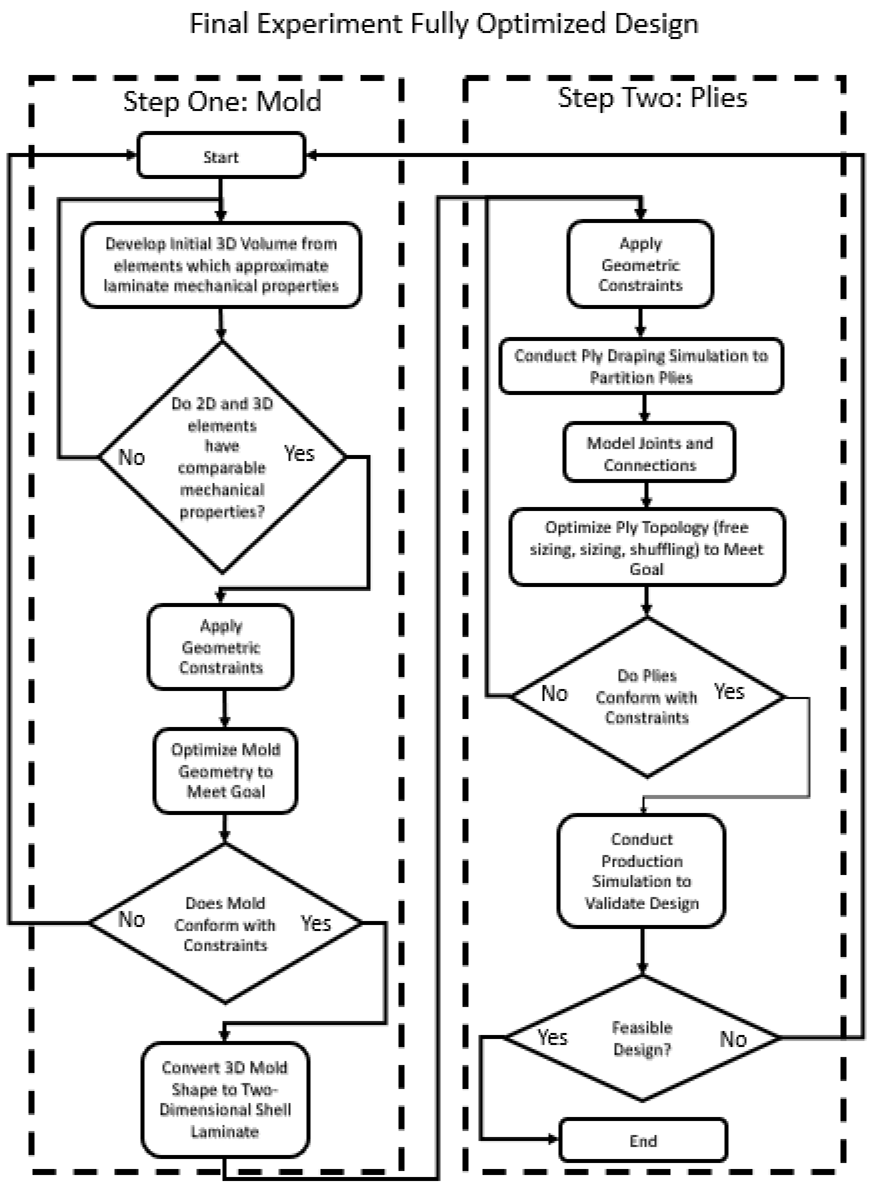

Figure 47 Integrated methodology to be applied to develop the fully optimized experimental design in the final experiment

To contrast the results obtained from the fully integrated model, a control design will be created which only applies the second major step of the proposed optimization methodology of ply optimization. Hereafter referred to as the *partially optimized design*, this model will represent the greatest extent that a structure can be optimized when only modifying ply geometry. The partially optimized model will serve as a control, and it is envisioned that it will demonstrate the importance of first developing an optimal mold shape for composite application.

To create the partially optimized design for the final experiment the black metal geometry used in the preliminary experiment of Chapter 3 will again be used. The partially optimized control design from the final experiment will be different from the model created in the preliminary experiment, however, because the ply optimization step will eliminate the identified simplifications and inaccuracies included in the preliminary experiment. Specifically, the partially optimized control model will replace all metal components with composite material, and include ply draping, partitioning, connection definition, and a production simulation, as shown in Figure 48. The same figure also provides a visual comparison of the methodologies applied in black metal design between the preliminary (a) and final experiment (b). It is predicted that the partially optimized design from the final experiment will be a more accurate representation of black metal structural performance, than what was demonstrated in the preliminary experiment.

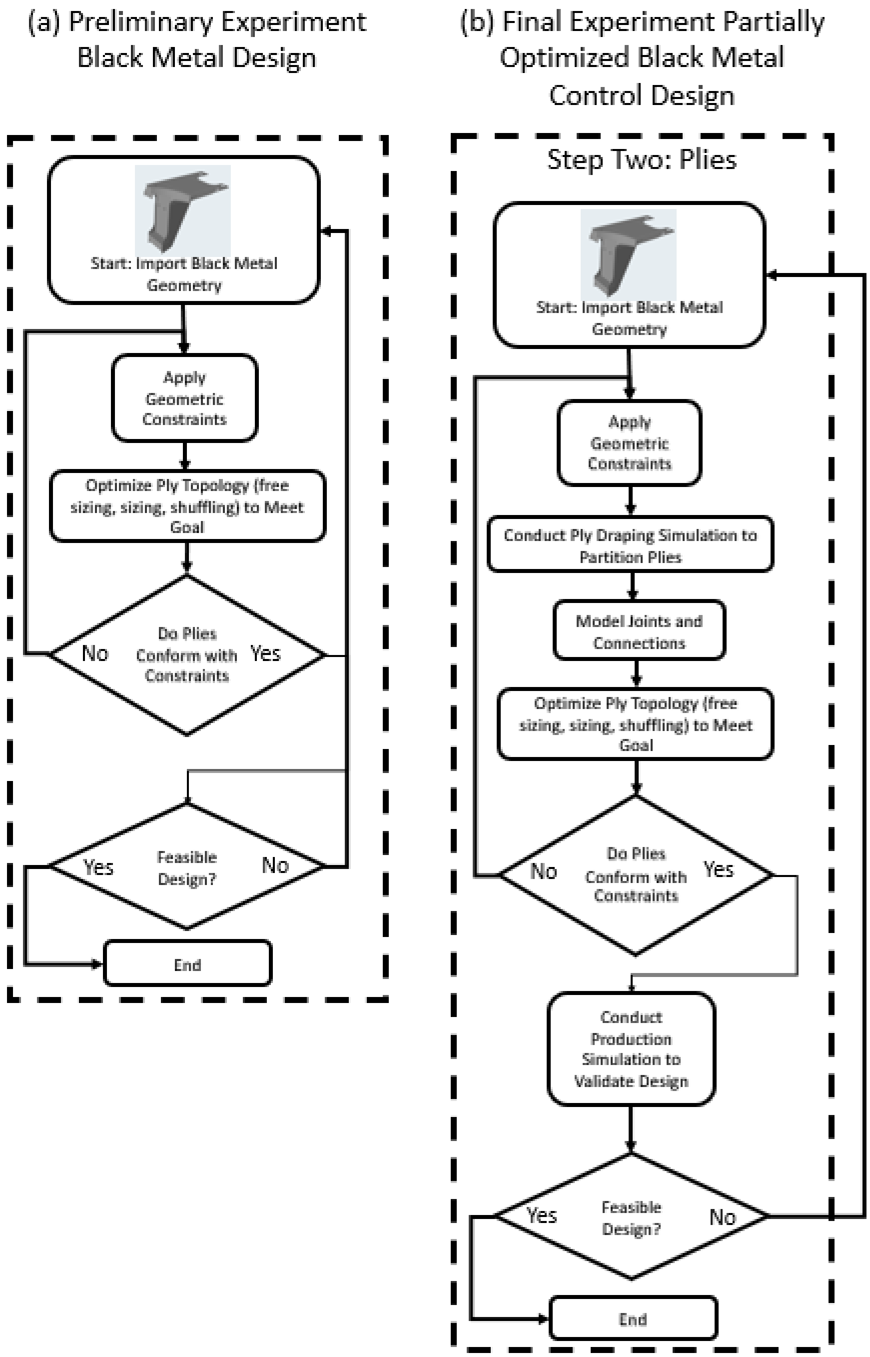

Figure 48 (a)Comparison of methodology applied to the black metal model in the preliminary experiment, and (b) partially integrated methodology to be applied to the black metal control model in the final experiment

To be consistent with the general scope of the literature reviewed, the objective of the final experiment remains to produce a low weight structure that has at least matching compliance to the existing steel design. Also like the preliminary experiment, the final designs will also be constrained with respect to composite failure criterion. The same materials and manufacturing processes assumed in the preliminary experiment of Chapter 3 will also be applied in the final experiment.

From this experimental design, the following hypothesis was developed:

6.1 Hypothesis

Hypothesis: A composite structure designed through a fully integrated methodology which optimizes both the mold and ply geometries will demonstrate reduced costs, mass and improved manufacturability compared to a black metal structure where only ply optimization functions have been integrated.

6.2 Step One: Mold Shape Optimization

As shown in Figure 47, the first step in the proposed methodology is to develop an optimal mold geometry for composite application. As also shown in Figure 47, the major subprocesses involved in mold shape optimization are the development of an initial 3D volume, comparison of three-dimensional and two-dimensional elements, establishment of geometric constraints, optimization of the mold shape, and conversion to a two-dimensional model.

6.2.1 Element and Material Definition

As discussed in Chapter 3, and demonstrated in past research, current FEA software only allows for the anisotropic material properties of composites to be modeled in two dimensions. This factor is likely contributing to the lack of established methodology for composite laminate optimization. However, recent research by Kuczek et al. has demonstrated that, when applying quasi-isotropic laminates, as is typical in vehicle design, it is acceptable to simplify the modeling of composites by applying the in-plane isotropic laminate mechanical properties to three-dimensional elements [83], [109]. Three-dimensional element optimization is also available in commercially available FEA software, including Altair's generative design tool Inspire, for isotropic materials. Therefore, in this study, laminate optimization was conducted using three-dimensional elements modeled with the quasi-isotropic properties listed in Table 5. For the final experiment, the same AS4 unidirectional carbon fiber material used in the preliminary experiment, produced through hand layup and autoclave, was modeled.

Table 5 Mechanical properties of composite ply and quasi-isotropic laminate

Material Property	**Individual AS4 8852 Carbon Ply** [78]	**8 Ply Quasi-Isotropic AS4 8852 Laminate** [136]
Modulus of Elasticity in Longitudinal Direction, E1	131.62 GPa	52.28 GPa
Modulus of Elasticity in Lateral Direction, E2	9.24 GPa	52.28 GPa
Modulus of Elasticity in Vertical Direction, E3	9.24 GPa	11.38 GPa
Poisson's Ratio, v	0.36	0.36
In-plane shear modulus, G12	4.83 GPa	19.96 GPa
Density, ρ	0.0018 g/mm^3	0.0018 g/mm^3
Thickness	0.188 mm (1 ply)	1.504 mm (8 plies)

Following the methodology developed by Kuczek et al. a test was conducted to confirm the accuracy of modeling the quasi-isotropic laminate with three-dimensional elements [83], [109]. To do this a two-dimensional element with anisotropic properties was modeled to represent an 8 ply quasi-isotropic laminate as shown in Figure 49 (a). This element was then compared to a three-dimensional element with the dimensions to match the thickness (1.504 X 1.504 X 1.504 mm) in plane mechanical properties of the quasi-isotropic laminate (provided in Table 5), as shown in Figure 49 (b). Consistent with the methodology proposed by Kuczek et al. a test was conducted within the FEA program which confirmed the two element types had matching in-plane properties.

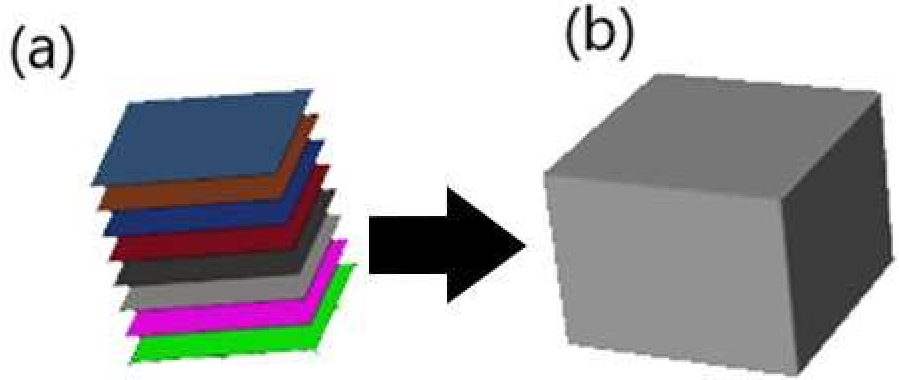

Figure 49 Comparison of two-dimensional anisotropic elements (a) compared to an isotropic element modeled to simulate quasi-isotropic properties (b)

6.2.2 Establish Geometric Constraints

Before beginning the optimization, constraints on the process had to be established. The first constraint established the spatial envelope under which a structural shape could be formed. As has been demonstrated in the literature reviewed, three-dimensional optimization begins with the definition of the initial volume to be eroded during optimization [135]. In this case study, the initial volume was defined as the maximum space that a new anchor bracket design could occupy under a rail vehicle. This initial volume was a 520-mm deep by 925-mm long by 525-mm-wide spatial envelope, as shown in maroon in Figure 50. The volume was modeled with three-dimensional elements to allow the optimization process maximum freedom to develop mold shapes.

The second constraint was based on composite manufacturability and mold design. The shape of the surface of a composite laminate is dependent on the shape of the surface of the mold that is used to manufacture the structure. Typically, FRPs are laid up on top of male or inside of female [133]. Therefore, a second constraint needed to be applied to the optimization process to dictate whether the anchor bracket would be manufactured in or on a mold. Although not explored in literature, this research theorized that mold shapes best suited for female molding, and mold shapes that are better suited for male molding, can be developed by altering the boundary constraints of the model prior to optimization.

When manufacturing a part through hand layup, as is assumed in this experiment, female molds impose one primary geometric constraint on a laminate's shape: hand access. The interior surface of the part must be accessible to lay in plies by hand. Furthermore, as plies are layered to build a laminate, that space is reduced due to the section of the layered plies. Therefore, prior to optimization, a geometric constraint had to be established to ensure the part was hollow and provided a cavity so that the selected manufacturing process could be performed inside the mold. To enforce this constraint, the boundary condition with the side sill was modeled as a hollow rectangle. This boundary constraint would force the developed geometry towards the outside of the side sill, providing access to lay plies on the inside of the part. Figure 50 (a) depicts the initial 3D volume and the boundary conditions applied to develop a female mold shape.

Conversely, male molds do not require internal hand access, as plies are layered on the outside of the mold. Therefore, as a point of comparison a second optimization model was conducted where the boundary constraint was applied along the entire top of the 3D volume. As shown in Figure 50 (b). It was theorized that this boundary constraint would develop a structural shape more suitable for a male mold.

A 30 kN load was also applied to both models, consistent with the preliminary experiment discussed in Chapter 2, and is shown in green in Figure 50 (a) and (b). As the steel anchor brackets load application point is not aligned with the centerline of the structure, the load application locations for the laminate optimization process were similarly aligned left of the centerline for both models.

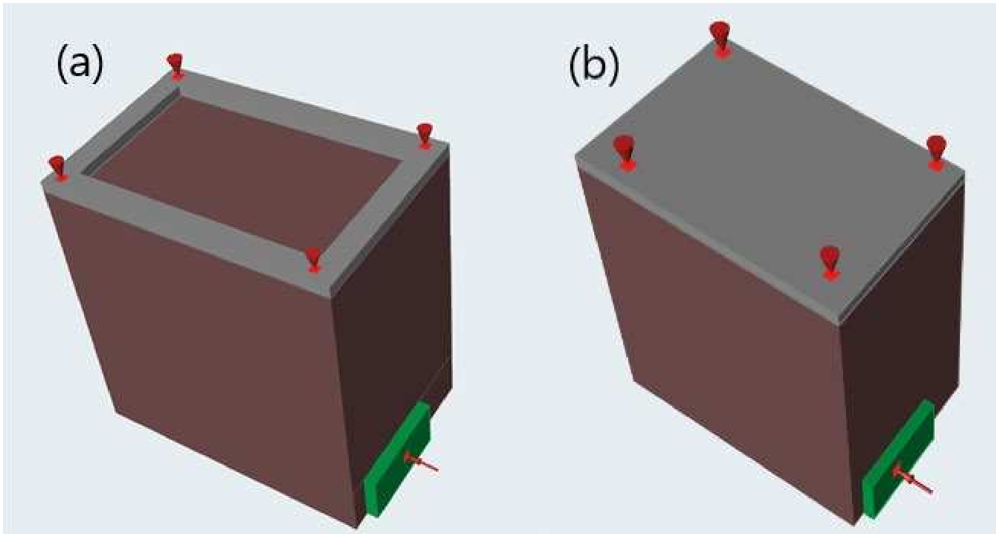

Figure 50 Initial 3D volume shown in maroon, and loading application location shown in green, boundary constraints shown in gray for female (a) and male (b) laminate optimization

6.2.3 Mold Shape Optimization Results and Discussion

With the constraints applied to the three-dimensional models, optimization was next conducted with the objective of minimizing compliance. Like ply topology optimization, the 3D optimization within Altair Inspire is a gradient based iterative process which continually evaluates structural performance with respect to constraints, while progressively eliminating and reorienting elements to support the goal of reducing mass. Inspire uses a process referred to as Non-Uniform Rational Basis Spline (NURBS) which re-meshes the structure throughout the process with 3D elements to create smooth contours on the developed structure [137]. NURBS 3D element modeling is advantageous for composite structures as it creates optimized shapes with smooth contours that would allow plies to be easily draped over the contours.

After the iterative optimization process was complete, the procedure was successful in developing two mold shapes, as shown in Figure 51 (a) and (b). The structural alternatives represent shapes that provide the minimum compliance achievable based on the in-plane laminate properties and established constraints. From the figure it can be noted that varying the boundary condition for the optimization did result in two unique mold geometries. The mold shown in Figure 51 (a) would be suitable for a female layup procedure as the spread-out contours towards the top of the part would allow for hand access to the interior of the mold. The mold shape shown in Figure 51 (b), however, would be better suited for a male molded part as the "V" shape developed would make interior hand access for female molding difficult.

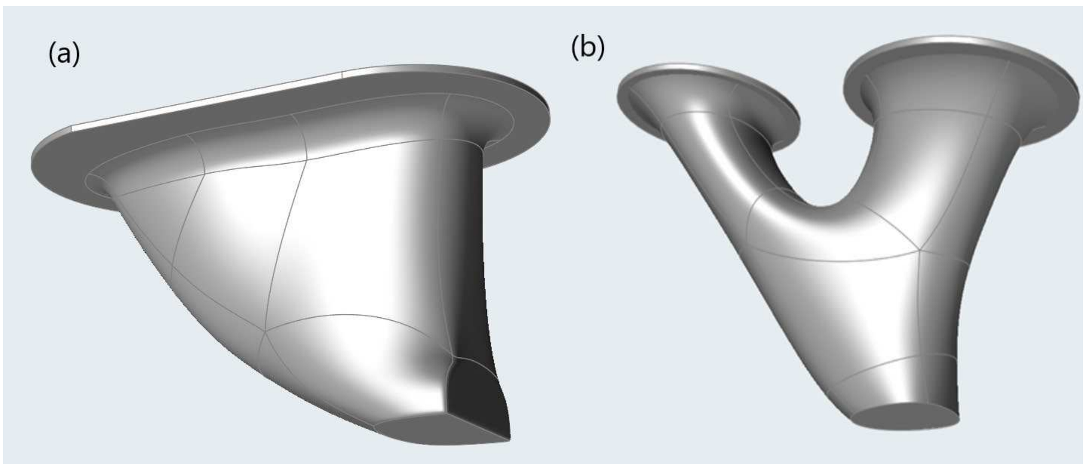

Figure 51 Optimized shape developed female (a) and male (b) mold shapes

The advantages of 3D element optimization are evident in the two developed mold shapes. The smooth contours of both molds would not have been developed through 2D element optimization. These smooth contours provide benefits to composite material application in the form of improved manufacturability and structural efficiency. As explained in Chapter 4, rounded contours are advantageous for composite manufacturability due to improved ply drapability. The smooth contours are also advantageous to structural efficiency as they allow for more efficient load transfer.

The advantages of the laminate optimization process are evident when comparing the optimized male molded structure to a common steel anchor bracket design currently used in rail vehicles. Figure 52 provides a visual comparison of the male molded shape developed for composites through optimization and a common cast steel anchor bracket on an actual US commuter train car. The development of the 'V' shaped contour for the male molded laminate provides validation that the process can automatically create structural shapes that have previously required detailed engineering efforts by vehicle designers to identify.

Figure 52 Comparison of the optimized male mold shape (a) compared with an actual steel anchor bracket design (b)

As explained in Chapter 2, many research studies have imported structural shapes such as those shown in Figure 52 (b), as a mold geometry and applied composites materials to that shape. As explained in Chapter 4, however, the sharp angles between the faces of the steel anchor bracket that are acceptable with steel castings would not be ideal for composite materials due to wrinkling that can occur when draping plies over tight curvatures[60]. As also explained in Chapter 4, those sharp angles between sections of cast steel structural shape can often necessitate laminates to be partitioned into numerous sections, increasing the complexity of the design [12]. Partitioning the structure also reduces efficiency as it does not allow fiber strands to extend between sections of the structure.

Instead of reusing a steel geometry like the one in Figure 52 (b), to create a black metal composite structure, as has been done in many studies, the fully optimized methodology of the final experiment created mold shapes that are better suited for composites. The rounded contours developed through mold optimization provides improved manufacturability and structural efficiency when compared a steel geometry like the one in Figure 52 (b). Furthermore, these smooth contours would also allow for reduced partitioning of the structures compared to a black metal design. Therefore, the mold optimization process demonstrates promise as a methodology that can be used to develop replacement structural geometries that are better suited for composite application than existing black metal structural shapes.

While both developed mold shapes represent promising geometries for composite application, the structure developed for a female mold would be the preferred alternative for an anchor bracket design. This is because parts produced in a female mold offer improved exterior environmental resistance that would be required of the service conditions [138]. During composite manufacturing surfaces in contact with a mold obtain an improved finish when compared to surfaces that cure without contact to a mold. A benefit of a finished surface is improved environmental resistance to water. As the anchor bracket structure is mounted underneath a rail car, this type of environmental resistance would be necessary. For the male molded part, either an outer surface coating could be added, or the part could be produced through a matched molding process where both the inner and outer surfaces of the laminate are in contact with a mold to provide the required environmental resistance. In both cases, however, additional manufacturing effort and complexity would be required, so the simpler female mold shape was selected for further analyses and experimentation.

6.2.4 Mold to Laminate Conversion

With the structural shape optimized for a female mold selected, the next step in the proposed optimization is to re-mesh the structure with two-dimensional elements to create a laminate model. As explained in Chapter 4, this is done by extracting the interior surfaces of the mold shape and meshing them with shell elements. Once completed the optimized volume created with three-dimensional elements is eliminated and a hollow contour representing the laminate surface remains. The hollow mold surface re-meshed with two-dimensional elements is shown in Figure 53. It can be seen from the figure that the resulting mold surface provides an interior cavity that would allow for access to conduct hand layup within the mold. This represents an improvement over many black metal designs, and the methodology applied in the literature reviewed, where the structural geometry was developed around metallic manufacturing procedures and are not suitable for composite manufacturing such as hand layup [22].

Figure 53 Developed mold cavity and mold shape, modeled from 3D elements with quasi-isotropic properties

Figure 53 also shows that holes were added to the laminate to represent connections to the vehicle side sill and the traction rods where loads would be applied. These types of features cannot be automatically generated or included in the laminate optimization process and must be added manually after completing the process.

6.3 Step Two: Ply Optimization

The process for ply optimization is summarized in Figure 47and Figure 48, and involves draping analyses, ply topology optimization, and production simulations. Although all of these processes have never been integrated together fully in previous research, recent studies have demonstrated the benefits of integrating multiple ply optimization processes [9]–[13], [46]. Therefore, the second step in the proposed methodology established during this research, and tested in the final experiment, represents the logical integration and advancement of established ply optimization methodologies.

6.3.1 Partially Optimized Black Metal Model

To test the hypothesis as part of the final experiment, and to serve as an experimental control, a second partially optimized design model was needed. The second model was to be developed only through the ply optimization step, summarized in Figure 48. This second model is a control because it does not incorporate the laminate optimization step. Without the laminate optimization, this means that the starting structure would be a black metal design, similar to that used in the preliminary experiment. As summarized in the discussion section of the preliminary experiment (Section 3.6), however, there were several assumptions and simplifications included in the modeling of the preliminary black metal design. Therefore, it was necessary for these assumptions and simplifications to be eliminated during the ply optimization step to improve the accuracy of the final experiment results for this black metal geometry.

The first simplification made during the preliminary experiment was the modeling of the cast piece at the base of the anchor bracket Structure. During the preliminary experiment this substructure was modeled as a steel cast block due to geometric complexity and to simplify the modeling effort. For the final experiment the cast steel block was removed from the control model and replaced by a hollow composite substructure that could realistically be molded with FRP material. Figure 54 illustrates the replacement of the cast steel block with composite material for the black metal control design used in the final experiment.

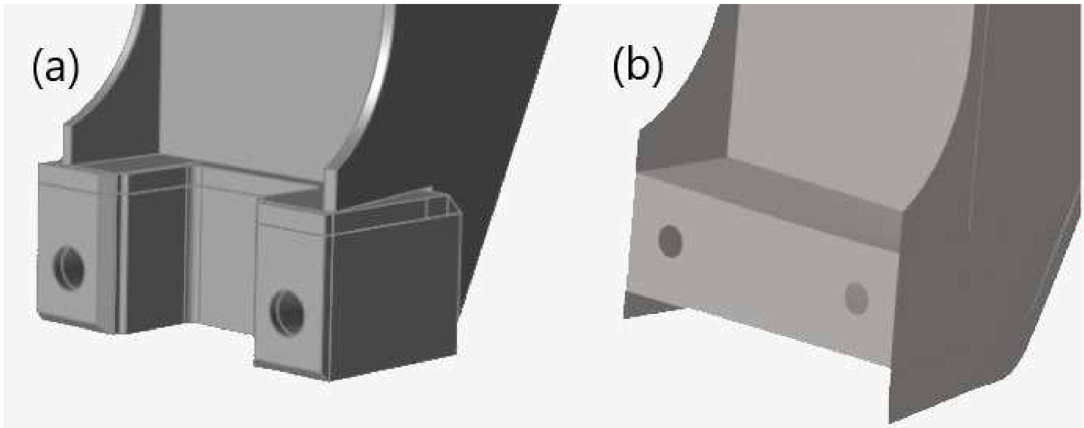

Figure 54 Replacement of solid casting used in the preliminary experiment (a) with hollow structure for composite application in the final experiment (b)

The other major simplification and assumption made during the preliminary experiment had to do with the modeling of connections between laminate regions. This modeling simplification was corrected through draping analysis and improved modeling of connections which will be explained in the following subsection.

6.3.2 Conduct Draping Analysis

Ply draping was not included in the preliminary experiment to simplify the modeling effort. As discussed in Section 4.3.1 ply draping can improve overall composite shape optimization by partitioning ply areas to improve manufacturability and performance. Ply draping also offers the additional benefit of providing preliminary validation of a design by simulating the effects of manufacturing on a structures shape and performance. As explained in Section 4.3.1, ply draping software simulates the effects that draping FRP over a mold can have on ply topology due to fabric shear and wrinkling. For large and complex structures, such as the anchor bracket, the effects of wrinkling and fabric shear on structural performance can be significant [123]. Based on the benefits demonstrated in the literature reviewed, ply draping was added to the ply optimization process for the final experiment [143]. The methodology included in the final experiment adds new knowledge to what has been published to date by combining ply topology optimization with ply draping to develop improved performance.

To investigate ply draping effects with respect to the anchor bracket designs, the two FEA models were next updated through simulation. In both models, plies were initially modeled with identical geometry to the overall part, forming an integral part. These integral ply shapes were formed so that an optimal partitioning of ply regions could be completed based on drapability in a later step. Integral quasi-isotropic laminates were created for both models that included two plies for each fiber angle orientation to assess the effects of ply draping on each of them. Like the preliminary experiment, the final experiment assumed all plies would be laid up in four typical unidirectional orientations: 0°, 45°, -45°, and 90° to form 8 ply quasi-isotropic laminates, as shown in Figure 55.

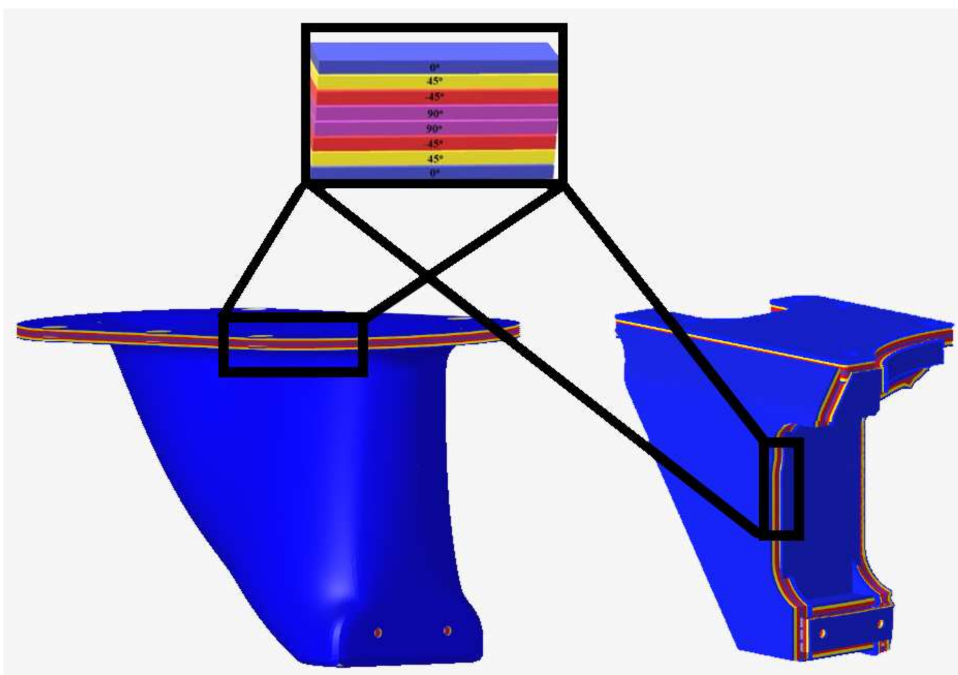

Figure 55 Integral quasi-isotropic laminates applied to both designs

When plies are draped over complex mold surfaces plies can bunch and wrinkle causing fabric shear which locally distorts fiber angle, but this detail is neglected in FEA modeling unless draping analysis is conducted [122]. As explained in Section 4.3.1, typical composite modeling practice is to orient fiber angles within each element to a model coordinate axis (X, Y, or Z). Figure 56 (a) shows this typical fiber orientation for the fully optimized model. Here fibers are all oriented in the same model direction, regardless of the complex geometry in some regions of the structure. During draping simulation, however, the fiber angle within each element is instead oriented to simulate the effects of a ply being draped those complex regions. In Figure 56 (b) fiber angles have been locally skewed following draping analyses. The high degree of fiber angle deviation in the structure would lead to wrinkling and suboptimal performance.

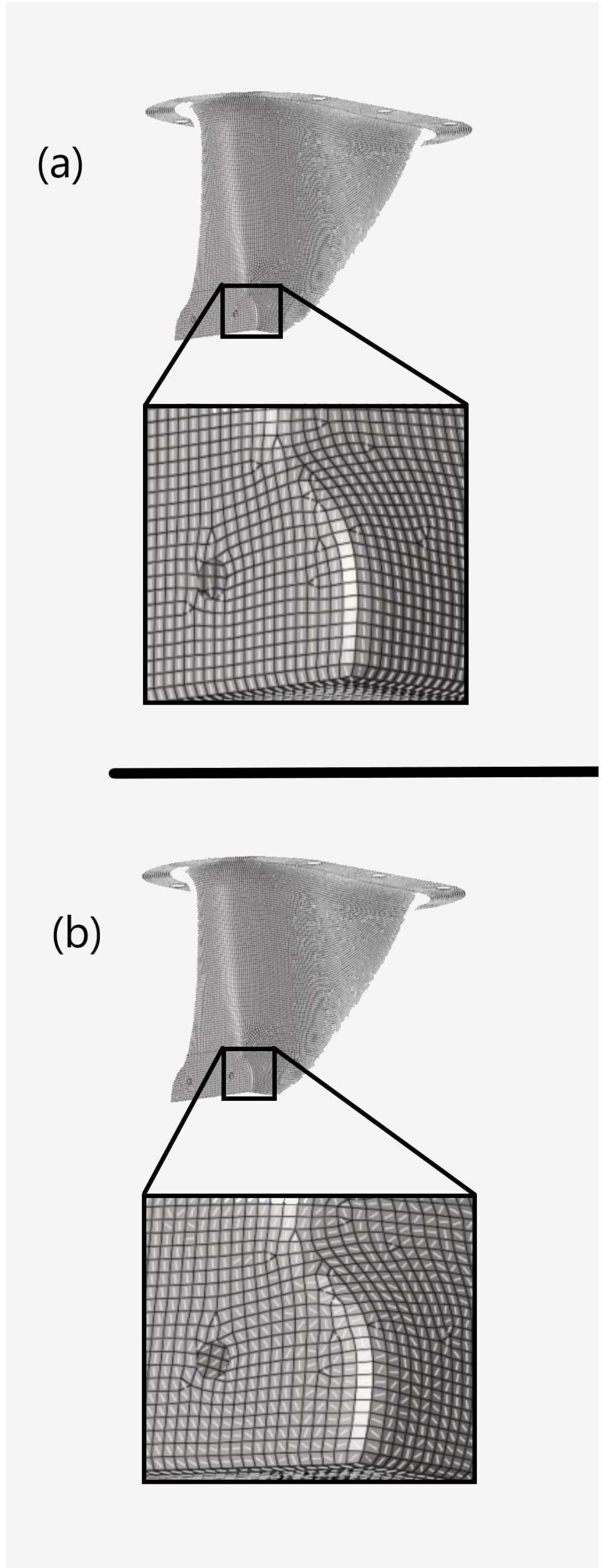

Figure 56 Example of fully optimized integral ply fiber angles without (a) and with (b) the effect of draping

FEA programs typically include a process called kinematic draping which assesses those local distortions and partitions ply regions to optimize drapability over a defined mold geometry. The next step in the optimization of the two design models was to conduct kinematic draping simulations. The kinematic process evaluates the initial integral ply geometries and partitions ply shapes to reduce fabric shear and wrinkling. Partitioning the fully optimized structure through kinematic draping analyses resulted in two segments, while the partially optimized structure was divided into five segments. Figure 57 depict the ply regions identified by the draping simulator for the fully optimized design. Figure 58 provides an example fiber angle definition within the fully optimized model following ply partitioning. Comparing these results to those shown in Figure 56 for the integral plies without kinematic draping shows improvement in fabric shear and wrinkling. The fiber angle definition following kinematic draping still accurately accounts for mold geometry, but through partitioning fiber angle transitions are more gradual, improving performance. Similarly, the partially optimized model was also partitioned using kinematic draping, Figure 59 shows the five identified ply regions for that design.

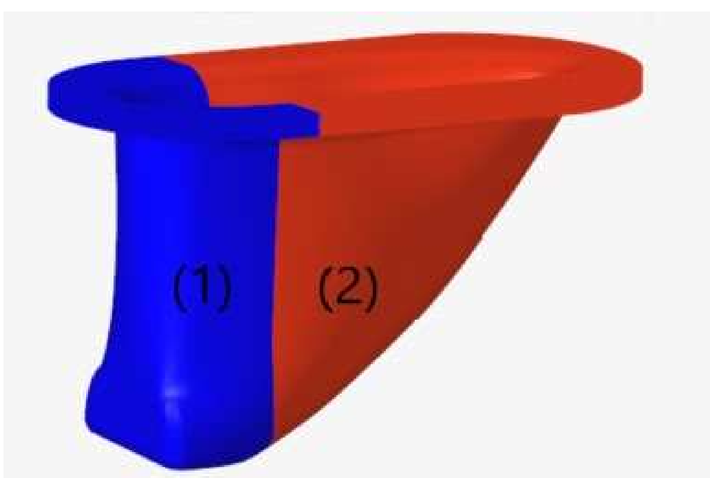

Figure 57 Fully optimized design segmented into two ply regions through kinematic draping

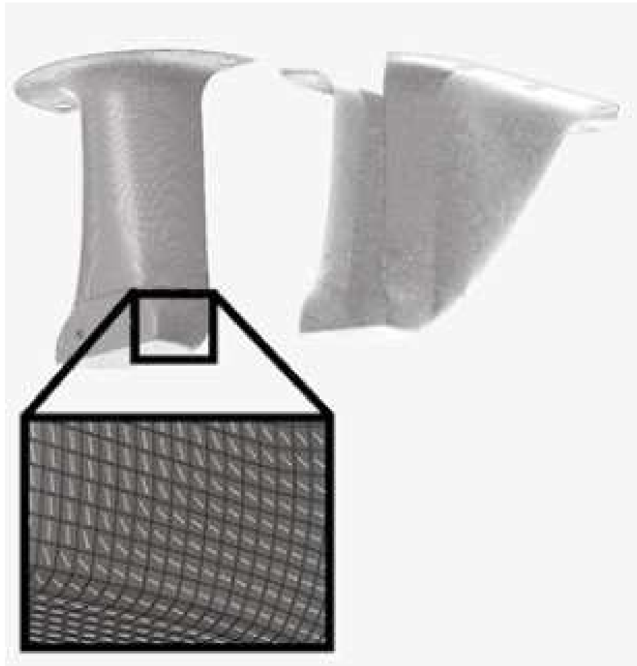

Figure 58 Reduced fabric shear in fully optimized plies following kinematic partitioning of the structure

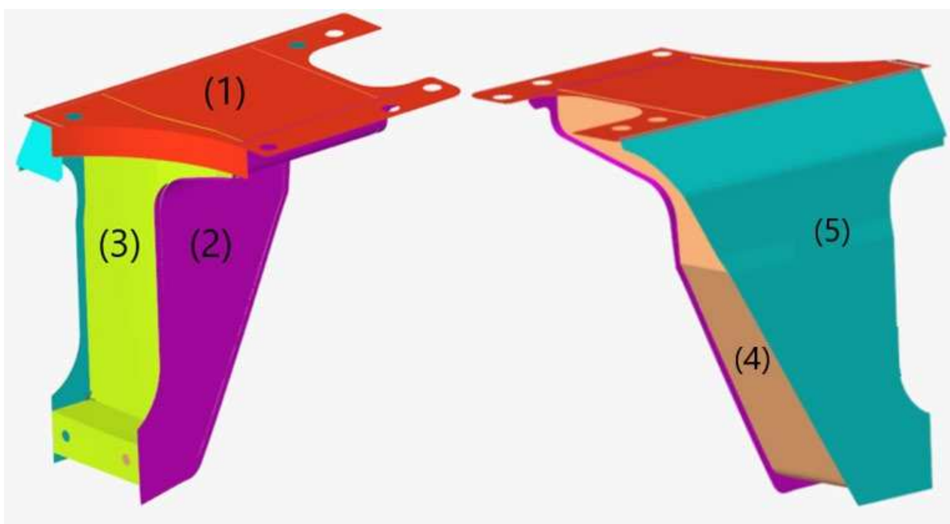

Figure 59 Partially optimized design segmented into five ply regions through kinematic draping

A feature not included in the kinematic draping analysis is the development of connections between the partitioned areas. This is, however, an important step in accurately modeling a composite structure, as joints can create stress concentration that reduces structural performance [144]. Based on an analysis of the draping results, connecting regions between the partitioned sections in both models were identified where joints of a maximum length could be formed without creating substantial fiber shear or wrinkling, as shown in Figure 60 and Figure 61. For the fully optimized model the overlap region could be formed by extending plies from the back portioned ply region towards the front of the structure to form an effective overlap for the joints. For the partially optimized black metal structure, however, extending plies to span the sharp angles between the 5 partitioned zones caused significant wrinkling and fabric shear, so "L" shaped ply regions, or clips, had to be created inside the structure, to carry the loads from one partitioned area to the next, effectively connecting the structure. These joints corrected the second, and final, major simplification made during the preliminary experiment for the black metal structure, that neglected the details of how the laminate areas were connected.

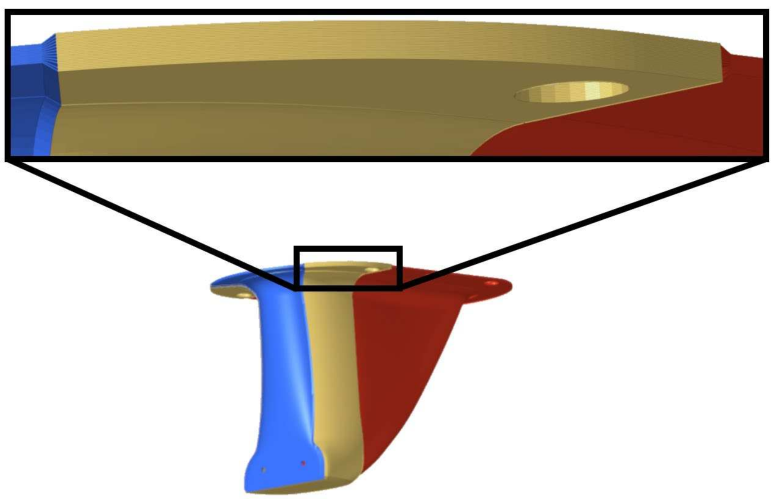

Figure 60 Ply regions with connections for fully optimized model

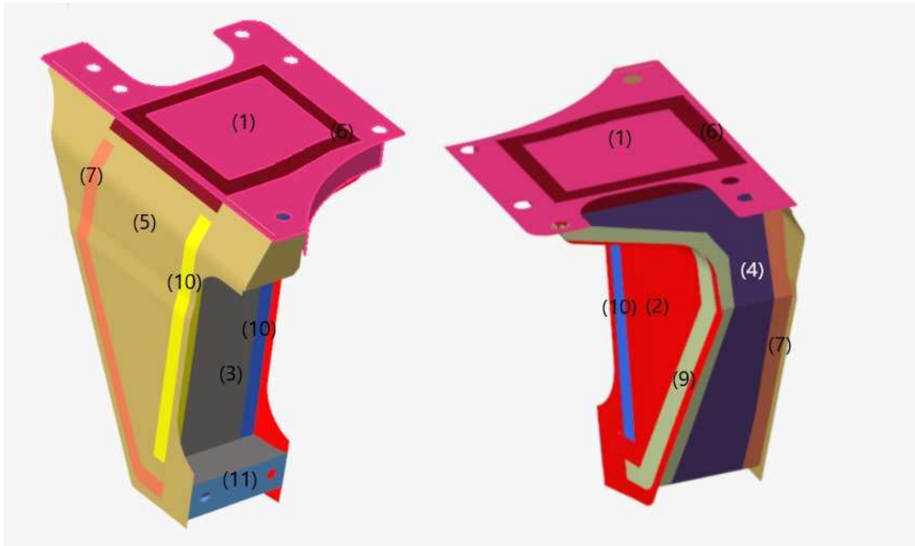

Figure 61 Ply laminate regions with connections for partially optimized model

As also explained in Section 4.3.1, an associated effect of fabric shear is thickness variations in the draped plies. These thickness variations simulate wrinkling, and the reduced performance of the ply. During draping simulation manufacturable ply thickness values are entered by the designer, and the FEA solver uses equation 7 (explained in Section 4.3.1) to calculate local thickness variations at each element. For the final experiment, the manufacturable ply thickness was set to 0.19 mm (based on material testing reports discussed in Section 3.3). Figure 62 through Figure 73 show the thickness variations in the ply regions for the fully optimized and partially optimized models following kinematic draping. The numbering in the figures is consistent with the ply region summaries shown in Figure 60 and Figure 61. The thickness plots demonstrate that except for minor localized wrinkling, the plies have relatively uniform thickness that is close to the 0.19 mm manufacturable target thickness following the partitioning process.

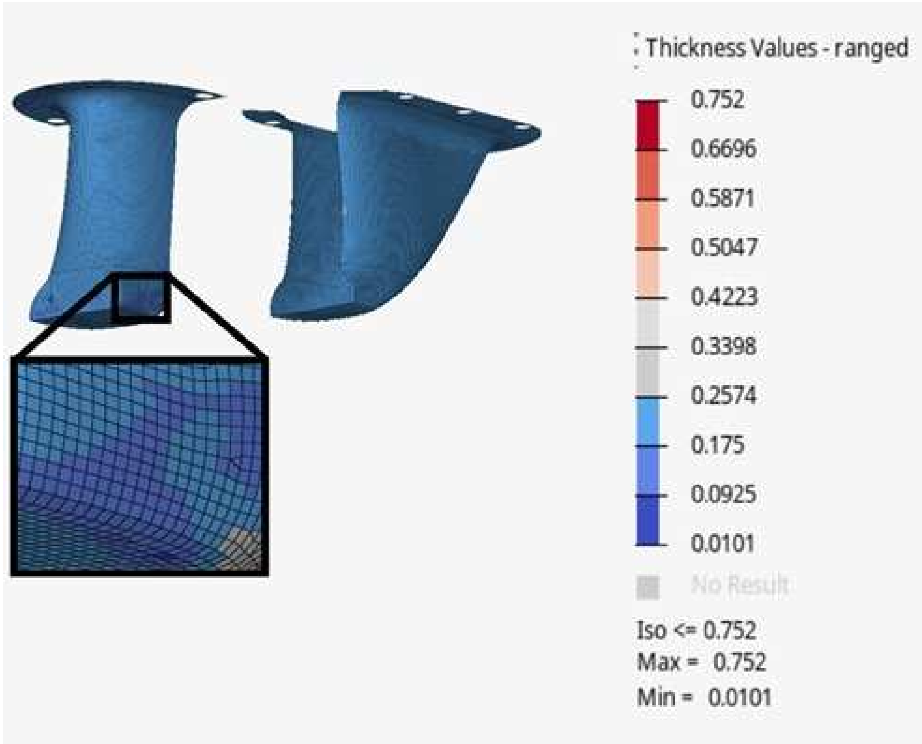

Figure 62 Draping thickness (mm) variation for fully optimized model ply regions 1 and 2

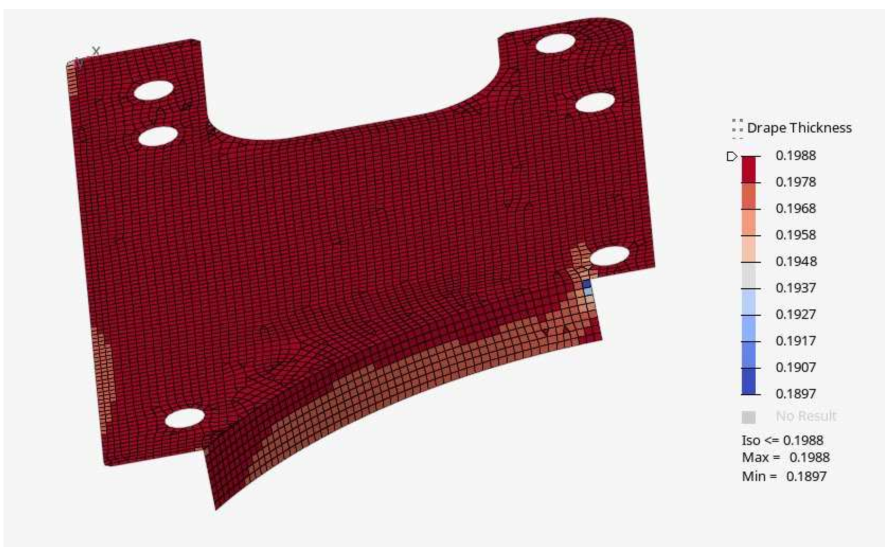

Figure 63 Draping thickness (mm) variation for partially optimized model ply region 1

Figure 64 Draping thickness (mm) variation for partially optimized model ply region 2

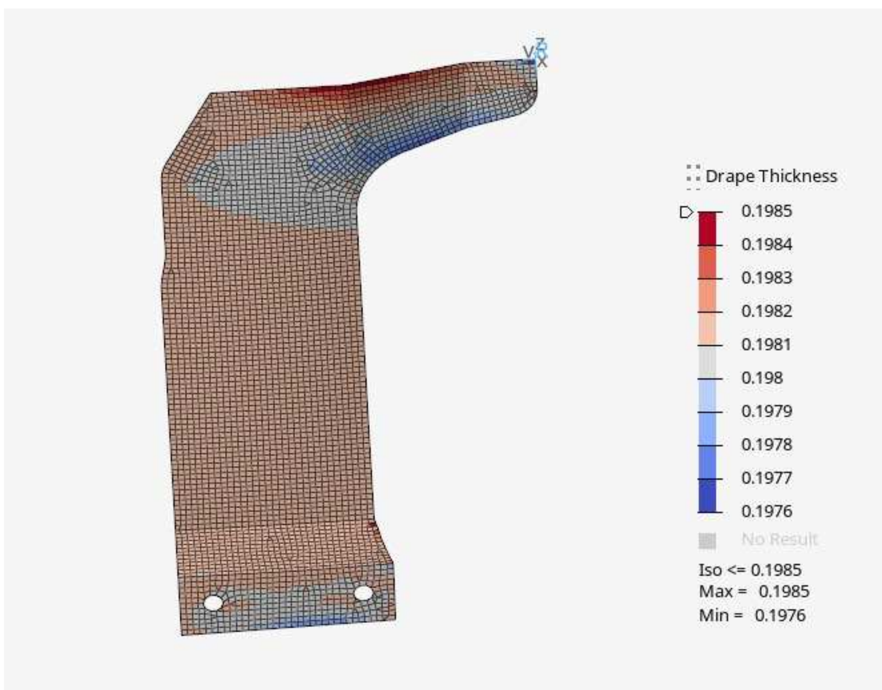

Figure 65 Draping thickness (mm) variation for partially optimized model ply region 3

Figure 66 Draping thickness (mm) variation for partially optimized model ply region 4

Figure 67 Draping thickness (mm) variation for partially optimized model ply region 5

Figure 68 Draping thickness (mm) variation for partially optimized model ply region 6

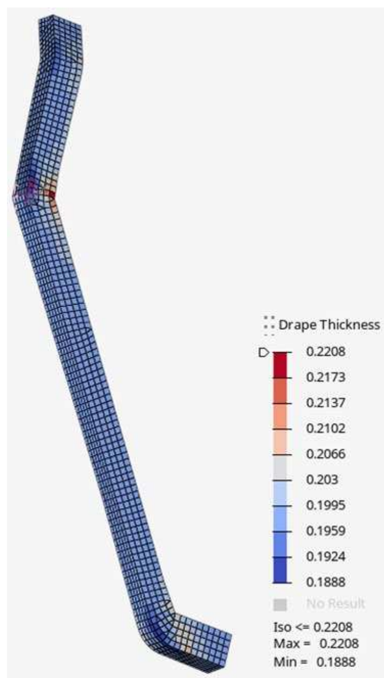

Figure 69 Draping thickness (mm) variation for partially optimized model ply region 7

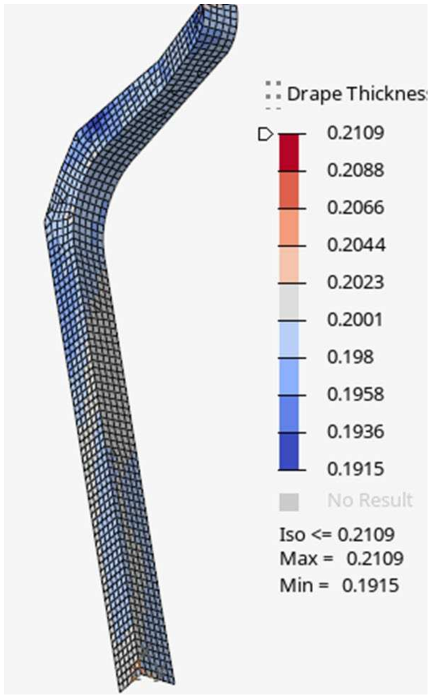

Figure 70 Draping thickness (mm) variation for partially optimized model ply region 8

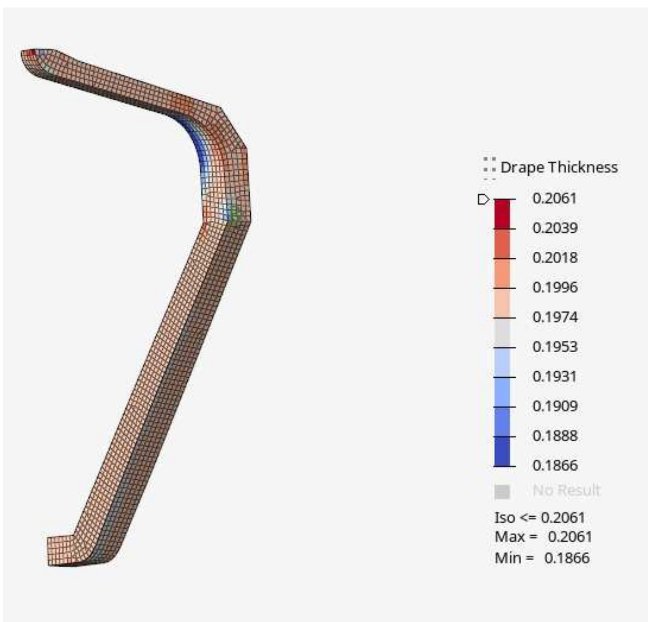

Figure 71 Draping thickness (mm) variation for partially optimized model ply region 9

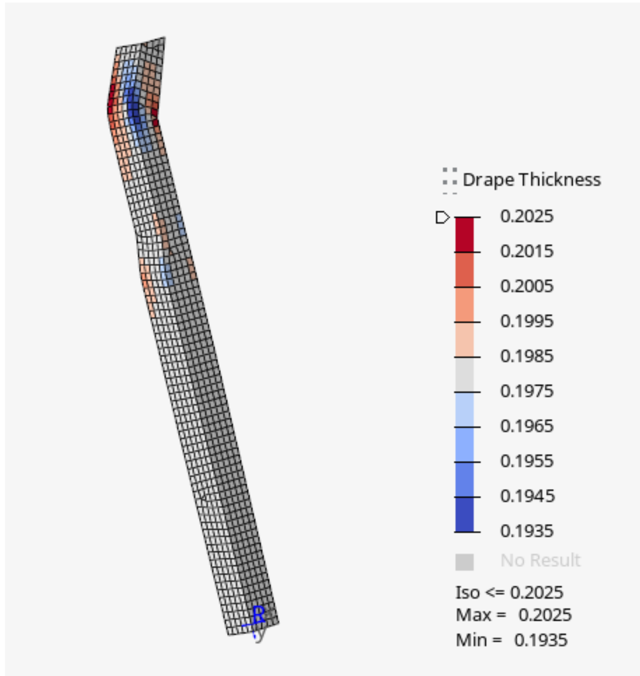

Figure 72 Draping thickness (mm) variation for partially optimized model ply region 10

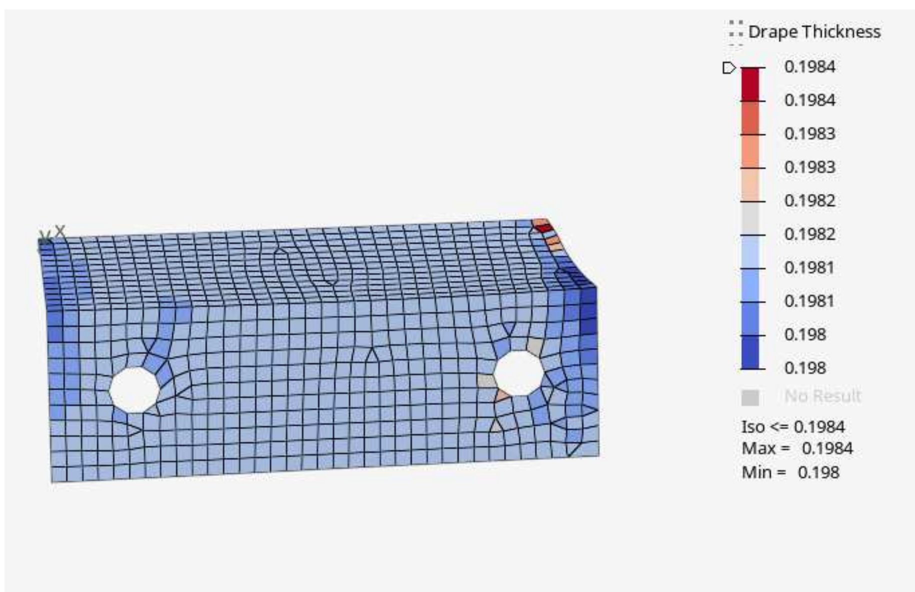

Figure 73 Draping thickness (mm) variation for partially optimized model ply region 11

6.3.2.1 Draping Analysis Results and Discussion

The kinematic draping process was successful in partitioning both structural geometries with respect to the composite specific design criteria of minimized fabric shear. This is an advantage over the methodology noted in many black metal optimization studies where partitioning was based on metallic material manufacturing constraints such as welding and plate forming [60]. The draping analysis also provided a preliminary validation of both designs by accurately simulating ply performance when molded to form all required structural shapes. For both structures the partitioned sections reduced fabric shear to acceptable levels, improving performance of the structure. Furthermore, all partitioned sections had minimal variations in ply thickness following partitioning, which is also preferred from a structural performance perspective.

For the partially optimized model, the kinematic draping process and joint detail definition further emphasizes the deficiencies of black metal design and optimization methodology. It is generally understood that composites offer the potential to reduce the number of structural components when replacing metallic materials [145]. This was initially the case following kinematic draping, as the number of components was reduced from 8 to 5. However, the often neglected process of defining and accurately modeling joints added another 6 components to the structure resulting in an actual increase in components from the 8 to 11.

For the fully optimized model, kinematic draping demonstrated the benefits that developing a mold geometry specific for composite applications can provide. Unlike the partially optimized model, the fully optimized design was able to reduce the number of components from 8 to 2. Additionally, the smooth contours of the fully optimized model allowed for overlap regions between partitioned sections to be formed without inducing additional fabric shear. Therefore, unlike the partially optimized model, the fully optimized design did not require additional ply regions or clips to join the partitioned regions. This decrease in components reduces the complexity of the design and would likely result in improved manufacturability, although that will be confirmed in the later process of manufacturing simulation.

6.3.3 Optimize Ply Topology

With the two FEA models draped, partitioned, and connections accurately modeled, the next step was to formulate the ply topology optimization process. The topology optimization methodology used in the final experiment was consistent with that applied in the preliminary experiment and explained in Sections 3.5. To re-summarize, the ply topology optimization process is governed by an algorithm that is formulated by the user. The algorithm for the final experiment matched that used in preliminary experiment, and is governed by the previously presented Equation 6:

$$\text{minimize } f(x) \tag{6}$$

subject to

$C \leq 3.820\text{E-}09 \text{ mm/N},$
$F \leq 1,$

$T = 0.19$ mm
$P \leq 2,$

Where *f(x)* is the objective function, set to minimize mass. The constraints on the optimization process are compliance (*C*), Max Stress failure criterion (*F*), minimum laminate thickness *(Lx),* manufacturable ply thickness used during the sizing optimization *(T),* and the maximum number of successive plies of any angle used during shuffling optimization (*P*).

As explained in Chapter 3 (subsection 3.5), the first step in ply optimization is to create models where the ply geometries match the partitioned sections for both structures. In the preliminary experiment the partitions were dictated by the black metal geometry, whereas in the final experiment the partitions were established through the ply draping process that was explained in the previous subsection.

As explained in Chapter 3 (subsection 3.5), during the early stages of ply optimization ply thickness is not accurate, and instead plies are treated as candidate "stacks" of plies for the optimizer to choose from. As also explained in that subsection, prior to ply optimization the thickness of the ply stacks should be increased from the values listed in the material testing reports, and used during the draping process, until the structures can meet all the constraints established in Equation 6. For the fully integrated model the plies had to be increased to a nominal thickness of 5 mm, whereas the partial integration model required plies to be 8 mm thick to start.

In the preliminary experiment ply stacks had uniform thickness following the thickening process, as ply draping was not integrated into the methodology. In the final experiment, however, ply draping caused the thickness to be non-uniform throughout the ply stacks due to fabric shear and wrinkling. Figure 74 provides a visual example of this for a 0° ply stack from partitioned section 1 of the fully optimized model. In the figure it can be seen that the majority of the ply stack area matches the nominal thickness input by the user of 5 mm. There are, however, local distortions within the ply stack that cause the overall thickness to vary between 0.27 and 20 mm prior to ply optimization.

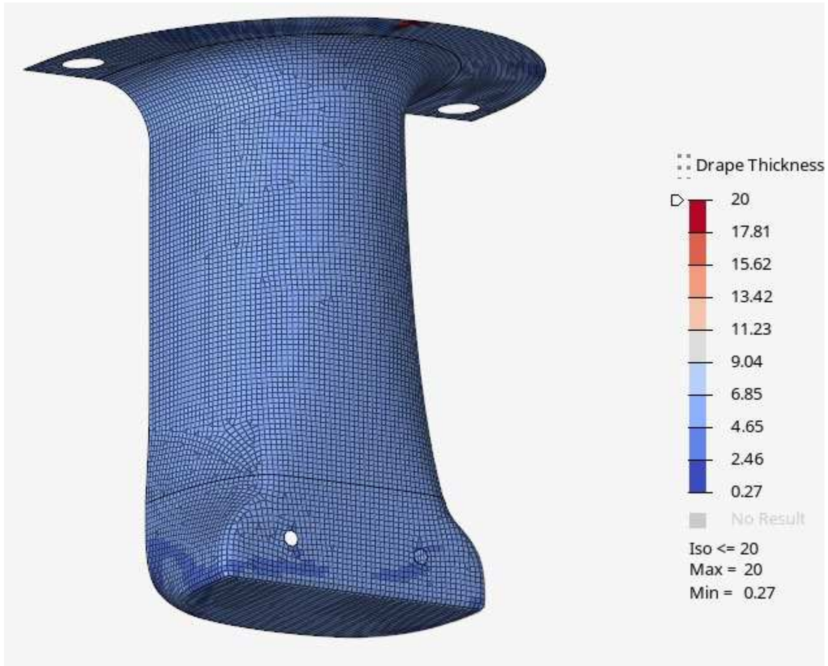

Figure 74 Example ply stack thickness (0° ply stack from partitioned section 1 of the fully optimized model) prior to ply optimization

With the nominal ply stack thickness set to values that met the constraints of the optimization algorithm, the models were ready to begin the ply topology optimization process. As explained in Chapter 3 (subsection 3.5), ply topology optimization is completed through three major subprocesses: free sizing, sizing and shuffling. During free-sizing the optimization process identifies optimal shapes and section thicknesses for each ply type from stacks in the initial models. Following free-sizing, the models have more ply stacks than the initial models, the overall laminate thicknesses have changed, the ply stacks do not have uniform shape or thickness, and the ply stacks are still unrealistically thick. During the second optimization step of sizing the stacks of each orientation developed during free-sizing are subdivided into actual manufacturable thicknesses. During sizing the nominal ply thickness is reset to match the 0.19 mm value listed in the NCAMP material report, but the plies still have variable thickness based on the draping simulation results [78]. Following sizing, there are numerous plies of the same fiber orientation stacked consecutively, so the third and final optimization process of shuffling reorganizes the plies within each laminate to ensure that plies of each fiber orientation are dispersed. This is done to reduce interlaminar forces that can develop when numerous plies of a particular orientation are stacked consecutively.

6.3.3.1 Ply Topology Optimization Results

Both the partially integrated and fully integrated optimization processes converged on solutions which offered mass savings over the 48.36 kg existing steel structure. As explained in Chapter 3, ply topology optimization is completed through iterative derivation of the defined algorithm until a solution is found. Figure 75 shows the iterative results during free size optimization for the partially optimized model. Prior to optimization the partially optimized model had a mass of 55.88 kg, as the 88 plies in the structure were thickened to meet the defined constraints. The figure shows that following 5 derivations of the optimization algorithm, the mass of the structure was reduced to 41.66 kg.

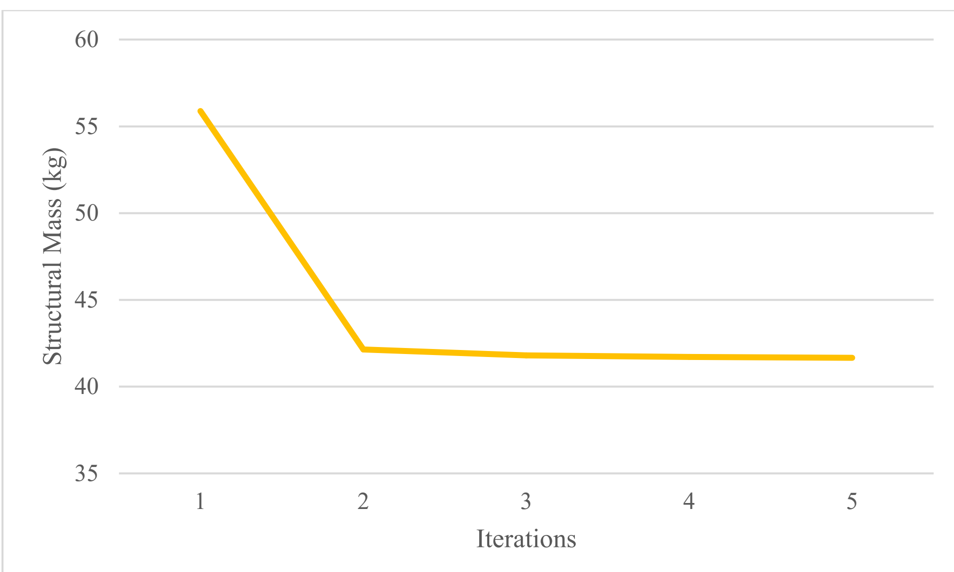

Figure 75 Iterative gradient descent free size results for the partially optimized model

While the mass of the structure was reduced following free size, the subsequent subprocess of sizing had to be conducted to resize the ply stacks to meet the nominal manufacturable ply thickness (0.19 mm) available commercially and defined in the material testing report [78]. Following free sizing the partially optimized model had 328 ply stacks of variable nominal thickness. Following the sizing subprocess, however, the structure had 3,149 plies each with a nominal thickness of 0.19 mm. Also following sizing, the thickness within each ply deviated from the nominal value based on the draping data generated previously. Because the ply stacks generated in the previous steps were not exactly divisible by the manufacturable thickness, the overall structural mass increased slightly during sizing from 41.66 kg to 42.50 kg.

The last subprocess of ply optimization is shuffling which is conducted following the sizing optimization. Shuffling reorganizes the plies within the laminate to disburse plies of the same orientation. As explained in the previous subsection the shuffling optimization process for the final experiment was set so that no more than two plies of any orientation could be stacked consecutively within a laminate. The shuffling subprocess was successful in shuffling the ply order within the two structures so that no more than two plies of any fiber orientation were laid up consecutively. Following shuffling the number of plies and overall structural mass remained the same from the sizing subprocess.

Figure 76 (a) shows that the partial optimization model met the failure criterion constraint following optimization. Comparing Figure 76 (a) to Figure 76 (b), it is apparent that the topology optimization process left the connection areas of the partially optimized structure thicker (up to 76.72 mm) to prevent failure. Figure 76 (b) also shows that the structure had an average laminate thickness of roughly 45 mm in areas outside of the connections. Figure 76 (c) shows the partial optimization model ply shapes following the topology optimization process. Table 6 provides a summary of how the partially optimized model was altered throughout the three topology optimization subprocesses.

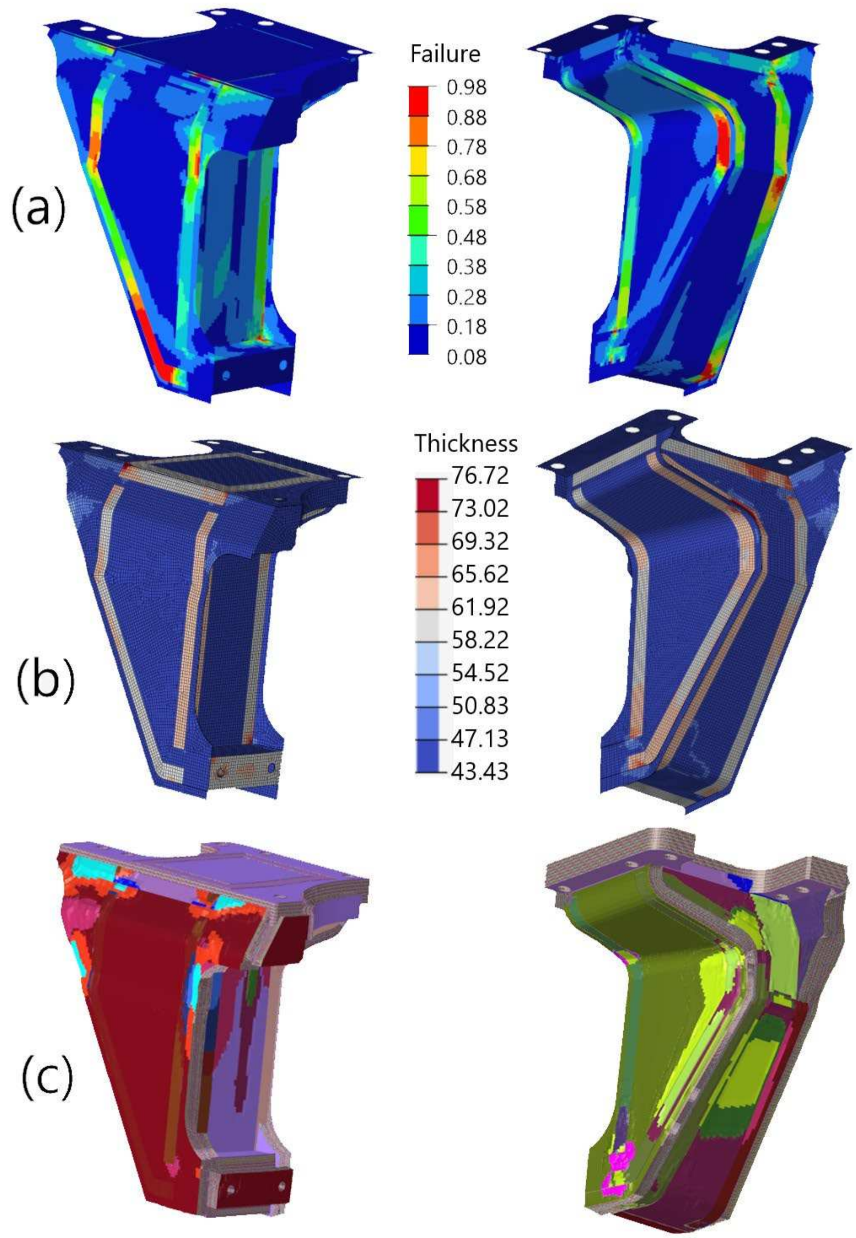

Figure 76 Partially optimized ply topology optimization results: (a) max failure criteria values, (b) laminate thickness plots, (c) and ply shape details

Table 6 Partially optimized model ply optimization results

Model Property	(e) Steel Structure	(f) Composite model prior to optimization	(g) Free-Size Model	(h) Sizing Model	(e) Shuffling Model
Plies in partitioned area 1	0	8	8	232	232
Plies in partitioned area 2	0	8	32	289	289
Plies in partitioned area 3	0	8	32	286	286
Plies in partitioned area 4	0	8	32	293	293
Plies in partitioned area 5	0	8	32	299	299
Plies in partitioned area 6	0	8	32	287	287
Plies in partitioned area 7	0	8	32	268	268
Plies in partitioned area 8	0	8	32	300	300
Plies in partitioned area 9	0	8	32	296	296
Plies in partitioned area 10	0	8	32	300	300
Plies in partitioned area 11	0	8	32	299	299
Total number of plies in structure	0	88	328	3,149	3,149
Average nominal ply thickness -mm	0	5	1.94	0.19	0.19
Total structural mass - kg	48.36	55.88	41.66	42.50	42.50

The fully optimized model was also able to achieve mass reduction compared to the original steel design following ply optimization. Figure 77 shows the iterative gradient based mass reductions for the fully optimized model. In the figure it can be seen that the mass of the structure was 66.79 kg after the plies were thickened to meet the optimization constraints, but after six iterations the mass was reduced to 24.19 kg.

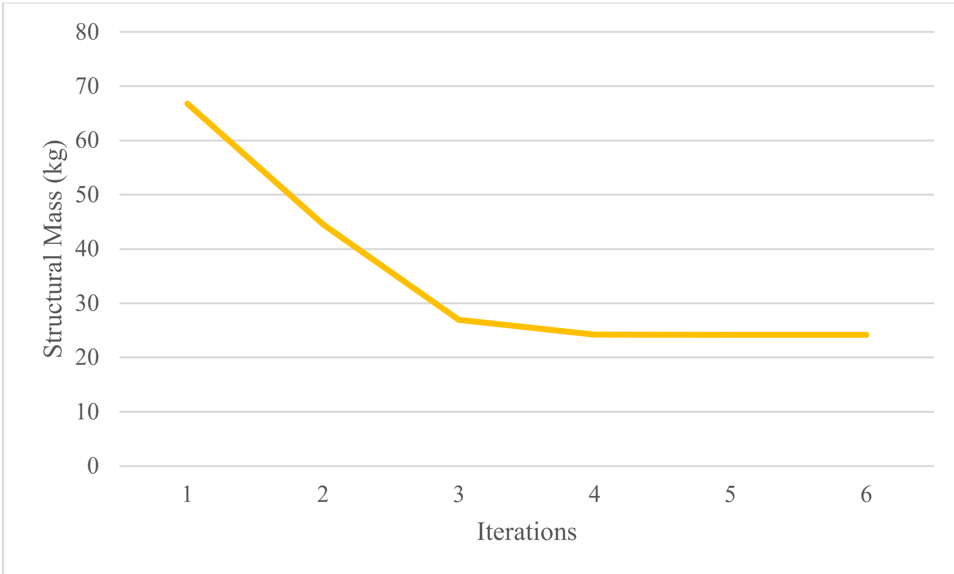

Figure 77 Iterative gradient descent free size results for the fully optimized model

Table 7 provides a summary of how the fully optimized model was modified throughout the three topology optimization subprocesses. Like the partially optimized model, the mass of the fully optimized model increased slightly during the sizing optimization to 26.72 kg. This increased mass was due to the fact that the ply stacks were again not exactly divisible by the nominal manufacturable ply thickness of 0.19 mm. The division of the ply stacks also resulted in an increase in ply stacks from 56 to 194 manufacturable plies. Also like the partially optimized model, the shuffling optimization was successful in dispersing plies of the same orientation within the laminate so that no more than two plies of any orientation were stacked consecutively. The mass and the number of plies for the fully optimized structure also remained constant following the shuffling subprocess.

Table 7 Fully optimized model ply optimization results

Model Property	(i) Steel Structure	(j) Composite model prior to optimization	(k) Free-Size Model	(l) Sizing Model	(e) Shuffling Model
Plies in partitioned area 1	0	8	32	106	106
Plies in partitioned area 2	0	8	24	88	88
Total number of plies in structure	0	16	56	194	194
Average nominal ply thickness -mm	0	5	0.78	0.19	0.19
Total structural mass - kg	48.36	66.79	24.19	26.72	26.72

Figure 78 shows the fully optimized structure following all topology optimization subprocesses. Figure 78 (a) shows that the fully optimized structure met the failure criteria constraint. Figure 78 (b) shows that the structure had an average laminate thickness of approximately 24 mm following the optimization process. Similar to the partially optimized model, the fully optimized structure had thicker sections in the connecting regions between the partitioned sections to support the structural performance. Finally, Figure 78 (c) shows the fully optimized structure ply shapes following topology optimization.

Figure 78 Fully optimized ply topology optimization results: (a) max failure criteria values, (b) laminate thickness plots, (c) and ply shape details

6.3.3.2 Ply Topology Optimization Discussion

Similar to the preliminary experiment, the results of the final experimentation demonstrate that composites can be used to create complex structures which support heavy loads. There are, however, new conclusions that can be drawn from the final experimentation's topology optimization process that were not apparent in the preliminary experiment. These conclusions are related to the improved accuracy when assumptions and simplifications are removed from ply optimization process, the advantages of optimizing mold shape prior to ply optimization, and the synergies between kinematic draping and ply optimization.

When comparing the black metal structure from the preliminary experiment to the partially optimized model in the final experiment, it can be concluded that the common assumptions and simplifications applied in the literature reviewed can result in inaccurate results. The total mass of the black metal structure from the preliminary experiment was 37.82 kg following ply optimization. During the final experiment the assumptions and simplifications included in the preliminary experiment relating to ignoring the connections between partitioned sections, modeling complex shapes with metals, and neglecting ply draping were eliminated. More accurately modeling the black metal structure through the partially optimized approach resulted in a total structural mass of 42.50 kg, an increase of over 12%. The number of plies also increased from 1,063 in the preliminary experiment model to 3,149 for the partially optimized model in the final experiment. This ply number increase of 196% once assumptions and simplifications were eliminated results in a structure that would be less feasible for manufacturing.

Accurately modeling connections between partitioned sections of the structures was one of the primary factors contributing to the differences in results from the preliminary and final experiments. Figure 79 provides a comparison of the thickness contours between the preliminary and final experimental models. From the Figure 79 (a) it can be seen that the maximum thickness in the preliminary experiment in the connection area was 38.71 mm, and that the thickness was inconsistent along the connection areas being as thin as 6.44 mmm in some areas. As previously discussed, however, the preliminary experiment mimicked common practice noted in literature where actual ply material was not modeled between the partitioned sections [60]. In the final experiment, however, the ply material and connections were accurately modeled which led to more consistent thickness in the connection area of the partially optimized structure of roughly 59 mm, as shown in Figure 79 (b).

When comparing the partially optimized and fully optimized models from the final experiment, it can also be concluded that optimizing mold shape prior to ply optimization offers advantages in structural performance and design. Comparing Figure 79 (b) with Figure 79 (c), it can be noted that the connection area of the fully optimized structure was able to be much thinner than the partially optimized structure. This is because the connection area on the fully optimized part was in an area where smooth contours were present. These contours led to lower failure criteria values and improved compliance, allowing the structure to be thinner in the connecting area.

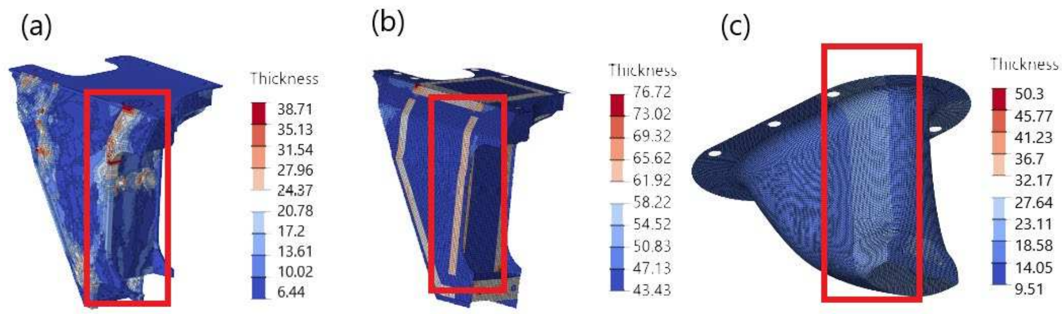

Figure 79 Comparison of laminate thickness (mm) for (a) the preliminary experiment model, (b) the partially optimized model, and (c) the fully optimized model

In addition to the connection areas, the fully optimized model also offered improvements in the form of greater mass reductions and reduced complexity for the overall structure. The fully optimized model had an overall structural mass of 26.72 kg following ply optimization, 37% lower than the partially optimized model. The fully optimized model also had only 194 plies, 94% fewer than the 3,149 plies for the partially optimized design. These results further emphasize that black metal geometries should not be used in applications where complex geometries or heavy loads are required. It also emphasizes that two-dimensional ply optimization is incapable of altering structural geometry to the extent necessary to make a black metal geometry suitable for composite application.

The final conclusion that can be drawn from this subprocess in the final experiment is that ply topology optimization and kinematic draping are complimentary processes that when properly integrated can improve the results of an optimization process. As discussed in subsection 6.3.2, the kinematic draping process defined partitioned ply geometries that minimized fabric shear. Following that process, however, there was some degree of fiber distortion and thickness variations within the plies. During ply topology optimization, however, each element within the ply is evaluated with respect to performance. Therefore, portions of ply area can be eliminated which further alleviates fabric shear and wrinkling. In industry these types of ply shape alterations are often made during prototyping and manufacturing as actual draping performance is better understood [146]. The integration of kinematic draping and topology optimization, however, presents a streamlined pathway for designers to efficiently develop ply shapes better suited for draping.

An example of how kinematic draping and ply topology optimization were complimentary in the design of the anchor bracket is illustrated in Figure 80. In the figure it can be seen that prior to optimization there was some degree of fabric shearing, wrinkling and thickness variation in the plies within partitioned region 1 of the fully optimized model. Following ply topology optimization, however, the ply was tailored in a way that almost completely eliminated these defects. Similar modifications were noted elsewhere in both structures.

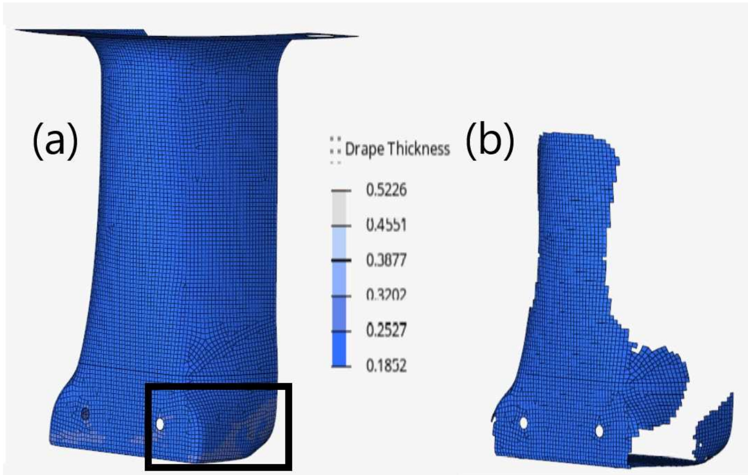

Figure 80 (a) Example of ply thickness (mm) following kinematic draping, and (b) tailoring following ply topology optimization to eliminate thickness variations and fabric shearing for a 0° ply within partitioned region 1 of the fully optimized model.

6.3.4 Conduct Production Simulation

As discussed in Chapter 4 (subsection 4.3), manufacturing simulation has been commonly cited as recommended practice to validate optimized composite structures [21]. This is because it can inform designers on the manufacturability of the developed geometry and structural details. Furthermore, manufacturing simulations can provide accurate costing data associated with the designs. In instances of light weighting, as was the intent of the final experiment, this can be important as extreme mass reductions may not be financially feasible. Instead, recommended practice is to review design alternatives, and determine if the mass reductions come with added costs. If weight savings do come with increased costs, the production simulation can provide a quantitative assessment of whether those increased costs are justified through operational benefit [10]. Therefore, conducting a production simulation of the partially optimized and fully optimized models was the final subprocess of the final experiment.

As also discussed in Chapter 4 (subsection 4.3), there are many types of production simulations used within the composites industry to validate designs. Bottom-up type simulations are recommended for new designs which have not been produced previously with composites, as they can most accurately predict the costs associated with new structural geometries [5]. Bottom-up simulation works by decomposing the production process into subprocesses. Costs for each subprocesses are then calculated by correlating industry pricing data against the specifics of the design being considered. As both the partially optimized and fully optimized designs have never been produced with composites before, a bottom-up simulation methodology was selected for integration into the final experiment.

SEER MFG by Galorath is the most widely cited and applied bottom-up cost estimation tool used within the composites industry, and therefore was selected for use as part of the final experiment [129]. SEER MFG simulations are comprehensive of all composite manufacturing subprocesses including engineering effort to design the production process and tooling, the labor to manufacture, finish, and inspect the parts for quality, and the composite and tooling materials required for production. SEER MFG contains a large set of proprietary equations to calculate costs and efforts to produce composite structures through a variety of manufacturing methods, including the hand layup and autoclave curing processes that were assumed in the design of the anchor brackets for the final experiment. The software also has a large library of materials and associated procurement costs, which included the carbon fiber epoxy prepreg materials that were modeled in the FEA program as part of the final experiment.

SEER MFG can import structural geometries, laminates, and ply details from FEA software to develop accurate costing for a specific part. The two composite structures, and associated laminate and ply information, were imported from the FEA program into SEER MFG to complete the simulation. SEER MFG assesses the ply and mold structural geometries imported from the FEA against its internal costing algorithms to complete the manufacturing simulation. The mold geometry is assessed within the program to determine curing details and the relative complexity of producing the tooling for the part. The ply geometries are used to calculate the labor required to lay the plies within the mold.

From the imported model details, and the prepreg material selected, a bottom-up production simulation framework was built up in the SEER MFG software, around two major subprocesses: hand layup and autoclave curing. As discussed in Chapter 4 (subsection 4.3), hand layup is the process of draping the prepreg plies into a mold to form the structural shape. The costs associated with the hand layup process are primarily due to the prepreg ply material and the labor-intensive process to drape the plies. Once hand layup is completed, the autoclave process is used to cure the epoxy resin that is impregnated into the plies of the structure. The autoclave uses heat and pressure to cure the resin. Multiple parts are typically loaded into a large, sealed autoclave and cured simultaneously. Unlike the layup process, curing is not labor intensive, but nitrogen gas is required to force out volatile gases that are produced during the process to avoid combustion at elevated temperature [147].

While specific parameters and equations within the software can be customized to represent specific manufacturing environments and material procurement details, for this study, the default equations and unit costs for labor and materials were used to provide average costs to produce the anchor bracket designs. A summary of key production parameters used within the program are provided in Table 8.

Table 8 Production simulation default parameters

Simulation Parameter	**Unit Detail**
Manufacturing Labor (Direct, Rework, Inspection)	$58.27/hour
Supervisory Labor (Setup)	$115.07/hour
AS4 Carbon Fiber Prepreg Material	$161/kg
Autoclave Nitrogen	$148.18/part

Like any manufacturing process, unit costs for composite manufacturing can be reduced in production environment as compared to a prototype part. As a result, for this case study, it was assumed that the anchor brackets were being manufactured as part of a 500-vehicle procurement. With four anchor brackets on every vehicle, this assumed a total production quantity of 2,000 brackets.

6.3.4.1 Production Simulation Results and Discussion

Table 9 provides a summary of the cost per unit associated with the partially optimized and fully optimized structures. The results of the simulation found that the fully optimized anchor bracket model could be produced for 56% less compared to the partially optimized structure. The cost differential was primarily associated with the increased complexity of the partially optimized design. Firstly, the partially optimized model required 2,955 more plies than the fully optimized model which resulted in a $2,500.46 higher material cost for that design. The increase in plies was also the primary driver in the $4,401.32 differential in labor costs required to produce the partially optimized design. Laying 3,149 plies per part is labor intensive, but also increases inspection and rework costs as the likelihood of defects increases. Finally, the tooling costs for the partially optimized design were more than ten times greater for the partially optimized model. This is because each partitioned region in a structure requires separate mold tooling during production. The partially optimized model had 11 partitioned regions, compared to only two for the fully optimized design, which created a significant increase in tooling costs per part.

Table 9 Cost summary for final designs

	Partially Optimized Design Cost/Unit	Fully Optimized Design Cost/Unit
LABOR TOTAL	**$5,540.24**	**$1,138.92**
Set-up	$446.18	$287.53
Direct	$4,741.86	$784.11
Inspection	$251.57	$48.06
Rework	$100.63	$19.22
ADDITIONAL COST	**$7,479.22**	**$4,490.22**
Material	$6,990.68	$4,450.10
Tooling	$488.54	$40.12
TOTAL COST	**$13,019.46**	**$5,629.14**

The production simulation provides useful insights into the manufacturing advantages offered by structures designed specifically for composites, and the potential detriments of black metal designs. The results of the simulation are logical, as the partially optimized structure has far greater complexity than the fully optimized design. Nonetheless, the process of conducting a production simulation was still valuable, as it provided validation that the fully optimized methodology provided improvements over a black metal partially optimized design. Furthermore, integrating this validation step into the overall optimization process can assist designers in avoiding major investments into the prototyping of a black metal structure.

6.4 Discussion of Final Experiment

In the final experiment a new integrated composite design and optimization methodology was tested. The methodology, which is summarized in Figure 46 of Chapter 5, consisted of two primary steps: mold and ply optimization. The methodology is divided into the steps to best utilize commercially available structural simulation tools. According to past research mold optimization should be conducted with three-dimensional elements to provide maximum geometric flexibility [115]. Unfortunately, current software does not allow for three-dimensional elements to be modeled with accurate anisotropic composite mechanical properties. Many applications, however, use laminate designs which have in-plane quasi-isotropic mechanical properties. As a method of approximation research has proposed applying the in-plane properties of a quasi-isotropic laminate to the three-dimensional elements, which is replicated in the first step of the proposed methodology.

In the second step, ply optimization, the developed three-dimensional geometry is converted to two-dimensional elements to more accurately model composite performance and to further optimize the design. Two dimensional elements are more commonly used in composite research, as commercially available software can accurately model anisotropic behaviors in two dimensions [7]. To date mold and ply optimization processes have never been integrated together to develop a fully optimized composite design, but the methodology proposed in this research and tested in this final experiment does so.

It was hypothesized that a composite structure designed through a fully integrated methodology that optimizes both the mold and ply geometry would demonstrate reduced costs, mass and improved manufacturability compared to a black metal structure that only ply optimization has been conducted on. To test this hypothesis a case study was conducted to design two composite anchor bracket structures for a rail vehicle. One anchor was created using the fully integrated optimization process, while the second black metal structure was only designed through the second step of ply optimization.

The first composite model created was a “fully optimized” design which fully integrated the two primary steps of the optimization process. During the first step of mold optimization the overall structural shape was formed by using three-dimensional elements. The structural shape was next converted to two-dimensional elements to complete the second step of ply optimization. In the second step the manufacturing process of draping was simulated on the overall structural shape to accurately model performance. The process of kinematic draping was also integrated into the ply optimization process to partition the structure into subcomponents to improve drapability and improve structural performance. The next design process integrated into the methodology leveraged the results of the kinematic draping process to inform the design of connections between the partitioned sections. Next the material allocation was determined by integrating ply topology optimization into the ply optimization step. Finally, a production simulation was integrated into the ply optimization step to provide feedback on the developed design and to validate the results.

As a control, a second "partially optimized" model was created which skipped the mold optimization step, and instead imported an overall structural geometry from a steel anchor bracket design. The design was representative of the types of black metal structures typically optimized in published research in that its geometry had features such as sharp angles and numerous subsections which are better suited for metallic materials [60]. Despite the issues with the overall structural geometry, composites application was simulated with the black metal structural shape. All ply optimization processes of kinematic draping, connection definition, ply topology optimization and production simulation were completed on the partially optimized model.

The result of the final experiment validated the hypothesis: the fully integrated optimization process developed a composite anchor bracket design with reduced costs, mass and improved manufacturability compared to a black metal structure where only partial integration of the ply optimization subprocesses had been applied. Through simulation the fully optimized design was predicted to have a 37% lower mass, 94% less plies, 9 less partitioned sections, and be 57% less expensive to manufacture. Table 10 summarizes the major results of the final experiment.

Table 10 Results for partially optimized and fully optimized designs

Design	Partially Optimized	Fully Optimized
Mass	42.50 kg	26.72 kg
Plies	3,149	194
Number of partitioned sections	11	2
Total cost to manufacture each part	$13,019.46	$5,629.14

As the optimization of the mold, or overall structural geometry, was the controlled variable between the partially optimized and fully optimized designs, it is a reasonable conclusion that this step in the optimization led to the improved results. These results are logical, as the final developed fully optimized design geometry is far less complicated and better suited for composite application. The mold step optimized three-dimensional elements to create the overall structural design which had smooth contours. Through the subsequent ply optimization steps these contours proved advantageous for composite application, as improved drapability, manufacturability, structural performance and production costs were confirmed when accurate composite properties were simulated.

CHAPTER 7: DISCUSSION OF INTEGRATED METHODOLOGY

Many industries have become interested in the application of composite materials in structural design [26]. Due to high specific properties and ability to be molded into complex shapes, the material type offers the potential to greatly reduce the mass of structures while improving performance when compared to traditional structural materials such as metals [137]. Unfortunately, despite the potential benefits, application remains limited in most industries due to a lack of established design principles specific to of the material class. Specifically, processes to develop structural geometries suited for composite application have not been adopted by many industries. Instead, industries have reused existing black metal structural shapes designed for metallic materials which do not fully exploit the benefits of composites [22].

Contributing to the issue, simulation and design tools specific to composite materials are less mature than those developed for metallic materials. Commercially available tools are, however, improving and there are now programs that can assist with developing structural shapes, optimizing the application of composite materials onto those structural shapes, simulating structural performance of a manufactured part, and accurately predicting costs [148]. These software tools have not been designed, however, to integrate these functionalities to provide a comprehensive design optimization and simulation process. Because of the lack of integration of the available tools, most researchers who have applied them have also developed methodologies which do not integrate between the multiple necessary functions, resulting in designs which are not accurately modeled or fully optimized [60].

A demand for integration is, however, evident in the literature reviewed. Industries which have more maturity in composite application, such as aerospace, have developed integrated design tools which combine the above mentioned functionality [103]. These tools are, however, proprietary and specific to the types of structural shapes that are used in aircraft design. Recently, researchers from less experienced industries have begun developing methodologies to integrate multiple composite design functions at a time using commercially available software tools [9]. While these studies have demonstrated progress and promising results, they have not yet created a fully integrated methodology. Several researchers have begun to formulate conceptual frameworks for a fully integrated solution but have not tested them in an actual application to determine their effectiveness [21].

This research aimed to meet the demand noted in literature through the development of a new integrated optimization methodology. Through a literature review, it is evident that the subprocesses required to optimize a composite structure can be grouped into two categories: mold and ply shape optimization. Mold shape optimization is aimed at developing the overall structural shape that can be readily manufactured through a molding process. Ply shape optimization is the allocation of material on the developed mold shape.

The overall effort of optimizing a composite design must be subdivided into the two steps of mold and ply shape optimization, again due to limitations of existing software tools. Past research has demonstrated that the mold shape should be developed using three-dimensional elements [83], [109]. Currently, simulation tools cannot optimize three-dimensional elements with anisotropic properties. Therefore, the established practice is to approximate in-plane isotropic properties of the designed laminate and apply them to three-dimensional elements. Once the mold shape is developed, the model is next re-meshed with two-dimensional elements to accurately simulate anisotropic properties.

Subsequently material allocation on the developed mold shape is completed through the subprocess of ply optimization. Ply optimization consists of draping simulation, kinematic partitioning, connection and joint design, ply topology optimization and production simulations [139]. Draping simulations are required to accurately represent the structural performance following the manufacturing process of laying plies up on the developed mold shape. Next, the results of the draping simulation are used to perform kinematic partitioning which subdivides ply area to optimize draping. Partitioning is necessary for composite structures which have complex shapes, as draping smaller ply areas over geometry details such as sharp curves can reduce material defects such as fabric shear and wrinkling. Once the structure is partitioned connections or joints between the ply subregions can be modeled to accurately capture structural performance. Topology optimization is the next function integrated which erodes ply areas within the partitioned regions to satisfy design objectives and constraints. Finally, production simulation is integrated to provide validation and feedback on the developed design with respect to cost.

To summarize, the methodology proposed in this research iteratively integrates the following composite design functions to progressively optimize a structure:

- Mold shape optimization
- Ply shape optimization
    - Ply draping simulation
    - Kinematic partitioning of the structure
    - Joint and connection definition and modeling
    - Ply topology optimization
    - Production simulation

7.1 Comparison to Past Research and New Knowledge Generated

While many studies were considered in this research, it primarily aimed to integrate two sets of composite design and optimization studies conducted by Kuzcek et al. and Mårtensson et al. The studies by Kuzcek et. al, established the mold optimization process that was integrated into the developed methodology [83], [109]. In those studies, the methodology of using three-dimensional elements with in-plane quasi-isotropic properties was used to identify the optimal shape of a rail vehicle body frame. The studies did not attempt to integrate the mold shape development process with any ply optimization functions.

While the studies were successful in creating a frame design, there were areas identified for improvement. First, the final structural mass was 48,000 kg, which is roughly 4,000 kg heavier than a typical steel design [73]. Therefore, a ply optimization process to identify mass savings would likely have improved results had it been integrated. Furthermore, the study only considered the use of composite tube structures and associated manufacturing constraints. While these types of molded tube shapes are logical for a frame structure, the manufacturing constraints associated with them are simpler than a hand layup process. In the final experiment from this dissertation a hand layup manufacturing process was assumed, along with the more complicated hand access and molding constraints associated with it.

Comparing the results of the studies by Kuczek et al., to the results obtained in the final experiment of this research, the improvements offered through an integrated methodology are evident. When the integrated methodology proposed in this research was applied in the design of a composite rail vehicle anchor bracket, as described in Chapter 6, it resulted in a structure which had a 45% lower mass than a typical steel design. This is an improvement over the 9% mass increase demonstrated in the studies by Kuczek et al. when comparing the composite rail vehicle frame structure to a typical steel design [83], [109]. Additionally, more complex manufacturing constraints were demonstrated in this research as hand layup manufacturing was considered. The integrated methodology proposed in this research was successful in developing a complex anchor bracket shape that could feasibly be manufactured through hand layup. The manufacturing constraints established during the mold optimization process resulted in a mold shape that provided hand access to the parts interior allowing it to be laid up in a female mold.

From a ply shape optimization perspective, this research primarily drew inspiration from a series of studies by Mårtensson et al. of Volvo which aimed to optimize a composite floor pan for an automobile. In one study the researchers integrated ply partitioning, ply topology optimization and manufacturing cost analyses, but excluded ply draping simulations [9]. In a separate study, the researchers combine ply partitioning, draping simulation and manufacturing cost analyses, but excluded ply topology optimization [118]. The research presented in this dissertation took the logical step of advancing the studies by the Volvo group through fully integrating all ply related design and optimization functions into the methodology proposed.

Both studies by Volvo also imported a pre-designed overall mold shape to complete the ply optimization subprocesses, rather than identifying an optimal overall structural shape as proposed by Kuczek et al. As a result, the results achievable with the methodology proposed by Volvo is limited based on the quality of the mold geometry that is imported for ply optimization. Without integration of the mold shape development, the methodology proposed by Volvo allows for black metal mold shapes to be used in composite design. Therefore, this dissertation also advanced the work by the Volvo group by integrating the mold optimization processes proposed by Kuczek et al. into the ply optimization methodology.

Other new knowledge generated by this research relating to the ply optimization subprocess is the confirmation that ply topology optimization, when not integrated with partitioning and draping, may result in inaccurate results. When comparing the black metal structure from the preliminary experiment (discussed in Chapter 3) to the partially optimized model in the final experiment (discussed in Chapter 7), those inaccuracies were apparent. During the preliminary experiment modeling of the structure was simplified in a manner that was noted in ply topology optimization literature [60]. Those assumptions included neglecting the effects of ply draping, partitioning the structure based on the original metallic design, not modelling the connections between partitioned regions, and leaving complex geometries modeled as steel. The total mass of the black metal structure from the preliminary experiment was 37.82 kg following ply optimization, which offered a mass savings of 22% compared to the original steel design.

During the final experiment the assumptions and simplifications included in the preliminary experiment were eliminated. More accurately modeling the black metal structure through the integrated ply optimization subprocess resulted in a total structural mass of 42.50 kg, an increase of over 12% compared to the preliminary experiment. Demonstrating the mass savings results of the preliminary experiment are not attainable in a manufactured solution. The number of plies also increased from 1,063 in the preliminary experiment model to 3,149 for the partially optimized model in the final experiment. This ply number increase of 196%, once assumptions and simplifications were eliminated, results in a structure that would be less feasible for manufacturing. This comparison indicates that many published ply topology optimization studies may be overly optimistic in their results due to the lack of an integrated methodology applied.

7.2 Other Potential Applications and Limits of Applicability

Because of the flexibility offered by the proposed methodology, there is potential for it to be applied in different applications other than the design of a rail vehicle anchor bracket. As previously discussed, software limitations only allow for the modeling of three-dimensional elements with isotropic material properties. Therefore, the application of the proposed mold optimization subprocess is limited to applications where quasi-isotropic laminate design is acceptable. In the literature reviewed quasi-isotropic design was common to applications that support dynamic loading, such as aerospace, vehicles, pressure vessels and wind turbines, as the laminate construction provides multi-axis support [149].

The integrated ply optimization subprocess proposed in this research is less constrained in its potential applications than mold optimization. The ply optimization methodology developed in this research is applicable to any structural application that uses FRP materials. In the literature reviewed ply optimization functionality has been applied to applications wide ranging from bathtubs to bridge structures [150].

7.3 Alternative Approaches

As discussed in Chapter 2 (subsection 2.1.3), this research aimed to develop a methodology leveraging commercially available software tools. As also explained in that chapter, shape optimization algorithms included in commercially available FEA solvers use a gradient based methodology to complete shape optimization. The gradient-based approach is preferred by FEA software developers as it is known to offer benefits such as reduced simulation time [8]. There are deficiencies of gradient based approaches, however, including the possibility that the solver arrives at local, rather than global, minima [6]. This occurs because the solver only considers one solution to reduce processing time. Despite these deficiencies, the methodology proposed in this research was developed around gradient-based algorithms. This approach was taken with the intent of encouraging more rapid acceptance of the methodology by industry and to encourage further development and advancement through research.

It was noted through the literature reviewed, however, that there are more customized alternative approaches that could be taken to achieve similar, or even improved, results. Some of the alternative optimization algorithms are more likely to arrive at global minima and may offer benefits in composite optimization [151]. Other algorithm types, include evolutionary, genetic, geometry projection, level-set, and phase field [7]. Unlike gradient based algorithms, these algorithms consider multiple design solutions to identify the global minima. Processing times for these algorithms are far longer than for gradient based optimization, however, as numerous solutions must be considered. As a result, commercially available FEA software does not include these algorithm types and they have been applied with less frequency in research. Custom software that uses non-gradient based algorithms have recently been developed in research but have only been developed to the point of assessing very simple composite structures [59]. Furthermore, the code is not commercially available, limiting the progression of research in this area.

It should be noted that, to date, none of the alternative algorithms have been formulated to simulate three-dimensional elements with anisotropic mechanical properties, which was another key deficiency noted with commercially available FEA tools. As a result, like the gradient-based approach, these alternative algorithms would either require custom programming or similar approximation methodology to what was used in this research to optimize mold shape. It should also be noted, the methodology and sequencing proposed in this research is specific to gradient based solutions. The methodology would likely need to be revised to be applied to other optimization algorithm types.

7.4 Future Work

Despite the success of the developed methodology and the results of the final experiment, there are still areas where this research could be advanced. These areas include exploration of alternative manufacturing methods, additional production simulation integration, further development of software tools, and physical testing and validation. Again, by developing the methodology for this research around commercially available software tools it is envisioned that the future work could be completed more rapidly than if custom solutions had been proposed.

The first area for potential future work would be exploration of alternative manufacturing methods. This research focused only on the most common manufacturing methods used in composite research (hand layup and autoclave curing). Further validation of the methodology to develop structures for manufacturing methods such as Resin Transfer Molding (RTM) or Automated Tape Placement (ATP), may result in fine tuning of the methodology. These manufacturing methods have separate and unique constraints from the manufacturing methods considered in this research and should be explored.

The second area that could be the focus of future work is further integration of production simulations. In the proposed methodology and final experiment, the production simulation was primarily used as a method of validation and feedback on the design. In future work parameters specific to the production simulation could be integrated into earlier steps to constrain the design to improve the cost efficiency of the design. For example, the ply topology optimization was not constrained during the experiments in this research to limit the number of plies required to produce the designs. This was done to achieve the maximum possible mass savings for each design considered. This did, however, result in the formation of many small plies which likely contribute little to the structural performance of the structure. By constraining the topology process to not form small ply geometries the mass of the structure would be increased to some degree, but it would also result in a more cost-effective design. Therefore, increased integration of the production simulation could be used to perform sensitivity analyses to balance cost and mass savings to achieve more balanced solutions.

The next area for future work relates to improvement of the commercially available simulation tools. First, software could be improved by allowing three-dimensional elements to be modeled with anisotropic mechanical properties. This has been demonstrated in custom software applications, but without it being incorporated into commercially available tools application will remain limited [37]. Should modeling and optimization of three-dimensional elements with anisotropic properties become possible with commercially available software tools, it would allow for the approximation method of using in-plane properties of quasi-isotropic laminates proposed by Kuczek et al. to be eliminated. Furthermore, it would increase the applicability of the methodology proposed in this research to any FRP composite structures.

Software could also be improved through further integration of the subprocesses identified in this research. As explained in Chapter 5, the progressive and iterative nature of the methodology proposed is due to the lack of integration between simulation tools. It is logical to assume that a methodology which simultaneously optimized composite structures with respect to laminate, draping, partitioning, connections, ply topology and manufacturability may yield improved results. For example, kinematic draping analyses have demonstrated effectiveness in partitioning composite structures but do not inform designers on connection and joint design between the partitioned regions. This requires manual analysis and interpretation by the designer to create connections. If the existing software tools were improved, however, connections could be developed automatically and optimized through the data present in the FEA model.

The final area for future work is physical testing and validation. The methodology proposed and experimentation in this research was conducted exclusively through simulation. While research has demonstrated that ply draping and manufacturing simulations are accurate in predicting composite performance, physical testing may lead to further refinement of the methodology [118]. As a starting point, these physical tests would likely be conducted on a structure that is much simpler than the anchor bracket that was the focus of this research.

CHAPTER 8: CONCLUSIONS

Shape is a key aspect of an optimal structural design. To date, an integrated methodology has not been developed to create optimal mold shapes for composite ply material lay-up. As a result, many industries and researchers have attempted to apply composites to existing structural geometries designed for metallic materials, in a process known as black metal design. This research proposed a new methodology which organizes, integrates and advances many established composite design methodologies to assist designers in replacing black metal geometries with more optimal mold and ply shapes.

To increase the rate of adoption by industry and the research community, the methodology is developed around commercially available composite simulation tools. The methodology sequentially optimizes the structural mold geometry and individual ply shapes to develop a final structural design. The methodology also incorporates ply draping and manufacturing simulation to act as design feedback and validation.

To test the methodology a case study was conducted to develop composite rail vehicle structures. As part of this case study, it was hypothesized that a composite structure designed through a fully integrated methodology which optimizes both the mold and ply geometries will demonstrate reduced costs, mass and improved manufacturability compared to a black metal structure where only ply optimization functions have been integrated.

When the proposed fully integrated methodology was applied to create a case study design, the hypothesis was validated. The design generated by the fully integrated optimization methodology had a 37% lower mass, 94% less plies, 9 less partitioned regions, and a 56% lower cost to manufacture than a design that was developed through a partially integrated methodology. Through the validation steps of ply draping and manufacturing simulations, the design produced with the proposed methodology is more feasible for manufacturing and application than the design produced from established methodologies.

Based on the literature reviewed there is a high demand for structural shape optimization techniques across many industries, meaning that the developed methodology could find widespread applicability. It is envisioned that this research will guide future optimization structural software development to provide additional integration and functionality to composite designers. It is also envisioned that the improved optimization methodology developed as part of this research will lead to increased adoption of composite materials by structural engineers.

REFERENCES

[1] F. Neveu, B. Castanié, and P. Olivier, “The GAP methodology: A new way to design composite structures,” *Materials and Design*, vol. 172, p. 107755, 2019, doi: 10.1016/j.matdes.2019.107755.

[2] N. Mayer, J. Prowe, T. Havar, R. Hinterhölzl, and K. Drechsler, “Structural analysis of composite components considering manufacturing effect,” *Composite Structures*, vol. 140, pp. 776–782, 2016, doi: 10.1016/j.compstruct.2016.01.023.

[3] S. Pilla, *CAE Design and Failure Analysis of Automotive Composites*. SAE, 2015.

[4] G. Kanesan, S. Mansor, and A. Abdul-Latif, “Validation of UAV wing structural model for finite element analysis,” *Jurnal Teknologi*, vol. 71, no. 2, pp. 1–5, 2014, doi: 10.11113/jt.v71.3710.

[5] C. Hueber, K. Horejsi, and R. Schledjewski, “Review of cost estimation: methods and models for aerospace composite manufacturing,” *Advanced Manufacturing: Polymer and Composites Science*, vol. 2, no. 1, pp. 1–13, 2016, doi: 10.1080/20550340.2016.1154642.

[6] K. T. Zuo, L. P. Chen, Y. Q. Zhang, and J. Yang, “Study of key algorithms in topology optimization,” *International Journal of Advanced Manufacturing Technology*, vol. 32, no. 7–8, pp. 787–796, 2007, doi: 10.1007/s00170-005-0387-0.

[7] O. Sigmund and K. Maute, “Topology optimization approaches: A comparative review,” *Structural and Multidisciplinary Optimization*, vol. 48, no. 6, pp. 1031–1055, 2013, doi: 10.1007/s00158-013-0978-6.

[8] D. Guirguis *et al.*, “Evolutionary Black-Box Topology Optimization: Challenges and Promises,” *IEEE Transactions on Evolutionary Computation*, vol. 24, no. 4, pp. 613–633, 2020, doi: 10.1109/TEVC.2019.2954411.

[9] M. Martensson, Per, Zenkart, Dan, Ankermo, "Effects of manufacturing constraints on the cost and weight efficiency of integral and differential automotive composite structures," *Composite Structures*, vol. 134, pp. 572–578, 2015.

[10] P. Mårtensson, "Cost and Weight Effective Composite Design of Automotive Body Structures," 2014. [Online]. Available: https://www.diva-portal.org/smash/get/diva2:717380/FULLTEXT01.pdf

[11] P. Mårtensson, D. Zenkert, and M. Åkermo, "Draping simulation-supported framework for cost- and weight- effective composite design," *International Journal of Automotive Composites*, vol. 3, no. 1, p. 1, 2017, doi: 10.1504/ijautoc.2017.10007631.

[12] P. Mårtensson, D. Zenkert, and M. Åkermo, "Cost and weight efficient partitioning of composite automotive structures," *Polymer Composites*, vol. 38, no. 10, pp. 2174–2181, 2017, doi: 10.1002/pc.23795.

[13] P. Mårtensson, D. Zenkert, and M. Åkermo, "Integral versus differential design for high-volume manufacturing of composite structures," *Journal of Composite Materials*, vol. 49, no. 23, pp. 2897–2908, 2015, doi: 10.1177/0021998314557684.

[14] D. Lang, Daniel, Radford, "Two-step Optimization of a Composite Rail Vehicle Anchor Bracket Structural Design," in *AREMA Conference 2021*, 2021, pp. 1–38. [Online]. Available: https://www.arema.org/AREMA_MBRR/AREMAStore/ProductCategory.aspx?Category=PRO

[15] D. Lang and D. Radford, "Design Optimization of a Composite Rail Vehicle Anchor Bracket," *Urban Rail Transit*, 2021, doi: 10.1007/s40864-021-00144-9.

[16] D. Lang and D. W. Radford, “Cost, Draping, Material and Partitioning Optimization of a Composite Rail Vehicle Structure,” *Materials*, vol. 15, no. 449, pp. 1–24, 2022, doi: doi.org/10.3390/ma15020449.

[17] D. Wennberg, “Multi-Functional Composite Design Concepts for Rail Vehicle Car Bodies,” KTH Royal Institute of Technology, Stockholm, 2013. [Online]. Available: http://kth.diva-portal.org/smash/get/diva2:622097/FULLTEXT01.pdf

[18] L. Vosteen and R. Hadcock, “Composite Chronicles: A Study of the Lessons Learned in the Development, Production, and Service of Composite Structures,” Hampton, 1994.

[19] M. Bruyneel and C. Diaconu, “Structural Composite Design: Concepts and Considerations,” *Wiley Encyclopedia of Composites*, pp. 1–10, 2012, doi: 10.1002/9781118097298.weoc238.

[20] A. K. Bledzki, H. Seidlitz, J. Krenz, K. Goracy, M. Urbaniak, and J. J. Rösch, “Recycling of carbon fiber reinforced composite polymers—review—part 2: Recovery and application of recycled carbon fibers,” *Polymers*, vol. 12, no. 12, pp. 1–10, 2020, doi: 10.3390/polym12123003.

[21] J. Kaspar and M. Vielhaber, “Fiber-reinforced composite design within a lightweight and material-oriented development process,” *Proceedings of the International Conference on Engineering Design, ICED*, vol. DS87-1, no., pp. 329–338, 2017.

[22] P. Bere, M. Dudescu, C. Neamțu, and C. Cocian, “Design, manufacturing and test of cfrp front hood concepts for a light-weight vehicle,” *Polymers*, vol. 13, no. 9, 2021, doi: 10.3390/polym13091374.

[23] A. Shivanagere, S. K. Sharma, and P. Goyal, “Modelling of glass fibre reinforced polymer (Gfrp) for aerospace applications,” *Journal of Engineering Science and Technology*, vol. 13, no. 11, pp. 3710–3728, 2018.

[24] M. v. Gandhi, B. S. Thompson, and F. Fischer, “Manufacturing-process-driven design methodologies for components fabricated in composite materials,” *Composites Manufacturing*, vol. 1, no. 1, pp. 32–40, 1990, doi: 10.1016/0956-7143(90)90272-X.

[25] S. Y. Yang, V. Girivasan, N. R. Singh, I. N. Tansel, and C. v. Kropas-Hughes, “Selection of optimal material and operating conditions in composite manufacturing. Part II: Complexity, representation of characteristics and decision making,” *International Journal of Machine Tools and Manufacture*, vol. 43, no. 2, pp. 175–184, 2003, doi: 10.1016/S0890-6955(02)00133-5.

[26] P. Beardmore and C. F. Johnson, “The potential for composites in structural automotive applications,” *Composites Science and Technology*, vol. 26, no. 4, pp. 251–281, 1986, doi: 10.1016/0266-3538(86)90002-3.

[27] Y. Wen, X. Yue, J. H. Hunt, and J. Shi, “Feasibility analysis of composite fuselage shape control via finite element analysis,” *Journal of Manufacturing Systems*, vol. 46, no. January, pp. 272–281, 2018, doi: 10.1016/j.jmsy.2018.01.008.

[28] A. D. Evans, “Hybrid carbon fibre architectures for high performance, high volume applications. PhD thesis,” no. June, 2017.

[29] K. Ho-Le, “Finite element mesh generation methods: a review and classification,” *Computer-Aided Design*, vol. 20, no. 1, pp. 27–38, 1988, doi: 10.1016/0010-4485(88)90138-8.

[30] A. W. Gebisa and H. G. Lemu, “A case study on topology optimized design for additive manufacturing,” *IOP Conference Series: Materials Science and Engineering*, vol. 276, no. 1, 2017, doi: 10.1088/1757-899X/276/1/012026.

[31] “The Finite Element Method (FEM),” *COMSOL*, 2017. https://www.comsol.com/multiphysics/finite-element-method (accessed Jul. 11, 2021).

[32] M. S. Hameed, S. K. Afaq, and F. Shahid, “Finite Element Analysis of a Composite VAWT Blade,” *Ocean Engineering*, vol. 109, pp. 669–676, 2015, doi: 10.1016/j.oceaneng.2015.09.032.

[33] G. Keifer and F. Effenberger, *Mathematics in Material Science*, 1st ed., vol. 6, no. 1. Mauritius: OmniScriptum Publishing Group, 2019.

[34] J. Huang, P. Boisse, N. Hamila, I. Gnaba, D. Soulat, and P. Wang, “Experimental and numerical analysis of textile composite draping on a square box. Influence of the weave pattern,” *Composite Structures*, vol. 267, no. January, p. 113844, 2021, doi: 10.1016/j.compstruct.2021.113844.

[35] R. M. Teli, H. V Lakshminarayana, and V. Kaup, “Analysis and Design Optimization of Composite Floor Panel of Mass Transit,” *International Journal of Engineering Research & Technology*, vol. 3, no. 7, pp. 874–882, 2014.

[36] M. N. Saleh, A. Yudhanto, G. Lubineau, and C. Soutis, “The effect of z-binding yarns on the electrical properties of 3D woven composites,” *Composite Structures*, vol. 182, no. September, pp. 606–616, 2017, doi: 10.1016/j.compstruct.2017.09.081.

[37] A. Drach, B. Drach, and I. Tsukrov, “Processing of fiber architecture data for finite element modeling of 3D woven composites Dedicated to Professor Zdeněk Bittnar in

occasion of his 70th birthday.,” *Advances in Engineering Software*, vol. 72, pp. 18–27, 2014, doi: 10.1016/j.advengsoft.2013.06.006.

[38] A. A. Safonov, “3D topology optimization of continuous fiber-reinforced structures via natural evolution method,” *Composite Structures*, vol. 215, no. December 2018, pp. 289–297, 2019, doi: 10.1016/j.compstruct.2019.02.063.

[39] X. Tong, W. Ge, X. Gao, and Y. Li, “Optimization of Combining Fiber Orientation and Topology for Constant-Stiffness Composite Laminated Plates,” *Journal of Optimization Theory and Applications*, vol. 181, no. 2, pp. 653–670, 2019, doi: 10.1007/s10957-018-1433-z.

[40] J. Chen, Y. Xu, and Y. Gao, “Topology optimization of metal and carbon fiber reinforced plastic (CFRP) laminated battery-hanging structure,” *Polymers*, vol. 12, no. 11, pp. 1–14, 2020, doi: 10.3390/polym12112495.

[41] X. Huang and Y. M. Xie, “A further review of ESO type methods for topology optimization,” *Structural and Multidisciplinary Optimization*, vol. 41, no. 5, pp. 671–683, 2010, doi: 10.1007/s00158-010-0487-9.

[42] S. M. Rohani, A. Vafaeesefat, M. Esmkhani, M. Partovi, and H. R. Molladavoudi, “Composite locomotive frontend analysis and optimization using Genetic Algorithm,” *Structural Engineering and Mechanics*, vol. 47, no. 5, pp. 729–740, 2013, doi: 10.12989/sem.2013.47.5.729.

[43] J. L. Cao, J. Y. Li, and C. Y. Wan, “Topology optimization for the light rail vehicle body based on sub-structure technology,” *Applied Mechanics and Materials*, vol. 367, pp. 145–150, 2013, doi: 10.4028/www.scientific.net/AMM.367.145.

[44] Y. Zhou and K. Saitou, “Topology optimization of composite structures with data-driven resin filling time manufacturing constraint,” *Structural and Multidisciplinary Optimization*, vol. 55, no. 6, pp. 2073–2086, 2017, doi: 10.1007/s00158-016-1628-6.

[45] J. Wu, A. Clausen, and O. Sigmund, “Minimum compliance topology optimization of shell–infill composites for additive manufacturing,” *Computer Methods in Applied Mechanics and Engineering*, vol. 326, pp. 358–375, 2017, doi: 10.1016/j.cma.2017.08.018.

[46] P. Mårtensson, D. Zenkert, and M. Åkermo, “Effects of manufacturing constraints on the cost and weight efficiency of integral and differential automotive composite structures,” vol. 134, pp. 572–578, 2015, doi: 10.1016/j.compstruct.2015.08.115.

[47] W. Zuo and K. Saitou, “Multi-material topology optimization using ordered SIMP interpolation,” *Structural and Multidisciplinary Optimization*, vol. 55, no. 2, pp. 477–491, 2017, doi: 10.1007/s00158-016-1513-3.

[48] B. Akay, D. Ragni, C. S. Ferreira, and G. J. W. van Bussel, “On the structural topology of wind turbine blades,” *Wind Energy*, no. April 2012, pp. 1–20, 2013, doi: 10.1002/we.

[49] L. Kupchanko, S. Roper, H. Lee, M. Huh, and I. Y. Kim, “A Comparison of Lightweight Design Concepts of a Passenger Aircraft Seat Using Topology and CFRP Laminate Optimization,” 2020. doi: 10.32393/csme.2020.104.

[50] B. Hassani, S. M. Tavakkoli, and H. Ghasemnejad, “Simultaneous shape and topology optimization of shell structures,” *Structural and Multidisciplinary Optimization*, vol. 48, no. 1, pp. 221–233, 2013, doi: 10.1007/s00158-013-0894-9.

[51] I. P. A. Papadopoulos, P. E. Farrell, and T. M. Surowiec, “Computing multiple solutions of topology optimization problems,” *SIAM Journal on Scientific Computing*, vol. 43, no. 3, pp. A1555–A1582, 2021, doi: 10.1137/20M1326209.

[52] G. D. Goh, Y. L. Yap, S. Agarwala, and W. Y. Yeong, “Recent Progress in Additive Manufacturing of Fiber Reinforced Polymer Composite,” *Advanced Materials Technologies*, vol. 4, no. 1, pp. 1–22, 2019, doi: 10.1002/admt.201800271.

[53] S. . M. Bharath.V.G, Ranjith .S, “Topology and Size Optimization of Composite Ply Cargo Door,” *International Journal of Engineering Research & Technology*, vol. 2, no. 10, pp. 2095–2100, 2013.

[54] N. P. van Dijk, K. Maute, M. Langelaar, and F. van Keulen, “Level-set methods for structural topology optimization: A review,” *Structural and Multidisciplinary Optimization*, vol. 48, no. 3, pp. 437–472, 2013, doi: 10.1007/s00158-013-0912-y.

[55] S. N. Sørensen and E. Lund, “Topology and thickness optimization of laminated composites including manufacturing constraints,” *Structural and Multidisciplinary Optimization*, vol. 48, no. 2, pp. 249–265, 2013, doi: 10.1007/s00158-013-0904-y.

[56] B. C. Cetin, J. W. Burdick, and J. Barhen, “Local Minima Problem in Learning with Artificial Neural Networks,” in *IEEE International Conference on Neural Networks*, 1993, pp. 836–842.

[57] S. Y. Wang, K. M. Lim, B. C. Khoo, and M. Y. Wang, “An extended level set method for shape and topology optimization,” *Journal of Computational Physics*, vol. 221, no. 1, pp. 395–421, 2007, doi: 10.1016/j.jcp.2006.06.029.

[58] R. H. Lopez, *Optimization of Structures and Components*, 1st ed., no. September. Santa Catarina: Springer, 2013. doi: 10.1007/978-3-319-00717-5.

[59] H. Smith and J. A. Norato, "A MATLAB code for topology optimization using the geometry projection method," *Structural and Multidisciplinary Optimization*, pp. 1579–1594, 2020, doi: 10.1007/s00158-020-02552-0.

[60] C. Wu, Y. Gao, J. Fang, E. Lund, and Q. Li, "Discrete topology optimization of ply orientation for a carbon fiber reinforced plastic (CFRP) laminate vehicle door," *Materials and Design*, vol. 128, no. April, pp. 9–19, 2017, doi: 10.1016/j.matdes.2017.04.089.

[61] V. v Toropov, R. Jones, T. Willment, and M. Funnell, "Weight and Manufacturability Optimization of Composite Aircraft Components Based on a Genetic Algorithm," *6th World Congresses of Structural and Multidisciplinary Optimization*, no. June, 2005.

[62] Y. Dai, M. Feng, and M. Zhao, "Topology optimization of laminated composite structures with design-dependent loads," *Composite Structures*, vol. 167, pp. 251–261, 2017, doi: 10.1016/j.compstruct.2017.01.069.

[63] J. W. Lee, J. J. Kim, and G. H. Yoon, "Stress constraint topology optimization using layerwise theory for composite laminates," *Composite Structures*, vol. 226, no. June, p. 111184, 2019, doi: 10.1016/j.compstruct.2019.111184.

[64] E. Lund, "Buckling topology optimization of laminated multi-material composite shell structures," *Composite Structures*, vol. 91, pp. 158–167, 2009, [Online]. Available: http://library1.nida.ac.th/termpaper6/sd/2554/19755.pdf

[65] L. Esposito *et al.*, "Topology optimization-guided stiffening of composites realized through Automated Fiber Placement," *Composites Part B: Engineering*, vol. 164, no. September 2018, pp. 309–323, 2019, doi: 10.1016/j.compositesb.2018.11.032.

[66] E. D. Sanders, M. A. Aguiló, and G. H. Paulino, "Multi-material continuum topology optimization with arbitrary volume and mass constraints," *Computer Methods in Applied*

Mechanics and Engineering, vol. 340, pp. 798–823, 2018, doi: 10.1016/j.cma.2018.01.032.

[67] M. Alfouneh and L. Tong, “Maximizing modal damping in layered structures via multi-objective topology optimization,” *Engineering Structures*, vol. 132, pp. 637–647, 2017, doi: 10.1016/j.engstruct.2016.11.058.

[68] J. P. Blasques, “Multi-material topology optimization of laminated composite beams with eigenfrequency constraints,” *Composite Structures*, vol. 111, no. 1, pp. 45–55, 2014, doi: 10.1016/j.compstruct.2013.12.021.

[69] Z. Hu, V. K. Gadipudi, and D. R. Salem, “Topology Optimization of Lightweight Lattice Structural Composites Inspired by Cuttlefish Bone,” 2018. doi: 10.1007/s10443-018-9680-6.

[70] D. Jiang, R. Hoglund, and D. E. Smith, “Continuous fiber angle topology optimization for polymer composite deposition additive manufacturing applications,” *Fibers*, vol. 7, no. 2, 2019, doi: 10.3390/FIB7020014.

[71] X. F. Sun, J. Yang, Y. M. Xie, X. Huang, and Z. H. Zuo, “Topology optimization of composite structure using Bi-directional Evolutionary Structural Optimization method,” *Procedia Engineering 14*, vol. 14, pp. 2980–2985, 2011, doi: 10.1016/j.proeng.2011.07.375.

[72] *Railway applications - Wheelsets and bogies - Method of specifying the structural requirements of bogie frames*. EUROPEAN COMMITTEE FOR STANDARDIZATION, 2011, p. 26.

[73] Parsons Brinckerhoff Quade & Douglas, “TCRP Report 57: Track Design Handbook for Light Rail Transit,” Herndon, VA, 2000.

[74] S. Yi, *Strengthening of the Railway Transport Capacity*. Academic Press, 2018. doi: 10.1016/b978-0-12-813487-0.00007-x.

[75] Y. Rong, G. Zhang, and Y. Huang, "Study on deformation and residual stress of laser welding 316L T-joint using 3D/shell finite element analysis and experiment verification," *International Journal of Advanced Manufacturing Technology*, vol. 89, no. 5–8, pp. 2077–2085, 2017, doi: 10.1007/s00170-016-9246-4.

[76] M. Bauccio, *ASM Metals Reference Book*, 3rd ed. Materials Park: ASM International, 1993.

[77] M. Kaufmann, D. Zenkert, and M. Åkermo, "Cost/weight optimization of composite prepreg structures for best draping strategy," *Composites Part A: Applied Science and Manufacturing*, vol. 41, no. 4, pp. 464–472, 2010, doi: 10.1016/j.compositesa.2009.11.012.

[78] K. Marlett, Y. Ng, J. Tomblin, A. By, and E. Hooper, "Hexcel 8552 AS4 Unidirectional Prepreg at 190 gsm & 35 % RC Qualification Material Property Data Report FAA Special Project Number SP4614WI-Q NCAMP Test Report Number : CAM-RP-2010-002 Rev A Prepared by : Reviewed by : Testing Facility :," Wichita, 2011. [Online]. Available: https://www.wichita.edu/research/NIAR/Research/hexcel-8552/AS4-Unitape-2.pdf

[79] P. Galvez, A. Quesada, M. A. Martinez, J. Abenojar, M. J. L. Boada, and V. Diaz, "Study of the behaviour of adhesive joints of steel with CFRP for its application in bus structures," *Composites Part B: Engineering*, vol. 129, pp. 41–46, 2017, doi: 10.1016/j.compositesb.2017.07.018.

[80] J. S. Kim, N. P. Kim, and S. H. Han, "Optimal stiffness design of composite laminates for a train carbody by an expert system and enumeration method," *Composite Structures*, vol. 68, no. 2, pp. 147–156, 2005, doi: 10.1016/j.compstruct.2004.03.009.

[81] M. E. Botkin, "Structural optimization of automotive body components based upon parametric solid modeling," *8th Symposium on Multidisciplinary Analysis and Optimization*, pp. 109–115, 2000, doi: 10.2514/6.2000-4707.

[82] D. H. Kim, H. G. Kim, and H. S. Kim, "Design optimization and manufacture of hybrid glass/carbon fiber reinforced composite bumper beam for automobile vehicle," *Composite Structures*, vol. 131, pp. 742–752, 2015, doi: 10.1016/j.compstruct.2015.06.028.

[83] T. Kuczek and B. Szachniewicz, "Topology optimization of passenger wagon composite structure," in *1st International Conference on Engineering and Applied Sciences Optimization, Proceedings*, 2014, pp. 1–9.

[84] F. G. Becker, "Lightweight design of automotive composite bumper system using modified particle swarm optimizer," *Composite Structures*, vol. 140, pp. 630–643, 2015.

[85] E. Lund, "Discrete Material and Thickness Optimization of laminated composite structures including failure criteria," *Structural and Multidisciplinary Optimization*, vol. 57, no. 6, pp. 2357–2375, 2018, doi: 10.1007/s00158-017-1866-2.

[86] R. Talreja, "Assessment of the fundamentals of failure theories for composite materials," *COMPOSITES SCIENCE AND TECHNOLOGY*, vol. 105, no. August, pp. 190–201, 2017, doi: 10.1016/j.compscitech.2014.10.014.

[87] S. D. Müzel, E. P. Bonhin, N. M. Guimarães, and E. S. Guidi, "Application of the finite element method in the analysis of composite materials: A review," *Polymers*, vol. 12, no. 4. MDPI AG, Apr. 01, 2020. doi: 10.3390/POLYM12040818.

[88] E. S. Barroso, E. Parente, and A. M. Cartaxo de Melo, “A hybrid PSO-GA algorithm for optimization of laminated composites,” *Structural and Multidisciplinary Optimization*, vol. 55, no. 6, pp. 2111–2130, 2017, doi: 10.1007/s00158-016-1631-y.

[89] M. Bruyneel, C. Beghin, G. Craveur, S. Grihon, and M. Sosonkina, “Stacking sequence optimization for constant stiffness laminates based on a continuous optimization approach,” *Structural and Multidisciplinary Optimization*, vol. 46, no. 6, pp. 783–794, 2012, doi: 10.1007/s00158-012-0806-4.

[90] J. M. Lee, B. J. Min, J. H. Park, D. H. Kim, B. M. Kim, and D. C. Ko, “Design of lightweight CFRP automotive part as an alternative for steel part by thickness and lay-up optimization,” *Materials*, vol. 12, no. 14, pp. 2309–2321, 2019, doi: 10.3390/ma12142309.

[91] D. Wennberg, *Light-weighting Methodology in Rail Vehicle Design through Introduction of Load Carrying Sandwich Panels*. 2011.

[92] D. Wennberg, S. Stichel, and P. Wennhage, “Optimisation of Sandwich Panels for the Load Carrying Structure of High-Speed Rail Vehicles,” *International Journal of Aerospace and Lightweight Structures (IJALS) -*, vol. 02, no. 01, p. 19, 2012, doi: 10.3850/s2010428612000207.

[93] M. M. S. Fakhrabadi, A. Rastgoo, and M. Samadzadeh, “Multi-objective design optimization of composite laminates using discrete shuffled frog leaping algorithm,” *Journal of Mechanical Science and Technology*, vol. 27, no. 6, pp. 1791–1800, 2013, doi: 10.1007/s12206-013-0430-2.

[94] R. le Riche and R. T. Haftka, “Improved genetic algorithm for minimum thickness composite laminate design,” *Composites Engineering*, vol. 5, no. 2, pp. 143–161, 1995, doi: 10.1016/0961-9526(95)90710-S.

[95] C. H. Park, W. il Lee, W. S. Han, and A. Vautrin, “Improved genetic algorithm for multidisciplinary optimization of composite laminates,” *Computers and Structures*, vol. 86, no. 19–20, pp. 1894–1903, 2008, doi: 10.1016/j.compstruc.2008.03.001.

[96] D. Liu and V. v. Toropov, “A lamination parameter-based strategy for solving an integer-continuous problem arising in composite optimization,” *Computers and Structures*, vol. 128, pp. 170–174, 2013, doi: 10.1016/j.compstruc.2013.06.003.

[97] A. Ulbricht, “Rail Vehicle in CFRP-intensive Design,” *Lightweight Design worldwide*, vol. 12, no. 2, pp. 36–41, 2019, doi: 10.1007/s41777-019-0009-4.

[98] M. Arian Nik, K. Fayazbakhsh, D. Pasini, and L. Lessard, “Optimization of variable stiffness composites with embedded defects induced by Automated Fiber Placement,” *Composite Structures*, vol. 107, no. 1, pp. 160–166, 2014, doi: 10.1016/j.compstruct.2013.07.059.

[99] K. Horejsi, J. Noisternig, O. Koch, and R. Schledjewski, “Process selection optimization of CFRP parts in the aerospace industry,” *ECCM 2012 - Composites at Venice, Proceedings of the 15th European Conference on Composite Materials*, no. June, pp. 24–28, 2012.

[100] R. Slayton and G. Spinardi, “Radical innovation in scaling up: Boeing’s Dreamliner and the challenge of socio-technical transitions,” *Technovation*, vol. 47, no. February 2016, pp. 47–58, 2016, doi: 10.1016/j.technovation.2015.08.004.

[101] A. Krzyzak, E. Kosicka, M. Borowiec, and R. Szczepaniak, “Selected tribological properties and vibrations in the base resonance zone of the polymer composite used in the aviation industry,” *Materials*, vol. 13, no. 6, 2020, doi: 10.3390/ma13061364.

[102] C. Monroy Aceves, M. P. F. Sutcliffe, M. F. Ashby, A. A. Skordos, and C. Rodríguez Román, “Design methodology for composite structures: A small low air-speed wind turbine blade case study,” *Materials and Design*, vol. 36, pp. 296–305, 2012, doi: 10.1016/j.matdes.2011.11.033.

[103] “Cost Optimization Software for Transport Aircarft Design Evaluation (COSTADE) Design Cost Methods,” Hampton, 1996. [Online]. Available: https://www.abbottaerospace.com/downloads/nasa-cr-4737-cost-optimization-software-for-transport-aircraft-design-evaluation-costade/

[104] J. Fortune and R. Valerdi, “Considerations for successful reuse in systems engineering,” *Space 2008 Conference*, pp. 1–8, 2008, doi: 10.2514/6.2008-7758.

[105] G. Wang, R. Valerdi, and J. Fortune, “Reuse in systems engineering,” *IEEE Systems Journal*, vol. 4, no. 3, pp. 376–384, 2010, doi: 10.1109/JSYST.2010.2051748.

[106] X. He, C. Xue, and Q. Zhou, “A system engineering approach for reusable software,” *Proceedings of 2015 the 1st International Conference on Reliability Systems Engineering, ICRSE 2015*, 2015, doi: 10.1109/ICRSE.2015.7366426.

[107] T. A. Zang, *Airfoil / Wing Optimization*, 1st ed. Washington D.C.: John Wiley & Sons, Ltd., 2010. doi: 10.1002/9780470686652.eae500.

[108] M. Zhou, R. Fleury, J. Wollschlager, and A. Engineering, “OPTIMIZATION OF COMPOSITES WITH REPEATING SUB-LAMINATES,” no. August, pp. 1–4, 2017.

[109] B. Kuczek,Tomasz, Szachniewicz, “Topology optimisation of railcar composite structure,” *International Journal of Heavy Vehicle Systems*, vol. 22, no. 4, pp. 375–385, 2015, doi: 10.1504/IJHVS.2015.073206.

[110] G. J. Kennedy and J. R. R. A. Martins, “A laminate parametrization technique for discrete ply-angle problems with manufacturing constraints,” *Structural and Multidisciplinary Optimization*, vol. 48, no. 2, pp. 379–393, 2013, doi: 10.1007/s00158-013-0906-9.

[111] S. Hernandez, A. Baldomir, and J. Mendz, “Size optimization of aircraft structures,” 2008.

[112] A. J. Sobey, J. I. R. Blake, and R. A. Shenoi, “Optimisation of composite boat hulls using first principles and design rules,” *Ocean Engineering*, vol. 65, pp. 62–70, 2013, doi: 10.1016/j.oceaneng.2013.03.001.

[113] J. Chen, Q. Wang, W. Z. Shen, X. Pang, S. Li, and X. Guo, “Structural optimization study of composite wind turbine blade,” *Materials and Design*, vol. 46, pp. 247–255, 2013, doi: 10.1016/j.matdes.2012.10.036.

[114] J. G. Cho, J. S. Koo, and H. S. Jung, “A lightweight design approach for an EMU carbody using a material selection method and size optimization,” *Journal of Mechanical Science and Technology*, vol. 30, no. 2, pp. 673–681, 2016, doi: 10.1007/s12206-016-0123-8.

[115] T. Mrzygłod, Mirosław; Kuczek, “Uniform crashworthiness optimization of car body for high-speed trains,” *Structural and Multidisciplinary Optimization*, vol. 49, no. February 2014, pp. 327–336, 2015, doi: 10.1007/s00158-013-0972-z.

[116] J. J. Lynch, “Advanced Composites Materials and their Manufacture Technology Assessment,” *Journal of Nervous and Mental Disease*, vol. 168, no. 11, pp. 701–703, 2015, [Online]. Available:

http://search.ebscohost.com/login.aspx?direct=true&db=psyh&AN=2011-11203-012&site=ehost-live

[117] S. L. Vatanabe, T. N. Lippi, C. R. de Lima, G. H. Paulino, and E. C. N. Silva, "Topology optimization with manufacturing constraints: A unified projection-based approach," *Advances in Engineering Software*, vol. 100, pp. 97–112, 2016, doi: 10.1016/j.advengsoft.2016.07.002.

[118] K. Vanclooster, S. v. Lomov, and I. Verpoest, "Simulating and validating the draping of woven fiber reinforced polymers," *International Journal of Material Forming*, vol. 1, no. SUPPL. 1, pp. 961–964, 2008, doi: 10.1007/s12289-008-0217-7.

[119] M. L. Herring, J. I. Mardel, and B. L. Fox, "The effect of material selection and manufacturing process on the surface finish of carbon fibre composites," *Journal of Materials Processing Technology*, vol. 210, no. 6–7, pp. 926–940, 2010, doi: 10.1016/j.jmatprotec.2010.02.005.

[120] P. Kulkarni, K. D. Mali, and S. Singh, "An overview of the formation of fibre waviness and its effect on the mechanical performance of fibre reinforced polymer composites," *Composites Part A: Applied Science and Manufacturing*, vol. 137, no. May, p. 106013, 2020, doi: 10.1016/j.compositesa.2020.106013.

[121] T. C. Lim and S. Ramakrishna, "Modelling of composite sheet forming: A review," *Composites - Part A: Applied Science and Manufacturing*, vol. 33, no. 4, pp. 515–537, 2002, doi: 10.1016/S1359-835X(01)00138-5.

[122] A. Iwata, T. Inoue, N. Naouar, P. Boisse, and S. v. Lomov, "Coupled meso-macro simulation of woven fabric local deformation during draping," *Composites Part A:*

Applied Science and Manufacturing, vol. 118, no. January, pp. 267–280, 2019, doi: 10.1016/j.compositesa.2019.01.004.

[123] J. Wang, R. Paton, and J. R. Page, “Draping of woven fabric preforms and prepregs for production of polymer composite components,” *Composites Part A: Applied Science and Manufacturing*, vol. 30, no. 6, pp. 757–765, 1999, doi: 10.1016/S1359-835X(98)00187-0.

[124] B. Fengler, L. Kärger, F. Henning, and A. Hrymak, “Multi-Objective Patch Optimization with Integrated Kinematic Draping Simulation for Continuous–Discontinuous Fiber-Reinforced Composite Structures,” *Journal of Composites Science*, vol. 2, no. 2, p. 22, 2018, doi: 10.3390/jcs2020022.

[125] D. Zenkert, M. Åkermo, and P. Mårtensson, “Draping simulation-supported framework for cost- and weight- effective composite design,” *International Journal of Automotive Composites*, vol. 3, no. 1, p. 1, 2017, doi: 10.1504/ijautoc.2017.10007631.

[126] J. M. Manter *et al.*, “Airframe Structures Technology for Future Systems,” Wright-Patterson Air Force Base, 2000.

[127] K. Balaji Thattaiparthasarathy, S. Pillay, H. Ning, and U. K. Vaidya, “Process simulation, design and manufacturing of a long fiber thermoplastic composite for mass transit application,” *Composites Part A: Applied Science and Manufacturing*, vol. 39, no. 9, pp. 1512–1521, 2008, doi: 10.1016/j.compositesa.2008.05.017.

[128] F. Henning, L. Kärger, D. Dörr, F. J. Schirmaier, J. Seuffert, and A. Bernath, “Fast processing and continuous simulation of automotive structural composite components,” *Composites Science and Technology*, vol. 171, no. December 2018, pp. 261–279, 2019, doi: 10.1016/j.compscitech.2018.12.007.

[129] J. Ceisel, P. Witte, T. Carr, S. Pogaru, and D. N. Mavris, "A non-weight based, Manufacturing Influenced Design (MIND) methodology for preliminary design," *28th Congress of the International Council of the Aeronautical Sciences 2012, ICAS 2012*, vol. 5, pp. 3995–4004, 2012.

[130] T. J. Tzong, G. D. Sikes, and M. J. Loikkanen, "Multidisciplinary design optimization of a large transport aircraft wing," *Aerospace Design Conference, 1992*, 1992, doi: 10.2514/6.1992-1002.

[131] M. Kaufmann, D. Zenkert, and P. Wennhage, "Integrated cost/weight optimization of aircraft structures," *Structural and Multidisciplinary Optimization*, vol. 41, no. 2, pp. 325–334, 2010, doi: 10.1007/s00158-009-0413-1.

[132] I. van Gent and C. Kassapoglou, "Cost-weight trades for modular composite structures," *Structural and Multidisciplinary Optimization*, vol. 49, no. 6, pp. 931–952, 2014, doi: 10.1007/s00158-013-1019-1.

[133] Q. Wang, L. Wang, W. Zhu, Q. Xu, and Y. Ke, "Design optimization of molds for autoclave process of composite manufacturing," *Journal of Reinforced Plastics and Composites*, vol. 36, no. 21, pp. 1564–1576, 2017, doi: 10.1177/0731684417718265.

[134] A. M. K. Esawi and M. F. Ashby, "Cost estimates to guide pre-selection of processes," *Materials and Design*, vol. 24, no. 8, pp. 605–616, 2003, doi: 10.1016/S0261-3069(03)00136-5.

[135] D. Zenkert, M. Kaufmann, and M. Åkermo, "Optimisation of Composite Stuctures : Design for Cost," *Composite Structures*, pp. 4–7, 2011.

[136] Galorath, "SEER-MFG Computer Program." Galorath, El Segundo, 2021.

[137] G. Motors, “A Three-Dimensional Shape Optimization System,” *Computers & Structures*, vol. 31, no. 6, pp. 881–890, 1989, doi: 10.5860/choice.32-5096.

[138] G. W. Burgreen and O. Baysal, “Three-dimensional aerodynamic shape optimization using discrete sensitivity analysis,” *AIAA Journal*, vol. 34, no. 9, pp. 1761–1770, 1996, doi: 10.2514/3.13305.

[139] S. Pierret, R. Filomeno Coelho, and H. Kato, “Multidisciplinary and multiple operating points shape optimization of three-dimensional compressor blades,” *Structural and Multidisciplinary Optimization*, vol. 33, no. 1, pp. 61–70, 2007, doi: 10.1007/s00158-006-0033-y.

[140] Autodesk, “Helius Composite.”

[141] M. Reshid *et al.*, “Mass Reduction of a Jet Engine Bracket using Topology Optimisation for Additive Manufacturing Application,” *International Journal of Advanced Science and Technology*, vol. 29, no. 8s, pp. 4438–4444, 2020, [Online]. Available: https://www.researchgate.net/publication/342378368

[142] R. R. Nagavally, “Composite Materials - History, Types, Fabrication Techniques, Advantages, and Applications,” *International Journal of Mechanical And Production Engineering*, pp. 25–30, 2016.

[143] A. Mallach, F. Härtel, F. Heieck, J. P. Fuhr, P. Middendorf, and M. Gude, “Experimental comparison of a macroscopic draping simulation for dry non-crimp fabric preforming on a complex geometry by means of optical measurement,” *Journal of Composite Materials*, vol. 51, no. 16, pp. 2363–2375, 2017, doi: 10.1177/0021998316670477.

[144] J. A. B. P. Neto, R. D. S. G. Campilho, and L. F. M. da Silva, "Parametric study of adhesive joints with composites," *International Journal of Adhesion and Adhesives*, vol. 37, pp. 96–101, 2012, doi: 10.1016/j.ijadhadh.2012.01.019.

[145] M. R. Mansor, S. M. Sapuan, E. S. Zainudin, A. A. Nuraini, and A. Hambali, "Conceptual design of kenaf fiber polymer composite automotive parking brake lever using integrated TRIZ-Morphological Chart-Analytic Hierarchy Process method," *Materials and Design*, vol. 54, pp. 473–482, 2014, doi: 10.1016/j.matdes.2013.08.064.

[146] K. a Fetfatsidis, D. Soteropoulos, A. Petrov, C. J. Mitchell, and J. a Sherwood, "Using Abaqus / Explicit to Link the Manufacturing Process to the Final Part Quality for Continuous Fiber-Reinforced Composite Fabrics," *2012 SIMULIA Community Conference*, no. March 2015, pp. 1–15, 2012.

[147] D. Abliz, Y. Duan, L. Steuernagel, L. Xie, D. Li, and G. Ziegmann, "Curing methods for advanced polymer composites -A review," *Polymers and Polymer Composites*, vol. 21, no. 6, pp. 341–348, 2013, doi: 10.1177/096739111302100602.

[148] Altair Engineering, "Generative Design and Topology Optimization," Troy, 2019. [Online]. Available: https://web.altair.com/generative-design-report?product__c=Inspire&msdcampaignid=CMP-06217-C9P7Y&detailed_lead_source=AdWords_Generative_Design_ad&campaign_source=AdWords&utm_campaign=Generative+Design&utm_term=%2Bgenerative %2Bdesign&utm_medium=ppc&utm

[149] V. B. Chandran, S. B. Tiwari, R. Suresh, C. K. Krishnadasan, B. Sivasubramonian, and A. S. Kumar, "Design and Analysis of Composite Overwrapped Pressure Vessel," *Proceedings of International Conference on Materials for the Future - Innovative*

Materials, Processes, Products and Applications, pp. 109–114, 2013, [Online]. Available: http://www.conference.bonfring.org/papers/gct_icmf2013/icmf146.pdf

[150] M. Pohlak, J. Majak, K. Karjust, and R. Küttner, "Multi-criteria optimization of large composite parts," *Composite Structures*, vol. 92, no. 9, pp. 2146–2152, 2010, doi: 10.1016/j.compstruct.2009.09.039.

[151] O. Sigmund, "On the usefulness of non-gradient approaches in topology optimization," *Structural and Multidisciplinary Optimization*, vol. 43, no. 5, pp. 589–596, 2011, doi: 10.1007/s00158-011-0638-7.